

---

# CHAPTER 3

---

# POLARIZERS

---

**Jean M. Bennett**

*Research Department*

*Michelson Laboratory*

*Naval Air Warfare Center*

*China Lake, California*

---

## GLOSSARY

---

$D$	optical density
$d$	grid spacing
$e$	extraordinary
$i$	angle of incidence
$i$	semi-cone angle
$M$	positive integer
$m$	number of plates
$N$	1/4, 1/2
$n$	refractive index
$o$	ordinary
$S$	cut angle
$T$	intensity transmittance
$\alpha$	faces angle
$\alpha$	angle ray makes with optical axis
$\alpha_i$	absorption coefficient for $i^{\text{th}}$ component
$\beta$	angle between normal and optical axis
$\gamma$	maximum variation plane of vibration
$\delta$	deviation angle
$\Delta n$	change in retardation
$\Delta n$	$n_e - n_o$
$\lambda$	wavelength
$\nu$	frequency (wave number)
$\phi$	angle $\phi$
$\phi$	angle to wave normal

## PRISM POLARIZERS

---

The material on prism polarizers is abridged from the much more complete treatment by Bennett and Bennett.<sup>1</sup> Basic relations for polarizers are given in Par. 3 of Chap. 5, "Polarization," in Vol. I of this handbook.

**1. Double Refraction in Calcite** Although many minerals, specifically those which do not have a cubic crystal structure, are doubly refracting, nearly all polarizing prisms used in the visible, near-ultraviolet, and near-infrared regions of the spectrum are made from optical calcite, which exhibits strong birefringence over a wide wavelength range. Polarizing prisms made from other birefringent crystals are used primarily in the ultraviolet and infrared at wavelengths for which calcite is opaque (Par. 33).

Next to quartz, calcite is the most widely distributed of all minerals and usually occurs in an impure polycrystalline form as marble, limestone, or chalk. Optical calcite, or Iceland spar, which is quite rare, originally came from a large deposit on the east coast of Iceland. This source is now exhausted, and optical calcite now comes principally from Mexico, Africa, and Siberia. It has been grown artificially by a hybrid gel-solution method,<sup>2</sup> but maximum edge lengths are only 3 to 4 mm.

Although calcite is much softer than glass, with care it can be worked to an excellent polish. Surfaces flat to one-fifth fringe, or even, with care, one-tenth fringe, which are free from surface defects or perceptible turned edges can be produced using more or less conventional pitch-polishing techniques.<sup>3</sup> Such techniques fail only for surfaces normal to the optic axis, in which case pitch polishing tends to cleave out small tetrahedra. Such surfaces can be polished to a lower surface quality using cloth polishers.

Crystals of calcite are negative uniaxial and display a prominent double refraction. The material can easily be cleaved along three distinct planes, making it possible to produce rhombs of the form shown in Fig. 1. At points *B* and *H*, a given face makes an angle of  $101^{\circ}55'$  with each of the other two. At all the other points, two of the angles are  $78^{\circ}5'$  and one is  $101^{\circ}55'$ . The *optic axis HI*, the direction in the crystal along which the two sets of refracted waves travel at the same velocity, makes equal angles with all three faces at point *H*.<sup>\*</sup> Any plane, such as *DBFH*, which contains the optic axis and is perpendicular to the two opposite faces of the rhomb *ABCD* and *EFGH* is called a *principal section*. A side view of the principal section *DBFH* is shown in Fig. 2. If light is incident on the rhomb so that the plane of incidence coincides with a principal section, the light is broken up into two components polarized at right angles to each other. One of these, the ordinary ray *o*, obeys Snell's law and has its plane of vibration (of the electric vector) perpendicular to the principal section. The second, the extraordinary ray *e*, has its plane of vibration parallel to the principal section. The refraction of the extraordinary ray in some cases violates Snell's law, at least in its simple form. The anomalous deflection of the ray is caused by the wavefront becoming ellipsoidal, so that the direction of propagation of the light is not along the wave normal. This ellipticity causes the velocity of the light in the crystal, and hence its refractive index, to be a function of angle. If light is incident on rhomb face *EFGH* parallel to edge *BF* of the rhomb, the *o* and *e* rays, both of which lie in a principal section, are as shown in Fig. 2. As the angle of incidence is changed in Fig. 2 so that the direction taken by the *o* ray approaches that of the optic axis *HI*, the separation between the *e* and *o* rays decreases. If the rhomb is rotated about an axis parallel to *HD*, the *e* ray

---

<sup>\*</sup> The direction of the optic axis in a uniaxial crystal such as calcite or crystalline quartz can be determined by observing the crystal between crossed polarizers. If the alignment is correct, so that the optic axis is parallel to the line of sight, there will be concentric colored circles with a black cross superimposed.<sup>4</sup>

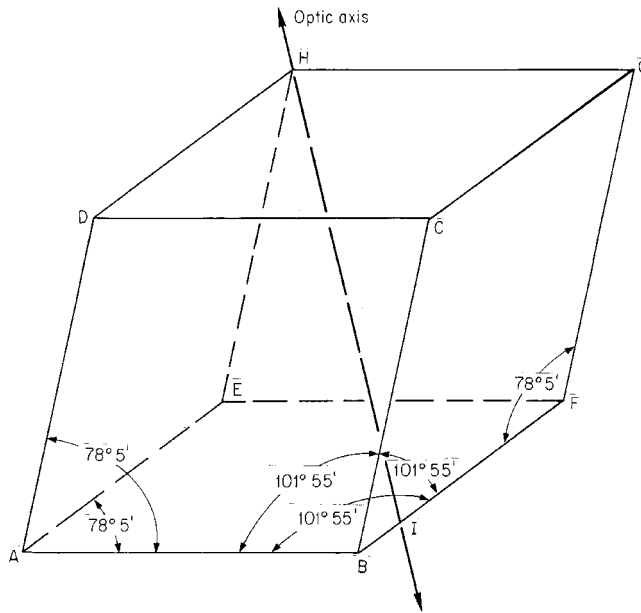


**FIGURE 1** Schematic representation of a rhombohedral calcite crystal showing the angles between faces. The optic axis passes through corner *H* and point *I* on side *BF*.

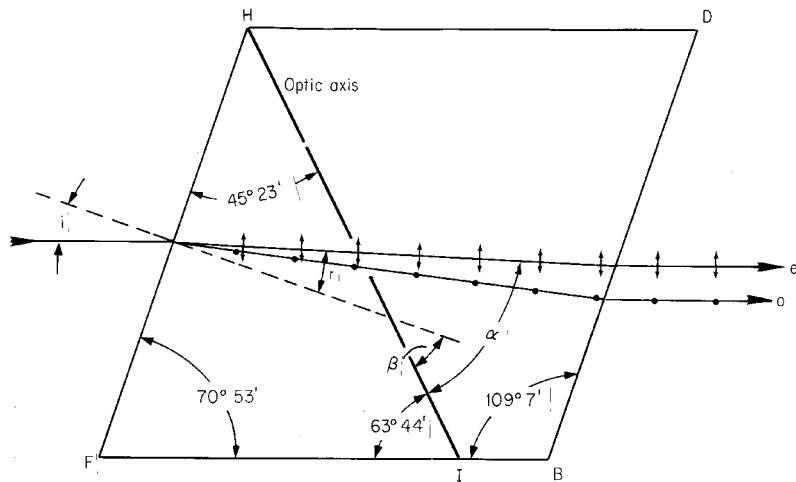


**FIGURE 2** Side view of a principal section for the calcite rhomb in Fig. 1. The direction of the optic axis and the angles of the principal section are indicated. The angle of incidence is *i*, angle of refraction is *r*, angle between the *e* ray and the optic axis is  $\alpha$ , and angle between the normal to the surface and the optic axis is  $\beta$ . The directions of vibration of the *e* and *o* rays are in the plane of the paper and perpendicular to it, respectively.

will precess about the  $o$  ray. However, unlike the  $o$  ray, it will not remain in the plane of incidence unless this plane coincides with the principal section.

The plane containing the  $o$  ray and the optic axis is defined as the *principal plane of the  $o$  ray*, and that containing the  $e$  ray and the optic axis as the *principal plane of the  $e$  ray*. In the case discussed above, the two principal planes and the principal section coincide. In the general case, they may all be different. However, in all cases, the  $o$  ray is polarized with its plane of vibration perpendicular to its principal plane and the  $e$  ray with its plane of vibration in its principal plane (see Fig. 2). In all cases, the vibration direction of the  $e$  ray remains perpendicular to that of the  $o$  ray.

The value of the index of refraction of the  $e$  ray which differs most from that of the  $o$  ray, i.e., the index when the  $e$  ray vibrations are parallel to the optic axis, is called the *principal index for the extraordinary ray  $n_e$* . Snell's law can be used to calculate the path of the  $e$  ray through a prism for this case. Snell's law can always be used to calculate the direction of propagation of the ordinary ray.

Table 1 lists values of  $n_o$  and  $n_e$  for calcite, along with the two absorption coefficients  $a_o$  and  $a_e$ , all as a function of wavelength. Since  $n_e < n_o$  in the ultraviolet, visible, and infrared regions, calcite is a negative uniaxial crystal. However, at wavelengths shorter than 1520 Å in the vacuum ultraviolet, the birefringence  $n_e - n_o$  becomes positive, in agreement with theoretical predictions.<sup>5,10</sup> For additional data in the 0.17 to 0.19- $\mu\text{m}$  region, see Uzan *et al.*<sup>11</sup> The range of transparency of calcite is approximately from 0.214 to 3.3  $\mu\text{m}$  for the extraordinary ray but only from about 0.23 to 2.2  $\mu\text{m}$  for the ordinary ray.

If the principal plane of the  $e$  ray and the principal section coincide (Fig. 2), the wave normal (*but not the  $e$  ray*) obeys Snell's law, except that the index of refraction  $n_\phi$  of this wave is given by<sup>12,13</sup>

$$\frac{1}{n_\phi^2} = \frac{\sin^2 \phi}{n_e^2} + \frac{\cos^2 \phi}{n_o^2} \quad (1)$$

where  $\phi$  is the angle between the direction of the *wave normal* and the optic axis ( $\phi \leq 90^\circ$ ). When  $\phi = 0^\circ$ ,  $n_\phi = n_o$ , and when  $\phi = 90^\circ$ ,  $n_\phi = n_e$ . The angle of refraction for the wave normal is  $\phi - \beta$ , where  $\beta$  is the angle the normal to the surface makes with the optic axis. Snell's law for the extraordinary-ray *wave normal* then becomes

$$n \sin i = \frac{n_e n_o \sin(\phi - \beta)}{(n_o^2 \sin^2 \phi + n_e^2 \cos^2 \phi)^{1/2}} \quad (2)$$

where  $i$  is the angle of incidence of light in a medium of refractive index  $n$ . Since all other quantities in this equation are known,  $\phi$  is uniquely determined but often must be solved for by iteration. Once  $\phi$  is known, the angle of refraction  $r$  for the extraordinary ray can be determined as follows. If  $\alpha$  is the angle the ray makes with the optic axis ( $\alpha \leq 90^\circ$ ), then  $r = \alpha - \beta$  and<sup>13</sup>

$$\tan \alpha = \frac{n_o^2}{n_e^2} \tan \phi \quad (3)$$

Although the angle of refraction of the extraordinary ray determines the path of the light beam through the prism, one must use the angle of refraction of the *wave normal*,  $\phi - \beta$ , in Fresnel's equation [Eq. (21) in Chap. 5, "Polarization," in Vol. I of this handbook] when calculating the reflection loss of the  $e$  ray at the surface of the prism.

For the special case in which the optic axis is parallel to the surface as well as in the plane of incidence,  $\alpha$  and  $\phi$  are the complements of the angles of refraction of the ray and wave normal, respectively. If the light is normally incident on the surface,  $\phi$  and  $\alpha$  are

TABLE 1 Refractive Indices<sup>a</sup> and Absorption Coefficients<sup>a</sup> for Calcite

$\lambda$ , $\mu\text{m}$	$n_o$	$\alpha_o$	$n_e$	$\alpha_e$	$\lambda$ , $\mu\text{m}$	$n_o$	$\alpha_o$	$n_e$	$\alpha_e$
0.1318	1.56 <sup>b</sup>	534,000 <sup>b</sup>	1.80 <sup>b</sup>	477,000 <sup>b</sup>	0.3195	—	0.059	—	—
0.1355	1.48	473,000	1.84	380,000	0.327	—	0.028	—	—
0.1411	1.40	561,000	1.82	196,000	0.330	1.70515	—	1.50746	—
0.1447	1.48	669,000	1.80	87,000	0.3355	—	0.028	—	—
0.1467	1.51	711,000	1.75	20,500	0.340	1.70078	—	1.50562	—
0.1478 <sub>5</sub>	1.54	722,000	1.75	17,000	0.3450	—	0.0170	—	—
0.1487	1.58	735,000	1.75	14,400	0.346	1.69833	—	1.50450	—
0.1495 <sub>5</sub>	1.62	714,000	1.75	12,600	0.3565	—	0.0112	—	—
0.1513	1.68	756,000	1.75	8,300	0.361	1.69316	—	1.50224	—
0.1518 <sub>5</sub>	1.72	753,000	1.74	10,700	0.3685	—	0.0056	—	—
0.1536	1.80	761,000	1.74	9,000	0.3820	—	0.0056	—	—
0.1544 <sub>5</sub>	1.87	748,000	1.74	6,500	0.394	1.68374	—	1.49810	—
0.1558 <sub>5</sub>	1.92	766,000	1.74	8,100	0.397	—	0.000	1.49640 <sup>f</sup>	—
0.1581 <sub>5</sub>	2.02	715,000	1.73	11,100	0.410	1.68014 <sup>c</sup>	—	1.49430	—
0.1596	2.14	669,000	1.72	12,600	0.434	1.67552	—	1.49373	—
0.1608	2.20	594,000	1.70	13,300	0.441	1.67423	—	1.48956	—
0.1620	2.10	566,000	1.65	14,000	0.508	1.66527	—	1.48841	—
0.1633	2.00	608,000	1.65	10,800	0.533	1.66277	—	1.48736	—
0.1662	2.00	559,000	1.64	7,500	0.560	1.66046	—	1.48640	—
0.1700	1.94	414,000	1.63	$\leq 4,400$	0.589	1.65835	—	1.48490	—
0.1800	1.70	391,000	1.61	$\leq 1,400$	0.643	1.65504	—	1.48459	—
0.1900	1.72	278,000	1.59	$\leq 321$ <sup>d</sup>	0.656	1.65437	—	1.48426	—
0.198	—	—	1.57796 <sup>c</sup>	—	0.670	1.65367	—	1.48353	—
0.200	1.90284 <sup>c</sup>	257,000	1.57649	133	0.706	1.65207	—	1.48259	—
0.204	1.88242	—	1.57081	—	0.768	1.64974	—	1.48215	—
0.208	1.86733	149,000	1.56640	—	0.795	1.64886	—	1.48216	—
0.211	1.85692	—	1.56327	—	0.801	1.64869	—	1.48176	—
0.214	1.84558	—	1.55976	$\sim 0.1$	0.833	1.64772	—	1.48137	—
0.219	1.83075	—	1.55496	—	0.867	1.64676	—	1.48098	—
0.226	1.81309	—	1.54921	—	0.905	1.64578	—	1.48060	—
0.231	1.80233	—	1.54541	—	0.946	1.64480	—	1.48022	—
0.242	1.78111	—	1.53782	—	0.991	1.64380	—	1.47985	—
0.2475	—	0.159 <sup>e</sup>	—	—	1.042	1.64276	—	1.47948	—
0.2520	—	0.125	—	—	1.097	1.64167	—	1.47910	—
0.256	—	0.109	—	—	1.159	1.64051	—	1.47870	—
0.257	1.76038	—	1.53005	—	1.229	1.63926	—	—	—
0.2605	—	0.102	—	—	1.273	1.63849	—	1.47831	—
0.263	1.75343	—	1.52736	—	1.307	1.63789	—	—	—
0.265	—	0.096	—	—	1.320	1.63767	—	—	—
0.267	1.74864	—	1.52547	—	1.369	1.63681	—	—	—
0.270	—	0.096	—	—	1.396	1.63637	—	1.47789	—
0.274	1.74139	—	1.52261	—	1.422	1.63590	—	—	—
0.275	—	0.102	—	—	1.479	1.63490	—	—	—
0.2805	—	0.096	—	—	1.497	1.63457	—	1.47744	—
0.286	—	0.102	—	—	1.541	1.63381	—	—	—
0.291	1.72774	—	1.51705	—	1.6	—	0.05 <sup>f</sup>	—	—
0.2918	—	0.109	—	—	1.609	1.63261	—	—	—
0.2980	—	0.118	—	—	1.615	—	—	1.47695	—
0.303	1.71959	—	1.51365	—	1.682	1.63127	—	—	—
0.305	—	0.118	—	—	1.7	—	0.09	—	—
0.312	1.71425	0.096	1.51140	—	1.749	—	—	1.47638	—

**TABLE 1** Refractive Indices<sup>a</sup> and Absorption Coefficients<sup>a</sup> for Calcite (*Continued*)

$\lambda$ , $\mu\text{m}$	$n_o$	$\alpha_o$	$n_e$	$\alpha_e$	$\lambda$ , $\mu\text{m}$	$n_o$	$\alpha_o$	$n_e$	$\alpha_e$
1.761	1.62974				2.4	—	2.3	—	0.09
1.8	—	0.16			2.5	—	2.7	—	0.14
1.849	1.62800				2.6	—	2.5	—	0.07
1.9	—	0.23			2.7	—	2.3	—	0.07
1.909	—	—	1.47573		2.8	—	2.3	—	0.09
1.946	1.62602				2.9	—	2.8	—	0.18
2.0	—	0.37			3.0	—	4.0	—	0.28
2.053	1.62372				3.1	—	6.7	—	0.46
2.100	—	0.62	1.47492	0.02 <sup>f</sup>	3.2	—	10.6	—	0.69
2.172	1.62099				3.3	—	15.0	—	0.92
2.2	—	1.1	—	0.05	3.324	—	—	1.47392	
2.3	—	1.7	—	0.07	3.4	—	19.0	—	1.2

<sup>a</sup> Refractive indexes  $n_o$  and  $n_e$  are the ordinary and extraordinary rays, respectively, and the corresponding absorption coefficients are  $\alpha_o = 4\pi k_o/\lambda \text{ cm}^{-1}$  and  $\alpha_e = 4\pi k_e/\lambda \text{ cm}^{-1}$ , where the wavelength  $\lambda$  is in centimeters. In the table, the wavelength is in micrometers.

<sup>b</sup> Uzan *et al.*, Ref. 5;  $\alpha_o$  and  $\alpha_e$  were calculated from the reported values of  $k_o$  and  $k_e$ .

<sup>c</sup> Ballard *et al.*, Ref. 6.

<sup>d</sup> Schellman *et al.*, Ref. 7;  $\alpha_e$  was calculated from the optical density for the extraordinary ray.

<sup>e</sup> Bouriau and Lenoble, Ref. 8; reported absorption coefficient in this paper was for both  $o$  and  $e$  rays.  $\alpha_o$  was calculated by assuming  $\alpha_e = 0$ .

<sup>f</sup> Ballard *et al.*, Ref. 9.

both  $90^\circ$  and the extraordinary ray is undeviated and has its minimum refractive index  $n_e$ . In other cases for which the optic axis is not parallel to the surface, the extraordinary ray is refracted even for normal incidence.

If the plane of incidence is neither in a principal section nor perpendicular to the optic axis, it is more difficult to determine the angle of refraction of the extraordinary ray. In such cases, Huygens' construction is helpful.<sup>13–15</sup>

**2. Types of Polarizing Prisms and Definitions** In order to make a polarizing prism out of calcite, some way must be found to separate the two polarized beams. In wavelength regions where calcite is absorbing (and hence only a minimum thickness of calcite can be used), this separation has been made simply by using a very thin calcite wedge cut so that the optic axis is parallel to the faces of the wedge to enable the  $e$  and  $o$  rays to be separated by a maximum amount. The incident light beam is restricted to a narrow pencil. Calcite polarizers of this type can be used at wavelengths as short as  $1900 \text{ \AA}$ .<sup>16</sup> In more favorable wavelength regions, where the amount of calcite through which the light passes is not so critical, more sophisticated designs are usually employed. Such prisms can be divided into two main categories, *conventional polarizing prisms* (Pars. 3 to 22) and *polarizing beam-splitter prisms* (Pars. 23 to 31), and a third category, *Feussner prisms* (Par. 32).

In conventional polarizing prisms, only light polarized in one direction is transmitted. This is accomplished by cutting and cementing the two halves of the prism together in such a way that the other beam suffers total internal reflection at the cut. It is usually deflected to the side, where it is absorbed by a coating containing a material such as lampblack. Since the ordinary ray, which has the higher index, is the one usually deflected, the lampblack is often mixed in a matching high-index binder such as resin of aloes ( $n_D = 1.634$ ) or balsam of Tolu ( $n_D = 1.628$ ) to minimize reflections.<sup>17</sup> When high-powered lasers are used, the coating is omitted to avoid overheating the prism, and the light is absorbed externally.

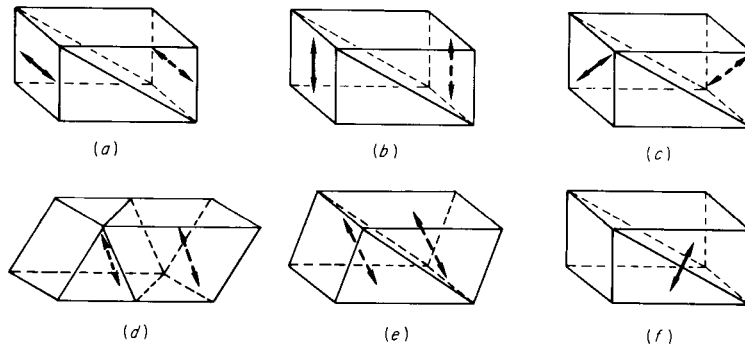


**FIGURE 3** Types of conventional polarizing prisms. Glan types: (a) Glan-Thompson, (b) Lippich, and (c) Frank-Ritter; Nicol types: (d) conventional Nicol, (e) Nicol, Halle form, and (f) Hartnack-Prizmowsky. The optic axes are indicated by the double-headed arrows.

Conventional polarizing prisms fall into two general categories: *Glan types* (Pars. 3 to 13) and *Nicol types* (Pars. 14 to 21), which are illustrated in Fig. 3. Glan types have the optic axis in the plane of the entrance face. If the principal section is parallel to the plane of the cut, the prism is a Glan-Thompson design (sometimes called a Glazebrook design); if perpendicular, a Lippich design; and if  $45^\circ$ , a Frank-Ritter design. In Nicol-type prisms, which include the various Nicol designs and the Hartnack-Prizmowsky, the principal section is perpendicular to the entrance face, but the optic axis is neither parallel nor perpendicular to the face.

Air-spaced prisms can be used at shorter wavelengths than cemented prisms, and special names have been given to some of them. An air-spaced Glan-Thompson prism is called a Glan-Foucault, and an air-spaced Lippich prism, a Glan-Taylor. In common practice, either of these may be called a Glan prism. An air-spaced Nicol prism is called a Foucault prism. Double prisms can also be made, thus increasing the prism aperture without a corresponding increase in length. Most double prisms are referred to as double Frank-Ritter, etc., but a double Glan-Thompson is called an Ahrens prism.

In polarizing beam-splitter prisms, two beams, which are polarized at right angles to each other, emerge but are separated spatially. The prisms have usually been used in applications for which both beams are needed, e.g., in interference experiments, but they can also be used when only one beam is desired. These prisms are also of two general types, illustrated in Fig. 10 in Par. 23; those having the optic axis in the two sections of the prism perpendicular and those having them parallel. Prisms of the first type include the Rochon, Sénarmont, Wollaston, double Rochon, and double Sénarmont. Prisms of the second type are similar to the conventional polarizing prisms but usually have their shape modified so that the two beams emerge in special directions. Examples are the Foster, the beam-splitting Glan-Thompson, and the beam-splitting Ahrens.

The Feussner-type prisms, shown in Fig. 12 in Par. 32, are made of isotropic material, and the film separating them is birefringent. For negative uniaxial materials the ordinary ray rather than the extraordinary ray is transmitted. These prisms have the advantage that much less birefringent material is required than for the other types of polarizing prisms, but they have a more limited wavelength range when calcite or sodium nitrate is used because, for these materials, the extraordinary ray is transmitted over a wider wavelength range than the ordinary ray.

The amount of flux which can be transmitted through a prism or other optical element depends on both its angular aperture and its cross-sectional area. The greater the amount of flux which can be transmitted, the better the *throughput* or *light-gathering power*

(sometimes called *étendue* or *luminosity*) of the system.<sup>18,19</sup> If a pupil or object is magnified, the convergence angle of the light beam is reduced in direct ratio to the increase in size of the image. The maximum throughput of a prism is thus proportional to the product of the prism's solid angle of acceptance and its cross-sectional area perpendicular to the prism axis. Hence, a large Glan-Taylor prism having an  $8^\circ$  field angle may, if suitable magnification is used, have a throughput comparable to a small Glan-Thompson prism with a  $26^\circ$  field angle. In general, to maximize prism throughput in an optical system, both the angular aperture and clear aperture (diameter of the largest circle perpendicular to the prism axis which can be included by the prism) should be as large as possible.

The quantities normally specified for a prism are its clear aperture, field angle, and length-to-aperture ( $L/A$ ) ratio. The *semi-field angle* is defined as the maximum angle to the prism axis\* at which a ray can strike the prism and still be completely polarized *when the prism is rotated about its axis*. The field angle is properly twice the semi-field angle.† (Some manufacturers quote a "field angle" for their polarizing prisms which is not symmetric about the prism axis and is thus in most cases unusable.) The *length-to-aperture ( $L/A$ ) ratio* is the ratio of the length of the prism base (parallel to the prism axis) to the minimum dimension of the prism measured perpendicular to the prism base. For a square-ended prism, the  $L/A$  ratio is thus the ratio of prism length to width.

In determining the maximum angular spread a light beam can have and still be passed by the prism, both the field angle and the  $L/A$  ratio must be considered, as illustrated in Fig. 4. If the image of a point source were focused at the center of the prism, as in Fig. 4a, the limiting angular divergence of the beam would be determined by the field angle  $2i$  of the prism.‡ However, if an extended source were focused there (Fig. 4b), the limiting angular divergence would be determined by the  $L/A$  ratio, not the field angle.

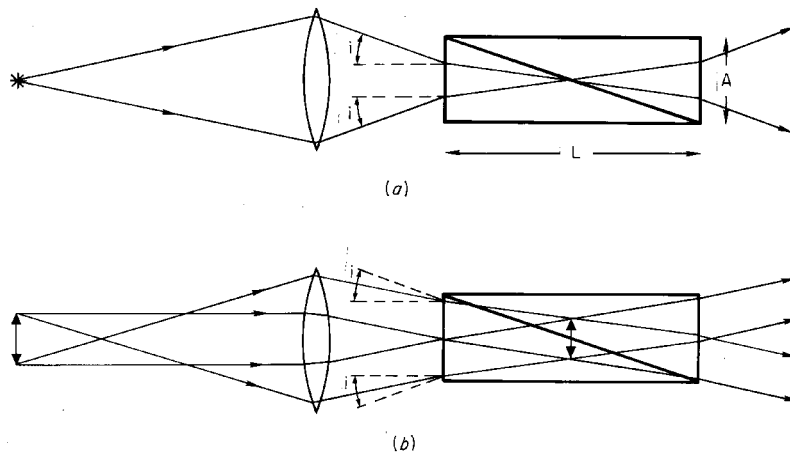


**FIGURE 4** The effect of field angle and length-to-aperture ratio of a prism polarizer on the maximum angular beam spread for (a) a point source and (b) an extended source. The field angle is  $2i$ , and  $L/A = 3$ . The field angle is exaggerated for clarity.

\* The prism axis, which is parallel to its base, is not to be confused with the optic axis of the calcite.

† In many prism designs, there is asymmetry about the prism axis, so that although light transmitted at a given angle to the prism axis may be completely polarized for one prism orientation, it will not be completely polarized when the prism is rotated about its axis. Thus, the semi-field angle is not necessarily the largest angle at which completely polarized light can be transmitted by the prism in any orientation.

‡ We are assuming that the prism is wide enough to ensure that the sides of the prism do not limit the angular width of the beam.

The field angle of a polarizing prism is strongly wavelength-dependent. For example, a Glan prism having an  $8^\circ$  field angle at  $0.4\ \mu\text{m}$  has only a  $2^\circ$  field angle at  $2\ \mu\text{m}$ . In designing optical systems in which polarizing prisms are to be used, the designer must allow for this variation in field angle. If he does not, serious systematic errors may occur in measurements made with the system.

## GLAN-TYPE PRISMS

---

3. Most prisms used at the present time are of the Glan type. Although they require considerably more calcite than Nicol types of comparable size, they are optically superior in several ways. (1) Since the optic axis is perpendicular to the prism axis, the index of the extraordinary ray differs by a maximum amount from that of the ordinary ray. Thus, a wider field angle or a smaller  $L/A$  ratio is possible than with Nicol types. (2) The light is nearly uniformly polarized over the field; it is not for Nicol types. (3) There is effectively no lateral displacement in the apparent position of an axial object viewed through a (perfectly constructed) Glan-type prism. Nicol types give a lateral displacement. (4) Since off-axis wander results in images which have astigmatism when the prism is placed in a converging beam, Glan types have slightly better imaging qualities than Nicol types.

Two other often-stated advantages of Glan-type prisms over Nicol types appear to be fallacious. One is that the slanting end faces of Nicol-type prisms have higher reflection losses than the square-ended faces of Glan types. Since the extraordinary ray vibrates in the plane of incidence and hence is in the  $p$  direction, increasing the angle of incidence toward the polarizing angle should decrease the reflection loss. However, the index of refraction for the extraordinary ray is higher in Nicol-type prisms (Glan types have the minimum value of the extraordinary index), so the reflection losses are actually almost identical in the two types of prisms. The second "advantage" of Glan-type prisms is that the slanting end faces of the Nicol type supposedly induce elliptical polarization. This widely stated belief probably arises because in converging light the field in Nicol-type polarizers is not uniformly polarized, an effect which could be misinterpreted as ellipticity (see Par. 22). It is possible that strain birefringence could be introduced in the surface layer of a calcite prism by some optical polishing techniques resulting in ellipticity in the transmitted light, but there is no reason why Nicol-type prisms should be more affected than Glan types.

## Glan-Thompson-Type Prisms

4. Glan-Thompson-type prisms may be either cemented or air-spaced. Since, as was mentioned previously, an air-spaced Glan-Thompson-type prism is called a Glan-Foucault or simply a Glan prism,\* the name Glan-Thompson prism implies that the prism is cemented. Both cemented and air-spaced prisms, however, have the same basic design. The cemented prisms are optically the better design for most applications and are the most common type of prisms in use today. The Glan-Thompson prism is named for P. Glan,<sup>20</sup> who described an air-spaced Glan-Thompson-type prism in 1880, and for S. P. Thompson,<sup>21</sup> who constructed a cemented version in 1881 and modified it to its present

---

\* An air-spaced Lippich prism, the Glan-Taylor (Par. 9), has similar optical properties to the Glan-Foucault prism but better transmission. It is also called a Glan prism.

square-ended design in 1882.<sup>22</sup> These prisms are also sometimes called Glazebrook prisms because R. T. Glazebrook<sup>23</sup> demonstrated analytically in 1883 that when rotated about its axis, this prism gives the most uniform rotation of the plane of polarization for a conical beam of incident light. The cut in a Glan-Thompson-type prism is made parallel to the optic axis, which may either be parallel to two sides, as in Fig. 3a, or along a diagonal. The end faces are always perpendicular to the axis of the prism and contain the optic axis.

The extinction ratio\* obtainable with a good Glan-Thompson-type prism equals or exceeds that of any other polarizer. Ratios of 5 parts in 100,000 to 1 part in 1 million can be expected, although values as high as 1 part in  $3 \times 10^7$  have been reported for small selected apertures of the prism.<sup>24</sup> The small residuals result mainly from imperfections in the calcite or from depolarization by scattering from the prism faces,<sup>24</sup> although if the optic axis is not strictly in the plane of the end face, or if the optic axes in the two halves of the prism are not accurately parallel, the extinction ratio will be reduced. Also, the extinction ratio may depend strongly upon which end of the prism the light is incident. When prisms are turned end for end, changes in the extinction ratio of as much as a factor of 6 have been reported.<sup>24</sup>

When measuring the extinction ratio, it is essential that none of the unwanted ordinary ray, which is internally reflected at the interface and absorbed or scattered at the blackened side of the prism, reach the detector. King and Talim<sup>25</sup> found that they had to use two 4-mm-diameter apertures and a distance of 80 mm between the photomultiplier detector and prism to eliminate the *o*-ray scattered light. With no limiting apertures and a 20-mm distance, their measured extinction ratio was in error by a factor of 80.

The field angle of the prism depends both on the cement used between the two halves and on the angle of the cut, which is determined by the  $L/A$  ratio. Calculation of the field angle is discussed in Par. 6 and by Bennett and Bennett.<sup>1</sup> Very large field angles can be obtained with Glan-Thompson prisms. For example, if the  $L/A$  ratio is 4, the field angle can be nearly  $42^\circ$ . Normally, however, smaller  $L/A$  ratios are used. The most common types of cemented prisms are the long form, having an  $L/A$  ratio of 3 and a field angle of  $26^\circ$ , and the short form, having an  $L/A$  ratio of 2.5 and a field angle of  $15^\circ$ .

**5. Transmission** In Fig. 5 the transmission of a typical Glan-Thompson prism is compared with curves for a Glan-Taylor prism and a Nicol prism. The Glan-Thompson is superior over most of the range, but its transmission decreases in the near ultraviolet, primarily because the cement begins to absorb. Its usable transmission range can be extended to about 2500 Å by using an ultraviolet-transmitting cement. Highly purified glycerin, mineral oil, castor oil, and Dow Corning DC-200 silicone oil, which because of its high viscosity is not as subject to seepage as lighter oils, have been used as cements in the ultraviolet, as have dextrose, glucose, and *gédamine* (a urea formaldehyde resin in butyl alcohol). Transmission curves for 1-mm thicknesses of several of these materials are shown in Fig. 6, along with the curve for Canada balsam, a cement formerly widely used for polarizing prisms in the visible region.<sup>8</sup> *Gédamine*, one of the best of the ultraviolet-transmitting cements, has an index of refraction  $n_D = 1.465_7$  and can be fitted to the dispersion relation<sup>8</sup>

$$n = 1.464 + \frac{0.0048}{\lambda^2} \quad (4)$$

where the wavelength  $\lambda$  is in micrometers.

Figure 7 shows ultraviolet transmission curves for Glan-Thompson prisms with  $L/A$

---

\* The extinction ratio is the ratio of the maximum to the minimum transmittance when a polarizer is placed in a plane polarized beam and is rotated about an axis parallel to the beam direction.

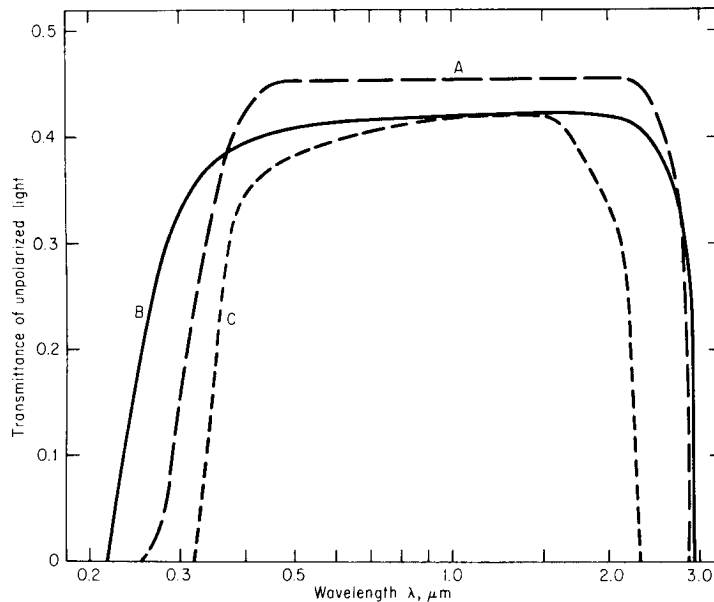


**FIGURE 5** Transmittance curves for typical polarizing prisms: A, Glan-Thompson, B, Glan-Taylor, and C, Nicol prism. (Measured by D. L. Decker, *Michelson Laboratory*.) In the visible and near infrared regions the Glan-Thompson has the best energy throughput. In the near ultraviolet the Glan-Thompson may still be superior because the Glan-Taylor has such an extremely small field angle that it may cut out most of the incident beam.

ratios of 2.5 and 3 which are probably cemented with *n*-butyl methacrylate, a low-index polymer that has largely replaced Canada balsam. Better ultraviolet transmission is obtained with a Glan-Thompson prism cemented with DC-200 silicone oil. Air-spaced prisms can be used to nearly 2140 Å in the ultraviolet, where calcite begins to absorb strongly. Transmission curves for two such prisms are shown in Fig. 7. The Glan-Taylor, which is an air-spaced prism of the Lippich design, has a higher ultraviolet transmission than the Glan-Foucault, an air-spaced Glan-Thompson prism. The reason for this difference is that multiple reflections occur between the two halves of the Glan-Foucault prism, resulting in a lowered transmission, but are largely absent in the Glan-Taylor design (see Par. 9).

The infrared transmission limit of typical Glan-Thompson prisms is about 2.7 μm although they have been used to 3 μm.<sup>26</sup> The same authors report using a 2.5-cm-long Glan-Thompson prism in the 4.4- to 4.9-μm region.

**6. Field Angle** Since many prism polarizers are used with lasers that have parallel beams of small diameter, field-angle effects are not as important as previously when extended area sources were used. Extensive calculations of the field angles for a Glan-Thompson prism are included in the earlier Polarization chapter.<sup>1</sup>

**7. Other Glan-Thompson-Type Prisms** Other types of Glan-Thompson-type prisms include the Ahrens prism (two Glan-Thompson prisms placed side-by-side), Glan-Foucault prism (an air-spaced Glan-Thompson prism), Grosse prism (an air-spaced Ahrens prism),

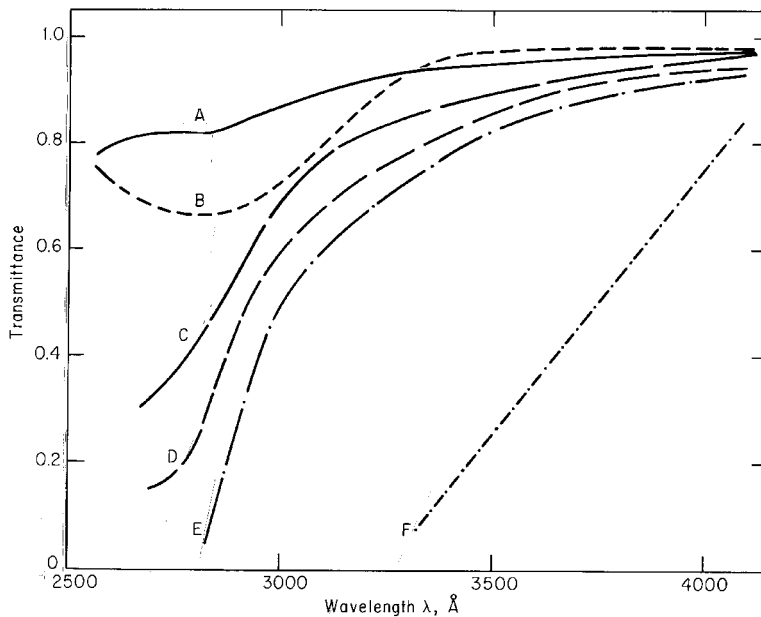


**FIGURE 6** Transmittance curves for 1-mm thicknesses of various cements: *A*, crystalline glucose, *B*, glycerine, *C*, gédamine (urea formaldehyde resin in butyl alcohol), *D*, Rhodopas N60A (polymerized vinyl acetate in alcohol), *E*, urea formaldehyde, and *F*, Canada balsam. (Modified from Bouriau and Lenoble, Ref. 8). The transmittance of these materials is adequate at longer wavelengths.

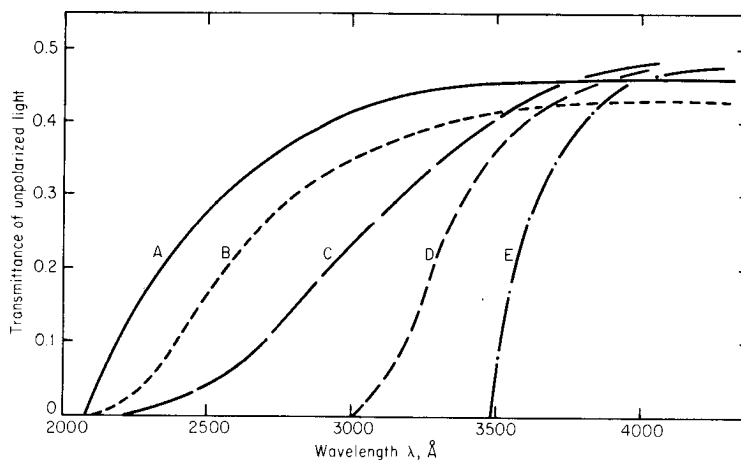


**FIGURE 7** Ultraviolet transmittance curves for various Glan-Thompson and air-spaced prisms: *A*, Glan-Taylor (air-spaced Lippich-type prism), *B*, Glan-Foucault (air-spaced Glan-Thompson prism), *C*, Glan-Thompson prism with  $L/A$  ratio of 2 cemented with DC-200 silicone oil, *D*, Glan-Thompson prism with  $L/A$  ratio of 2.5 probably cemented with *n*-butyl methacrylate, and *E*, Glan-Thompson prism similar to *D* except with  $L/A = 3$ . (Modified from curves supplied by Karl Lambrecht Corporation, Chicago.)

and those constructed of glass and calcite. Information about these prisms can be found in the earlier Polarization chapter.<sup>1</sup>

## Lippich-Type Prisms

8. Lippich<sup>27</sup> (1885) suggested a polarizing-prism design similar to the Glan-Thompson but with the optical axis in the entrance face and at right angles to the intersection of the cut with the entrance face (Fig. 3*b*).<sup>\*</sup> For this case, the index of refraction of the extraordinary ray is a function of angle of incidence and can be calculated from Eq. (1) after  $\phi$ , the complement of the angle of refraction of the wave normal is determined from Eq. (2). In the latter equation,  $\beta$ , the angle the normal to the surface makes with the optic axis, is  $90^\circ$  since the optic axis is parallel to the entrance face. Since the directions of the ray and the wave normal no longer coincide, the ray direction must be calculated from Eq. (3). Lippich prisms are now little-used because they have small field angles, except for two; the air-spaced Lippich, often called a Glan-Taylor prism, and the Marple-Hess prism (two Glan-Taylor prisms back-to-back) that is described in Par. 10. Further information about all Lippich-type prisms is given in the earlier Polarization chapter.<sup>1</sup>

9. **Glan-Taylor Prism** The Glan-Taylor prism, first described in 1948 by Archard and Taylor,<sup>29</sup> has substantial advantages over its Glan-Thompson design counterpart, the Glan-Foucault prism (Par. 7). Since air-spaced prisms have a very small field angle, the light must be nearly normally incident on the prism face, so that the difference in field angles between the Glan-Taylor and Glan-Foucault prisms (caused by the difference in the refractive index of the extraordinary ray) is negligible.

The major advantages of the Glan-Taylor prism are that its calculated transmission is between 60 and 100 percent higher than that of the Glan-Foucault prism and the intensity of multiple reflections between the two sides of the cut, always a principal drawback with air-spaced prisms, is reduced to less than 10 percent of the value for the Glan-Foucault prism.

The calculated and measured transmittances of a Glan-Taylor prism are in reasonable agreement, but the measured transmittance of a Glan-Foucault prism (Fig. 7) may be considerably higher than its theoretical value.<sup>29</sup> Even so, the transmission of the Glan-Taylor prism is definitely superior to that of the Glan-Foucault prism, as can be seen in Fig. 7. Extinction ratios of better than 1 part in  $10^3$  are obtainable for the Glan-Taylor prism.<sup>30</sup>

A final advantage of the Glan-Taylor prism is that it can be cut in such a way as to conserve calcite. Archard and Taylor<sup>29</sup> used the Ahrens method of spar cutting described by Thompson<sup>22</sup> and found that 35 percent of the original calcite rhomb could be used in the finished prism.

In a modified version of the Glan-Taylor prism becoming popular for laser applications, the cut angle<sup>†</sup> is increased, the front and back faces are coated with antireflection coatings, and portions of the sides are either covered with absorbing black glass plates or highly polished to let the unwanted beams escape.<sup>30</sup> The effect of increasing the cut angle is twofold: a beam normally incident on the prism face will have a smaller angle of incidence

<sup>\*</sup> The Lippich prism should not be confused with the Lippich half-shade prism, which is a device to determine a photometric match point. The half-shade prism consists of a Glan-Thompson or Nicol prism placed between the polarizer and analyzer such that it intercepts half the beam and is tipped slightly in the beam. The prism edge at the center of the field is highly polished to give a sharp dividing line. The eye is focused on this edge; the disappearance of the edge gives the photometric match point.<sup>28</sup>

<sup>†</sup> The cut angle is the acute angle the cut makes with the prism base.

on the cut and hence a smaller reflection loss at the cut than a standard Glan-Taylor prism, but, at the same time, the semi-field angle will be reduced throughout most of the visible and near-infrared regions.

A new type of air-spaced prism<sup>31</sup> has a very high transmittance for the extraordinary ray. It resembles the Glan-Taylor prism in that the optic axis is parallel to the entrance face and at right angles to the intersection of the cut with the entrance face. However, instead of striking the prism face at normal incidence, the light is incident at the Brewster angle for the extraordinary ray ( $54.02^\circ$  for the 6328-Å helium-neon laser wavelength), so that there is no reflection loss for the  $e$  ray at this surface. Since the ordinary ray is deviated about  $3^\circ$  more than the extraordinary ray and its critical angle is over  $4^\circ$  less, it can be totally reflected at the cut with tolerance to spare while the extraordinary ray can be incident on the cut at only a few degrees beyond its Brewster angle. Thus this prism design has the possibility of an extremely low light loss caused by reflections at the various surfaces. A prototype had a measured transmission of 0.985 for the extraordinary ray at 6328 Å.<sup>31</sup> If the prism is to be used with light sources other than lasers, its semi-field angle can be calculated.<sup>1</sup>

A major drawback to the Brewster angle prism is that since the light beam passes through a plane-parallel slab of calcite at nonnormal incidence, it is displaced by an amount that is proportional to the total thickness of the calcite. Some of the prisms are made with glass in place of calcite for the second element. In this case, the beam will usually be deviated in addition to being displaced. Measurements on a calcite-glass prototype at 6328 Å showed that the output beam was laterally displaced by several millimeters with an angular deviation estimated to be less than  $0.5^\circ$ .<sup>31</sup>

**10. Marple-Hess Prism** If a larger field angle is required than can be obtained with a Glan-Taylor prism, a Marple-Hess prism may be used. This prism, which was first proposed in 1960 as a double Glan-Foucault by D. T. F. Marple of the General Electric Research Laboratories and modified to the Taylor design by Howard Hess of the Karl Lambrecht Corporation,<sup>32</sup> is effectively two Glan-Taylor prisms back-to-back. The analysis for this prism is made in the same way as for the Glan-Taylor prism (Par. 9) and Lippich-type prisms in general, keeping in mind that the refractive index of the “cement” is 1 since the components are air-spaced.

Since the ordinary ray is totally reflected for all angles of incidence by one or the other of the two cuts, the field angle is symmetric about the longitudinal axis of the prism and is determined entirely by the angle at which the extraordinary ray is totally reflected at one of the two cuts. This angle can be readily calculated.<sup>1</sup> The field angle is considerably larger than for the Glan-Foucault or Glan-Taylor prism and does not decrease as the wavelength increases.

Unlike the Glan-Foucault or Glan-Taylor prisms, which stop being efficient polarizers when the angle of incidence on the prism face becomes too large, the Marple-Hess prism continues to be an efficient polarizer as long as the axial ordinary ray is not transmitted. If the prism is used at a longer wavelength than the longest one for which it was designed (smallest value of  $n_o$  used to determine the cut angle), the value of  $n_o$  will be still smaller and the critical angle for the axial ordinary ray will not be exceeded. Thus the axial  $o$  ray will start to be transmitted before off-axis rays get through. When this situation occurs, it only makes matters worse to decrease the convergence angle. Thus, there is a limiting long wavelength, depending on the cut angle, beyond which the Marple-Hess prism is not a good polarizer. At wavelengths shorter than the limiting wavelength, the Marple-Hess prism has significant advantages over other air-spaced prism designs.

It is not easy to make a Marple-Hess prism, and the extinction ratio in the commercial model is given as between  $1 \times 10^{-4}$  and  $5 \times 10^{-5}$ , somewhat lower than for a Glan-Taylor prism.<sup>30</sup> On the other hand, even though the Marple-Hess prism has an increased  $L/A$

ratio, 1.8 as compared to 0.85 for a Glan-Taylor prism, its ultraviolet transmission is still superior to commercially available ultraviolet transmitting Glan-Thompson prisms of comparable aperture.

### Frank-Ritter-Type Prisms

11. The third general category of Glan-type polarizing prisms is the Frank-Ritter design. Prisms of this type are characterized by having the optic axis in the plane of the entrance face, as in other Glan-type prisms, but having the cut made at  $45^\circ$  to the optic axis (Fig. 3c) rather than at  $0^\circ$ , as in Glan-Thompson prisms, or at  $90^\circ$ , as in Lippich prisms. Frank-Ritter prisms are particularly popular in the Soviet Union, and over 80 percent of the polarizing prisms made there have been of this design.<sup>33</sup> Usually double prisms comparable to the Ahrens modification of the Glan-Thompson are used,<sup>1</sup> primarily because from a rhombohedron of Iceland spar two Frank-Ritter double prisms can be obtained but only one Ahrens of the same cross section or one Glan-Thompson of smaller cross section.<sup>33</sup> However, this apparent advantage can be illusory since Iceland spar crystals often are not obtained as rhombs. For example, if the natural crystal is in the form of a plate, it may be less wasteful of material to make a Glan-Thompson or Ahrens prism than a Frank-Ritter prism.<sup>33</sup>

Optically, Frank-Ritter prisms should be similar to Glan-Thompson and Ahrens types, although the acceptance angle for a given  $L/A$  ratio is somewhat smaller since the refractive index of the extraordinary ray is larger than  $n_e$  in the prism section containing the longitudinal axis and perpendicular to the cut. In practice, the degree of polarization for a Frank-Ritter prism seems to be quite inferior to that of a good Glan-Thompson or even an Ahrens prism.<sup>33</sup>

### Use of Glan-Type Prisms in Optical Systems

12. Several precautions should be taken when using Glan-type prisms in optical systems: (1) the field angle of the prism should not be exceeded, (2) there should be an adequate entrance aperture so that the prism does not become the limiting aperture of the optical system, and (3) baffles should be placed preceding and following the prism to avoid incorrect collection of polarized light or extraneous stray light. The reason why these precautions are important are discussed in the earlier Polarization chapter.<sup>1</sup>

### Common Defects and Testing of Glan-Type Prisms

13. Several common defects are found in the construction of Glan-type prisms and limit their performance:

1. The axial beam is displaced as the prism is rotated. This defect, called *squirm*, results when the optic axes in the two halves of the prism are not strictly parallel. A line object viewed through the completed prism will oscillate as the prism is turned around the line of sight.<sup>34</sup>
2. The axial ray is deviated as the prism is rotated. This defect is caused by the two

prism faces not being parallel. A residual deviation of 3 minutes of arc is a normal tolerance for a good Glan-Thompson prism; deviations of 1 minute or less can be obtained on special order.

3. The optic axis does not lie in the end face. This error is often the most serious, since if the optic axis is not in the end face and the prism is illuminated with convergent light, the planes of vibration of the transmitted light are no longer parallel across the face of the prism. This effect, which in Nicol-type prisms gives rise to the Landolt fringe, is illustrated in the following practical case.<sup>35</sup> For a convergent beam of light of semi-cone angle  $i$ , the maximum variation of the plane of vibration of the emergent beam is  $\pm\gamma$ , where, approximately,

$$\tan \gamma = n_e \sin i \tan \phi \quad (5)$$

and  $\phi$  is the angle of inclination of the optic axis to the end face, caused by a polishing error. For  $i = 3^\circ$  and  $p = 5^\circ$ , the plane of vibration of the emergent beam varies across the prism face by  $\pm 23$  minutes of arc. Thus, good extinction cannot be achieved over the entire aperture of this prism even if nearly parallel light is incident on it. The field angle is also affected if the optic axis is not in the end face or is not properly oriented in the end face, but these effects are small.

4. The cut angle is incorrect or is different in the two halves of the prism. If the cut angle is slightly incorrect, the field angle may be decreased. This error is particularly important in Glan-Foucault or Glan-Taylor prisms, for which the angular tolerances are quite severe, and a small change in cut angle for these prisms may greatly alter the field angle, as discussed in Par. 9 and Ref. 1. If the cut angles are different in the two halves of the prism, the field angle will change when the prism is turned end-for-end. The field angle is determined by the cut angle in the half of the prism toward the incident beam. Differences in the two cut angles may also cause a beam deviation. If the angles in the two halves differ by a small angle  $\alpha$  that makes the end faces nonparallel, the beam will be deviated by an angle  $\delta = \alpha(n_e - 1)$ .<sup>35</sup> If instead, the end faces are parallel and the difference in cut angle is taken up by the cement layer which has a refractive index of approximately  $n_e$ , there will be no deviation. However, if the prism is air-spaced, the deviation  $\delta'$  caused by a nonparallel air film is approximately  $\delta' = \alpha n_e$ , illustrating one reason why air-spaced prisms are harder to make than conventional Glan-Thompson prisms.<sup>35</sup>

5. The transmittance is different when the prism is rotated through  $180^\circ$ . A potentially more serious problem when one is making photometric measurements is that the transmission of the prism may not be the same in two orientations exactly  $180^\circ$  apart.<sup>36</sup> This effect may be caused by the presence of additional light outside the entrance or exit field angle, possibly because of strain birefringence in the calcite.

Two factors which limit other aspects of polarizer performance in addition to the extinction ratio are *axis wander*, i.e. variation of the azimuth of the transmitted beam over the polarizer aperture, and the ellipticity of the emergent polarized beams<sup>25</sup> caused by material defects in the second half of the prism. Further details are discussed in the earlier Polarization chapter.<sup>1</sup>

In order to determine the cut angle, field angle, parallelism of the prism surfaces, thickness and parallelism of the air film or cement layer, and other prism parameters, one can use the testing procedures outlined by Decker *et al.*,<sup>37</sup> which require a spectrometer with a Gauss eyepiece, laser source, and moderately good polarizer. (Other testing procedures have been suggested by Archard.<sup>35</sup>) Rowell *et al.*<sup>38</sup> have given a procedure for determining the absolute alignment of a prism polarizer. However, they failed to consider some polarizer defects, as pointed out by Aspnes<sup>39</sup> who gives a more general alignment procedure that compensates for the prism defects. (There is also a response from

Rowell.<sup>40)</sup> Further information about testing Glan-type prisms and reasons why prism errors are important can be found in the earlier Polarization chapter.<sup>1</sup>

## NICOL-TYPE PRISMS

**14.** Nicol-type prisms are not generally used at the present time, as Glan types are optically preferable. However, they were the first kind made and were once so common that Nicol became a synonym for polarizer. There is much more calcite wastage in making Glan-type prisms than in making the simpler Nicol types so that, even though Glan polarizers were developed in the nineteenth century, it was only following the recent discoveries of new calcite deposits that they became popular. Many of the older instruments are still equipped with Nicol prisms so they will be briefly described here.

**15. Conventional Nicol Prism** The first polarizing prism was made in 1828 by William Nicol<sup>41</sup> a teacher of physics in Edinburgh. By cutting a calcite rhomb diagonally and symmetrically through its blunt corners and then cementing the pieces together with Canada balsam, he could produce a better polarizer than any known up to that time. A three-dimensional view of Nicol's prism is shown in Fig. 3*d*. The cut is made perpendicular to the principal section (defined in Par. 1), and the angle is such that the ordinary ray is totally reflected and only the extraordinary ray emerges. When the rhomb is intact, the direction of polarization can be determined by inspection. However, the corners are sometimes cut off, making the rhomb difficult to recognize.

The principal section of Nicol's original prism is similar to that shown in Fig. 2 except that the ordinary ray is internally reflected at the cut along diagonal *BH*. The cut makes an angle of  $19^{\circ}8'$  with edge *BF* in Fig. 2 and an angle of about  $90^{\circ}$  with the end face of the rhomb. Since the obtuse angle is  $109^{\circ}7'$  (Fig. 3*d*), the angle between the cut and the optic axis is  $44^{\circ}36'$ . The field of the prism is limited on one side by the angle at which the ordinary ray is no longer totally reflected from the balsam film, about  $18.8^{\circ}$  from the axis of rotation of the prism, and on the other by the angle at which the extraordinary ray is totally reflected by the film, about  $9.7^{\circ}$  from the axis. Thus the total angle is about  $28.5^{\circ}$  but is not by any means symmetric about the axis of rotation; the field angle (Par. 2) is only  $2 \times 9.7^{\circ} = 19.4^{\circ}$ .

In order to produce a somewhat more symmetric field and increase the field angle, the end faces of Nicol prisms are usually trimmed to an angle of  $68^{\circ}$ . This practice was apparently started by Nicol himself.<sup>22</sup> If the cut is made at  $90^{\circ}$  to the new face, as shown in Fig. 8, the new field angle is twice the smaller of  $\theta_1$  and  $\theta'_1$ . The field angles are computed as described in the earlier Polarization chapter.<sup>1</sup>

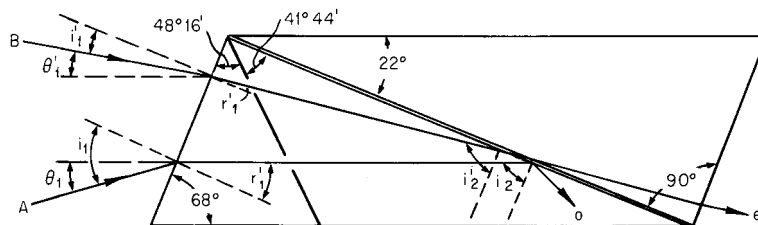


**FIGURE 8** Principal section of a conventional Nicol prism with slightly trimmed end faces. Ray *A* gives the limiting angle  $\theta_1$  beyond which the ordinary ray is no longer totally internally reflected at the cut; ray *B* gives the limiting angle  $\theta'_1$  for which the extraordinary ray starts to be totally internally reflected at the cut.

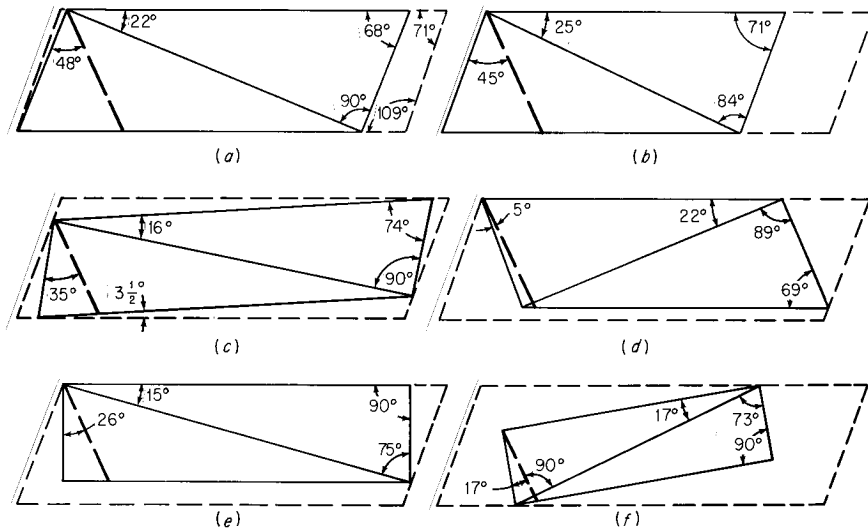


**FIGURE 9** Principal sections of various types of trimmed cemented Nicol prisms shown superimposed on the principal section of a cleaved calcite rhomb (see Fig. 2): (a) conventional trimmed Nicol; (b) Steeg and Reuter shortened Nicol (*Thompson, Ref. 22*); (c) Ahrens Nicol (*Thompson, Ref. 22*); (d) Thompson reversed Nicol (*Thompson, Ref. 42*); (e) square-ended Nicol; and (f) Hartnack-Prazmowski reversed Nicol. In all cases, the angle between the prism face and the optic axis (*heavy dashed line*), the angle of the cut, and the acute angle of the rhomb are indicated.

### Trimmed Nicol-Type Prisms

**16.** The angle at which the cut is made in a Nicol-type prism is not critical. The field angle is affected, but a useful prism will probably result even if the cut is made at an angle considerably different from  $90^\circ$ . The conventional trimmed Nicol, discussed in Par. 15, is shown again in Fig. 9a. In this and the other five parts of the figure, principal sections of various prisms are shown superimposed on the principal section of the basic calcite rhomb (Fig. 2). Thus, it is clear how much of the original rhomb is lost in making the different types of trimmed Nicols.

In the Steeg and Reuter Nicol shown in Fig. 9b, the rhomb faces are not trimmed, and the cut is made at  $84^\circ$  to the faces instead of  $90^\circ$ , giving a smaller  $L/A$  ratio. The asymmetry of the field which results is reduced by using a cement having a slightly higher index than Canada balsam.

Alternately, in the Ahrens Nicol shown in Fig. 9c, the ends are trimmed in the opposite direction, increasing their angles with the long edges of the rhomb from  $70^\circ 53'$  to  $74^\circ 30'$  or more. By also trimming the long edges by  $3^\circ 30'$ , the limiting angles are made more symmetric about the prism axis.

**17. Thompson Reversed Nicol** In the Thompson reversed Nicol shown in Fig. 9d, the ends are heavily trimmed so that the optic axis lies nearly in the end face. As a result, the blue fringe is thrown farther back than in a conventional Nicol, and although the resulting prism is shorter, its field angle is actually increased.

**18. Nicol Curtate, or Halle, Prism** The sides of the calcite rhomb may also be trimmed so that they are parallel or perpendicular to the principal section. Thus, the prism is square (or sometimes octagonal). This prism is of the Halle type<sup>43,44</sup> and was shown in Fig. 3e.

Halle, in addition, used thickened linseed oil instead of Canada balsam and altered the angle of the cut. In this way he reduced the length-to-aperture ratio from about 2.7 to 1.8 and the total acceptance angle from  $25^\circ$  to about  $17^\circ$ . Such shortened prisms cemented with low-index cements are often called Nicol curtate prisms (curtate means shortened).

**19. Square-ended Nicol** The slanting end faces on conventional Nicol prisms introduce some difficulties, primarily because the image is slightly displaced as the prism is rotated. To help correct this defect, the slanting ends of the calcite rhomb can be squared off, as in Fig. 9e, producing the so-called square-ended Nicol prism. The angle at which the cut is made must then be altered since the limiting angle  $\theta_1$  for an ordinary ray depends on the angle of refraction at the end face in a conventional prism, in which the limiting ray travels nearly parallel to the prism axis inside the prism (ray *A* in Fig. 8). If the cut remained the same, the limiting value of  $\theta_1$  would thus be zero. However, if the cut is modified to be  $15^\circ$  to the sides of the prism, the total acceptance angle is in the  $24$  to  $27^\circ$  range, depending on the type of cement used.<sup>22</sup>

Some image displacement will occur even in square-ended Nicol prisms since the optic axis is not in the plane of the entrance face. Therefore, the extraordinary ray will be bent even if light strikes the entrance face of the prism at normal incidence. There is considerable confusion on this point in the literature.<sup>22,45</sup>

**20. Hartnack-Prazmowski Prism** A reversed Nicol which has the cut at  $90^\circ$  to the optic axis<sup>46</sup> is shown in Figs. 3f and 9f. If it is cemented with linseed oil, the optimum cut angle calculated by Hartnack is  $17^\circ$  to the long axis of the prism, giving a total acceptance angle of  $35^\circ$  and an  $L/A$  ratio of 3.4.<sup>22</sup> If Canada balsam is used, the cut should be  $11^\circ$ , in which case the total acceptance angle is  $33^\circ$  and the  $L/A$  ratio is 5.2.

**21. Foucault Prism** A modified Nicol prism in which an air space is used between the two prism halves instead of a cement layer<sup>47</sup> consists of a natural-cleavage rhombohedron of calcite which has been cut at an angle of  $51^\circ$  to the face. The cut nearly parallels the optic axis. Square-ended Foucault-type prisms, such as the Hofmann prism, have also been reported.<sup>22</sup> The angle at which the cut is made can be varied slightly in both the normal Foucault prism and the Hofmann variation of it. In all designs the  $L/A$  ratio is 1.5 or less, and the total acceptance angle about  $8^\circ$  or less. The prisms suffer somewhat from multiple reflections, but the principal trouble, as with all Nicol prisms, is that the optic axis is not in the plane of the entrance face. This defect causes various difficulties, including nonuniform polarization across the field and the occurrence of a Landolt fringe (Par. 22 and Ref. 1) when two Nicol-type prisms are crossed.

**22. Landolt Fringe** If an intense extended light source is viewed through crossed polarizing prisms, careful observation will reveal that the field is not uniformly dark. In Nicol-type prisms the darkened field is crossed by a darker line whose position is an extremely sensitive function of the angle between the polarizer and analyzer. Other types of polarizing prisms also exhibit this anomaly but to a lesser extent. The origin of the Landolt fringe is given in the earlier Polarization chapter<sup>1</sup> and the references cited therein.

## POLARIZING BEAM-SPLITTER PRISMS

---

**23.** The three classic polarizing beam-splitter prisms are the Rochon, Sénarmont, and Wollaston, shown in perspective in Fig. 10a to c and in side view in Fig. 11a to c. In

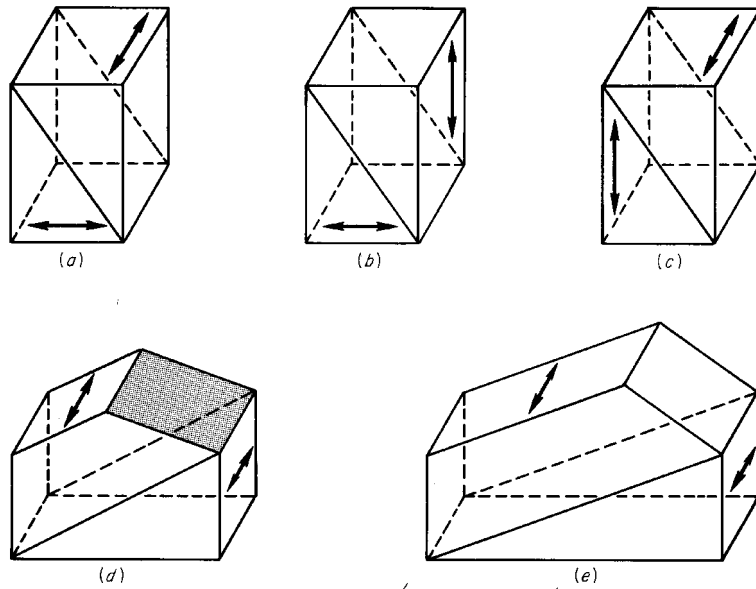


**FIGURE 10** Three-dimensional views of various types of polarizing beam-splitter prisms: (a) Rochon; (b) Sénarmont; (c) Wollaston; (d) Foster (shaded face is silvered); and (e) beam-splitting Glan-Thompson.

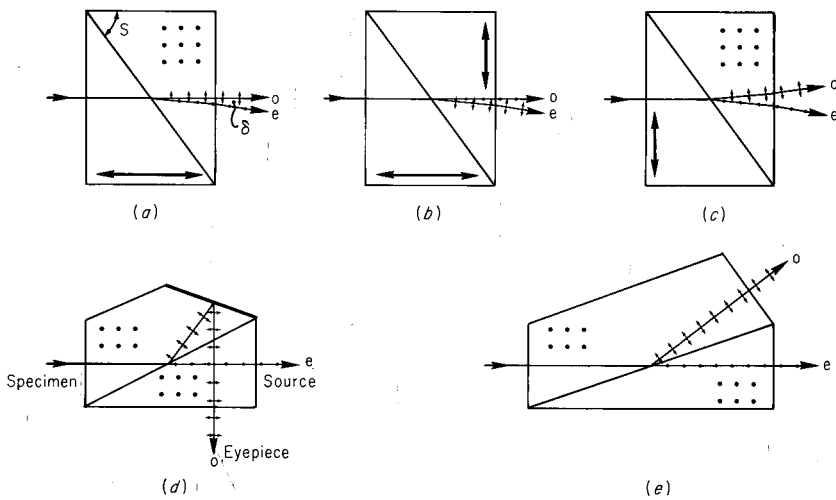


**FIGURE 11** Side views of the polarizing beam-splitter prisms in Fig. 10. The directions of the optic axes are indicated by the dots and the heavy double-pointed arrows. The angle of the cut for the Rochon prism is  $S$ . When the Foster prism is used as a microscope illuminator, the source, specimen, and eyepiece are in the positions indicated.

addition, any polarizing prism can be used as a polarizing beam splitter by changing the shape of one side and removing the absorbing coating from its surface. Two examples of such prisms are the Foster prism, in which the ordinary and extraordinary rays emerge at right angles to each other, and the beam-splitting Glan-Thompson prism, in which the ordinary ray emerges normal to one side (Figs. 10*d* and *e* and 11*d* and *e*). Another prism of this type, the beam-splitting Ahrens prism, is a double beam-splitting Glan-Thompson prism (see Par. 7).

In polarizing prisms, the optic axes are always parallel to each other in the two halves of the prism. By contrast, the optic axes in the two halves of the Rochon, Sénarmont, and Wollaston polarizing beam-splitter prisms are at right angles to each other. Crystal quartz is often used to make these beam splitters, and such prisms can be used down to the vacuum ultraviolet. In applications not requiring such short wavelengths, calcite is preferable because it gives a greater angular separation of the beams (typically 10° as compared to 0.5° for quartz) and does not produce optical rotation.

**24. Rochon Prism** The Rochon prism, invented in 1783,<sup>48</sup> is the most common type of polarizing beam splitter. It is often used in photometric applications in which both beams are utilized. It is also used as a polarizing prism in the ultraviolet, in which case one of the beams must be eliminated, e.g., by imaging the source beyond the prism and blocking off the deviated image.

The paths of the two beams through the prism are shown in Fig. 11*a*. A ray normally incident on the entrance face travels along the optic axis in the first half of the prism, so that both ordinary and extraordinary rays are undeviated and have the same refractive index  $n_o$ . The second half of the prism has its optic axis at right angles to that in the first half, but the ordinary ray is undeviated since its refractive index is the same in both halves. The extraordinary ray, however, has its minimum index in the second half, so that it is refracted at the cut according to Snell's law (see Par. 1). Since the deviation angle depends on the ratio  $n_e/n_o$ , it is a function of wavelength. If the angle of the cut is  $S$ , to a good approximation the beam deviation  $\delta$  of the extraordinary ray depends on the cut angle in the following manner, according to Steinmetz *et al.*,<sup>49</sup>

$$\tan S = \frac{n_o - n_e}{\sin \delta} + \frac{\sin \delta}{2n_e}. \quad (6)$$

This relation holds for light normally incident on the prism face. The semifield angle  $i_{\max}$  is given by<sup>49</sup>

$$\tan i_{\max} = \frac{1}{2}(n_e - n_o) \cot S. \quad (7)$$

If the prism is to be used as a polarizer, the light should be incident as shown. Rochon prisms also act as polarizing beam splitters when used backward, but the deviation of the two beams is then slightly less.

When a Rochon prism is used backward, both the dispersion and the optical activity (for quartz) will adversely affect the polarization. Thus, one generally uses a Rochon in the normal manner. However, an exception occurs when a quartz Rochon is to be used as an analyzer. In this case it is best to reverse the prism and use a detector that is insensitive to polarization to monitor the relative intensities of the two transmitted beams.

A Rochon prism is achromatic for the ordinary ray but chromatic for the extraordinary ray. Since total internal reflection does not occur for either beam, the type of cement used between the two halves of the prism is less critical than that used for conventional polarizing prisms. Canada balsam is generally used, although the two halves are sometimes optically contacted for high-power laser applications or for use in the ultraviolet at wavelengths shorter than 3500 Å. Optically contacted crystalline-quartz Rochon prisms

can be used to wavelengths as short as  $1700 \text{ \AA}$ , and a double Rochon of  $\text{MgF}_2$  has been used to  $1300 \text{ \AA}$  in the vacuum ultraviolet.<sup>49</sup> Optically contacted single Rochon prisms of  $\text{MgF}_2$  have also been constructed, and the transmission of one has been measured from  $1400 \text{ \AA}$  to  $7 \mu\text{m}$ .<sup>50</sup> Ultraviolet-transmitting cements such as *gédamine* can be used to extend the short-wavelength limit of calcite prisms to about  $2500 \text{ \AA}$  (see Par. 5).

**25. Defects** Quartz and calcite Rochon prisms suffer from several defects. Quartz exhibits optical activity when light is transmitted through it parallel to the optic axis, and although two mutually perpendicular, polarized beams will emerge from a quartz Rochon prism used in the conventional direction, their spectral composition will not faithfully reproduce the spectral compositions of the horizontal and vertical components of the input. If such a prism is used backward, different wavelengths emerge from the prism vibrating in different planes. Hence the output consists of many different polarizations instead of the desired two.<sup>51</sup>

Calcite Rochon prisms do not exhibit optical activity but are difficult to make, since when calcite surfaces are cut normal to the optic axis, small tetrahedra tend to cleave out from the surface during pitch polishing. These tetrahedra may also cleave out during attempts to clean the prisms, and occasionally glass plates are cemented to such surfaces to prevent damage. Some image distortion will occur in calcite prisms; if nonnormally incident rays pass through the prism, both beams will be distorted along their directions of vibration; i.e., the undeviated beam (*o* ray), which vibrates in a vertical plane, will be distorted vertically, and the deviated beam (*e* ray), which vibrates in a horizontal plane, will be distorted horizontally.<sup>51</sup>

**26. Glass-Calcite Rochons** Some of the difficulties mentioned in Par. 25 can be minimized or eliminated by making the entrance half of the Rochon prism out of glass of matching index instead of quartz or calcite. Both *o* and *e* rays travel along the same path and have the same reflective index in this half of the prism, so that the birefringent qualities of the quartz or calcite are not being used and an isotropic medium would serve just as well. By properly choosing the index of the glass, either the ordinary or the extraordinary ray can be deviated, and glasses are available for matching either index of calcite reasonably well over much of the visible region.<sup>51</sup> The extraordinary ray always suffers some distortion in its direction of vibration, but the distortion of the ordinary ray can be eliminated in the glass-calcite construction. By properly choosing the refractive index of the glass, we can determine whether the *e* ray will be the deviated or the undeviated beam. (Some distortion also arises for deviated beams in the direction of the deviation because of Snell's law and cannot be corrected in this way.) Another method of obtaining an undeviated beam was used by Hardy;<sup>52</sup> unable to find a glass with refractive index and dispersion matching those of calcite, he selected a glass with the correct dispersive power and then compensated for the difference in refractive index by putting a slight wedge angle on the calcite surface. Now a wider selection of glasses is available, but glass-calcite prisms cannot be made strictly achromatic over an extended wavelength range, and thermally induced strains caused by the difference in expansion coefficients in the two parts of the prism may be expected unless the cement yields readily.

**27. Total Internal Reflection in Rochons** When normal Rochon prisms are used as polarizers, one of the beams must be screened off and eliminated. This restriction might be removed by making the cut between halves of the prism at a sufficiently small angle for the extraordinary ray to be totally reflected. Calculations indicate that this approach should be feasible,<sup>53</sup> but it has apparently not been followed.

**28. Sénarmont Prism** The Sénarmont polarizing beam splitter, shown in Figs. 10*b* and 11*b*, is similar to the Rochon prism except that the optic axis in the exit half of the prism is coplanar with the optic axis in the entrance half, i.e., at right angles to the Rochon

configuration. As a result, light whose plane of vibration is initially vertical is deviated in the Sénarmont prism, while in the Rochon prism the deviated beam has its plane of vibration horizontal (assuming no optical activity in either case) (compare Fig. 11*a* and *b*). The amount of the deviation in the Sénarmont prism is slightly less than in the Rochon because the extraordinary ray does not have its minimum refractive index [Eq. (1)].

An alternate form of Sénarmont prism, the right-angle Sénarmont or Cotton polarizer,<sup>54</sup> consists of only the first half of the Sénarmont prism. Unpolarized light normally incident on the prism face is totally internally reflected at the hypotenuse and is then resolved into two planes of vibration, one parallel to the optic axis and the other perpendicular to it. Double refraction will then occur just as in a normal Sénarmont prism. Such a prism has a transmission equivalent to that of an optically contacted Sénarmont or Rochon but is much less expensive.

**29. Wollaston Prism** The Wollaston prism (Figs. 10*c* and 11*c*) is a polarizing beam splitter, also used as a polarizing prism in the vacuum ultraviolet,<sup>55</sup> that deviates both transmitted beams. The deviations, indicated in Fig. 11*c*, are nearly symmetrical about the incident direction, so that the Wollaston has about twice the angular separation of a Rochon or Sénarmont prism. A normally incident beam is undeviated upon entering the prism, but the *o* ray, vibrating perpendicular to the optic axis, has a refractive index  $n_o$  while the *e* ray, vibrating parallel to the optic axis has its minimum (or principal) index  $n_e$ . At the interface the *e* ray becomes the *o* ray and vice versa because the direction of the optic axis in the second half is perpendicular to its direction in the first half. Thus the original *o* ray enters a medium of lower refractive index and is refracted away from the normal at the cut, while the original *e* ray passes into a medium of higher refractive index and is refracted toward the normal. On leaving the second half of the prism, both rays are refracted away from the normal, so that their divergence increases.

The deviation of each beam is chromatic in Wollaston prisms, which are most commonly used to determine the relative intensities of two plane-polarized components. Since the light never travels along the optic axis, optical activity does not occur and the relative intensities of the two beams are always proportional to the intensities of the horizontal and vertical polarization components in the incident beam. For an  $L/A$  ratio of 1.0, the angular separation between beams is about  $1^\circ$  for a crystalline-quartz Wollaston prism; it can be as high as  $3^\circ 30'$  for an  $L/A$  ratio of 4.0. With a calcite prism, the beams would have an angular separation of about  $19^\circ$  for an  $L/A$  ratio of 1.0, but severe image distortion and lateral chromatism results when such large angular separations are used. These effects can be minimized or the angular separation can be increased for a given  $L/A$  ratio by using a three-element Wollaston prism, a modification, apparently suggested by Karl Lambrecht.<sup>30</sup> Divergences as large as  $30^\circ$  can be obtained.<sup>1</sup>

The ellipticity in the emergent polarized beams has been measured by King and Talim.<sup>25</sup> For calcite Wollaston prisms, the ellipticities were in the  $0.004$  to  $0.025^\circ$  range, comparable to those of Glan-Thompson prisms (Par. 13). Larger values, between  $0.12$  and  $0.16^\circ$ , were measured for crystalline-quartz Wollaston prisms. The major contribution, which was from the combined optical activity and birefringence in the quartz rather than from defects within the crystal, cannot be avoided in quartz polarizers.

**30. Foster Prism** This prism, shown in a three-dimensional view in Fig. 10*d* and in cross section in Fig. 11*d*, can be used to form two plane-polarized beams separated by  $90^\circ$  from each other.<sup>56</sup> Its construction is similar to that of a Glan-Thompson prism except that one side is cut at an angle and silvered to reflect the ordinary ray out the other side.

The Foster prism is often used backward as a polarizing microscope illuminator for observing reflecting specimens. For this application, the light source is at *e* in Fig. 11*d*, and unpolarized light enters the right-hand face of the prism. The ordinary ray (not shown) is reflected at the cut and absorbed in the blackened side of the prism, while the extraordinary ray is transmitted undeviated out the left face of the prism. It then passes

through the microscope objective and is reflected by the specimen, returning on its same path to the prism. Light that is unchanged in polarization will be transmitted undeviated by the prism along the path to the light source. If, however, the plane of vibration has been rotated so that it is at right angles to the optic axis (in the plane of the figure), the light will be reflected into the eyepiece. The prism thus acts like a crossed polarizer-analyzer combination.

If a correctly oriented quarter-wave plate is inserted in the beam between the prism and the microscope objective, the light striking the sample will be circularly polarized, and, after being reflected back through the quarter-wave plate, it will be linearly polarized again but with the plane of vibration rotated by  $90^\circ$ . This light is vibrating perpendicular to the optic axis and will be reflected into the eyepiece, giving bright-field illumination. Foster prisms used in this manner introduce no astigmatism since the light forming the image enters and leaves the prism normal to the prism faces and is reflected only by plane surfaces.

**31. Beam-splitting Glan-Thompson Prism** If a prism design similar to the Foster is used but the side of the prism is cut at an angle so that the ordinary ray, which is deflected, passes out normal to the surface of the prism rather than being reflected, the prism is called a beam-splitting Glan-Thompson prism (Figs. 10e and 11e). Since no refraction occurs for either beam, the prism is achromatic and nearly free from distortion. The angle between the two emerging beams is determined by the angle of the cut between the two halves of the prism and hence depends on the  $L/A$  ratio of the prism. For an  $L/A$  ratio of 2.414, the angle is  $45^\circ$ . The field angle around each beam is calculated for different  $L/A$  ratios just as for a conventional Glan-Thompson prism. By making the prism double, i.e., a beam-splitting Ahrens prism, the incident beam can be divided into three parts, one deflected to the left, one to the right, and one undeviated.

**32. Feussner Prisms** The polarizing prisms discussed so far require large pieces of birefringent material, and the extraordinary ray is the one usually transmitted. Feussner<sup>57</sup> suggested an alternate prism design in which only thin plates of birefringent material are required and the ordinary ray rather than the extraordinary ray is transmitted for negative uniaxial materials. A similar suggestion was apparently made by Sang in 1837, although he did not publish it until 1891.<sup>58</sup> In essence, Feussner's idea was to make the prisms isotropic and the film separating them birefringent, as shown in Fig. 12. The isotropic prisms should have the same refractive index as the higher index of the birefringent material so that for negative uniaxial materials, e.g., calcite or sodium nitrate, the ordinary ray is transmitted and the extraordinary ray totally internally reflected. Advantages of this design are (1) since the ordinary ray is transmitted, the refractive index does not vary with angle of incidence and hence the image is anastigmatic, (2) large field angles or prisms of compact size can be obtained, and (3) the birefringent material is used economically.

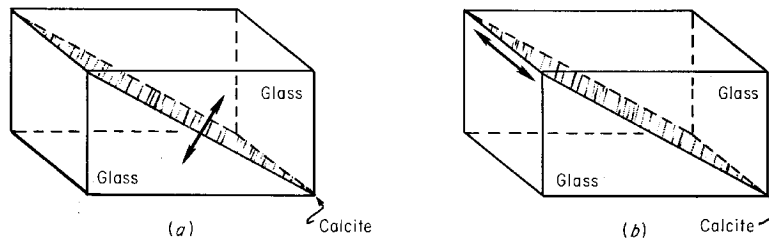


**FIGURE 12** Types of Feussner prisms: (a) original Feussner prism and (b) Bertrand type. The arrows indicate the orientation of the optic axis in the calcite (or other birefringent material).

Furthermore, because the path length of the ray through the birefringent material is short, a lower-quality material can be used.

Disadvantages are (1) for both calcite and sodium nitrate, the extraordinary ray is transmitted over a larger wavelength range than the ordinary ray so that Feussner prisms do not transmit over as large a wavelength range as conventional prisms, and (2) the thermal-expansion coefficients of the isotropic and birefringent materials are different, making thermally induced strains likely. Solutions to the second problem are to use a thixotropic cement, which flows more readily with increasing stress, or to enclose the system in a metal sleeve and use oil instead of cement. If the ordinary index is matched by the oil, the birefringent material does not even need to be polished very well. Even a cleavage section of calcite can be used, with only a tolerable loss in angular field.<sup>59</sup>

Feussner suggested orienting the optic axis of the birefringent slab perpendicular to the cut, as indicated in Fig. 12*a*. Since the thermal expansion of the slab is the same in all directions perpendicular to the optic axis, thermally induced strains are minimized in this way. Field angles for Feussner prisms employing calcite and sodium nitrate slabs are given in the earlier Polarization chapter.<sup>1</sup>

Shortly after Feussner's article was published, Bertrand<sup>60</sup> pointed out that the optic axis of the birefringent slab should be parallel to the entrance face of the prism to give the maximum difference between the refractive indices of the ordinary and extraordinary rays. A prism made in this way, sometimes called a Bertrand-type Feussner prism, is shown in Fig. 12*b*.

Since sodium nitrate is easily obtainable and has a birefringence even larger than that of calcite, attempts have been made to produce polarizing prisms of this material by Wulff,<sup>61</sup> Stöber,<sup>62-64</sup> Tzekhovitzer,<sup>65</sup> West,<sup>66</sup> Huot de Longchamp,<sup>67</sup> and Yamaguti.<sup>68,69</sup> However, it is not only deliquescent but also very soft, so that although large single crystals can be obtained, they are difficult to work. They can be crystallized in the desired orientation from a melt using a technique discovered by West.<sup>66</sup> When sodium nitrate crystallizes from a melt on a mica cleavage surface, one of its basal planes is oriented parallel to the mica cleavage and hence its optic axis is perpendicular to the mica surface. West reports growing single crystals as large as  $38 \times 19 \times 2$  cm using this technique. Yamaguti<sup>68,69</sup> has produced polarizing prisms of sodium nitrate by placing thin, closely spaced glass plates on edge on a mica sheet and then immersing the assembly in a melt of sodium nitrate. The thin single crystal thus formed was annealed and cemented between glass prisms to form a Bertrand-type Feussner prism. Conceivably, the sodium nitrate could have been grown directly between the glass prisms themselves, but when such thick pieces of glass are used, it is difficult to avoid setting up strains in the crystal and consequently reducing the polarization ratio. Yamaguti used SK5 glass prisms ( $n_D = 1.5889$ ) cut at an angle of  $23^\circ$  to form his polarizing prism and reports a field of view of  $31^\circ$ , symmetric about the normal to the entrance face.

Another possible birefringent material suitable for a Feussner prism is muscovite mica, and such prisms have actually been constructed and tested.<sup>70,71</sup> A  $6^\circ$  field angle can be obtained,<sup>59</sup> which is adequate for many optical systems illuminated by lasers.

## Noncalcite Polarizing Prisms

**33.** Polarizing prisms made of materials other than calcite have been used primarily in the ultraviolet region at wavelengths for which calcite is opaque. Prism materials used successfully in this region include crystalline quartz, magnesium fluoride, sodium nitrate, and ammonium dihydrogen phosphate. Rutile polarizing prisms have been used beyond the calcite cutoff in the infrared. A new prism material, yttrium orthovanadate, has been used to make high-transmission polarizers for the visible and near-infrared spectral regions.<sup>72</sup> Properties of this material were described in the earlier Polarization chapter.<sup>1</sup>

Rochon or Wollaston prisms (Pars. 24 and 29) are sometimes made of crystalline

quartz for use in the far ultraviolet. The short-wavelength cutoff of the quartz is variable, depending on the impurities present, but can be as low as 1600 Å.

By utilizing magnesium fluoride instead of quartz for the polarizing prisms, the short-wavelength limit can be extended to 1300 Å. Magnesium fluoride transmits to about 1125 Å, but below 1300 Å its birefringence decreases rapidly and changes sign at 1194 Å.<sup>55,73</sup> Although it is the most birefringent material available in this region, MgF<sub>2</sub> has a much smaller birefringence than that of calcite; hence, a small cut angle and large  $L/A$  ratio for the prism are unavoidable. Since absorption does occur, it is desirable to minimize the length of the prism. Johnson<sup>55</sup> solved this problem by constructing a MgF<sub>2</sub> Wollaston prism which requires only half the path length necessary for a Rochon prism. However, both beams are deviated, creating instrumental difficulties.

Steinmetz *et al.*<sup>49</sup> constructed a double Rochon prism of MgF<sub>2</sub> which has the same  $L/A$  ratio as the Wollaston prism but does not deviate the desired beam. Problems with the prism included fluorescence, scattered light, and nonparallelism of the optic axes.<sup>1</sup> In principle, however, a MgF<sub>2</sub> double Rochon polarizing prism should be an efficient, high-extinction-ratio, on-axis polarizer for the 1300- to 3000-Å wavelength range and should also be useful at longer wavelengths. Morris and Abramson<sup>50</sup> reported on the characteristics of optically contacted MgF<sub>2</sub> single Rochon prisms.

A different type of polarizer suggested by Chandrasekharan and Damany<sup>74</sup> to take the place of a Rochon or Wollaston prism in the vacuum ultraviolet consisted of a combination of two MgF<sub>2</sub> lenses, one planoconcave and the other planoconvex of the same radius of curvature, combined so that their optic axes were crossed. The combination acted as a convergent lens for one polarization and as a divergent lens for the other. It had the advantage that the polarized beam remained on axis and was focused. A measured degree of polarization of 98.5 percent was obtained at 1608 Å, in good agreement with the calculated value.

Prism polarizers can also be constructed for use in the infrared at wavelengths longer than those transmitted by calcite. Rutile, TiO<sub>2</sub>, a positive uniaxial mineral with a large birefringence and good transmittance to 5 μm in the infrared, has been used by Landais<sup>75</sup> to make a Glan-Foucault-type crystal polarizer. Since rutile has a positive birefringence (in contrast to the negative birefringence of calcite), the ordinary ray is transmitted undeviated and the extraordinary ray is reflected out one side. Other characteristics are given in the earlier Polarization chapter.<sup>1</sup>

## DICHROIC AND DIFFRACTION-TYPE POLARIZERS

---

**34.** Some of the most useful polarizers available employ either dichroism or diffraction effects. These polarizers come in sheet form, sometimes in large sizes, are easily rotated, and produce negligible beam deviation. Also, they are thin, lightweight, and rugged, and most can be made in any desired shape. The cost is generally much less than that of a prism-type polarizer. Furthermore, both types are insensitive to the degree of collimation of the beam, so that dichroic or diffraction-type polarizers can be used in strongly convergent or divergent light.

A dichroic\* material is one which absorbs light polarized in one direction more strongly than light polarized at right angles to that direction. Dichroic materials are to be distinguished from birefringent materials, which may have different refractive indexes for the two electric vectors vibrating at right angles to each other but similar (usually

---

\* The term *dichroic* is also used in three other ways: (1) to denote the change in color of a dye solution with change in concentration, (2) to denote a color filter that has two transmission bands in very different portions of the visible region and hence changes color when the spectral distribution of the illuminating source is changed, and (3) to denote an interference filter that appears to be of a different color when viewed in reflected or transmitted light.

negligible) absorption coefficients. Various materials are dichroic, either in their natural state or in a stretched condition. The most common materials used as dichroic polarizers are stretched polyvinyl alcohol sheets treated with absorbing dyes or polymeric iodine, commonly marketed under the trade name Polaroid. These and similar materials are discussed in Par. 35. Another type of dichroic polarizer is prepared by rubbing a glass or plastic surface in a single direction and then treating it with an appropriate dye. Polarizers of this type are sold under the trade name Polacoat and will be described in Par. 36. In certain portions of the infrared spectral region, calcite is strongly dichroic and makes an excellent high-extinction polarizer.<sup>76</sup> Pyrolytic graphite is electrically and optically anisotropic and has been successfully used as an infrared polarizer; it is described in Par. 37. Other materials which exhibit dichroism in the infrared include single-crystal tellurium,<sup>77</sup> ammonium nitrate,<sup>78</sup> mica, rubber under tension, polyvinyl alcohol, and polyethylene.<sup>79</sup> In the visible region, gold, silver, and mercury in the form of microcrystals,<sup>80</sup> needles of tellurium,<sup>81</sup> graphite particles,<sup>82</sup> and glasses containing small elongated silver particles<sup>83</sup> are all dichroic.

A sodium nitrate polarizer described by Yamaguti<sup>84</sup> is not dichroic in the strict sense of the word but acts like a dichroic polarizer. Roughened plates of SK5 glass are bonded together by a single crystal of sodium nitrate, which has a refractive index for the ordinary ray nearly equal to that of the glass. The extraordinary ray has a much lower index, so that it is scattered out of the beam by the rough surfaces, leaving the ordinary ray to be transmitted nearly undiminished. (Yamaguti has also made Feussner prisms out of single-crystal sodium nitrate described in Par. 32.)

Diffraction-type polarizers include diffraction gratings, echelettes, and wire grids. These are all planar structures that have properties similar to those of dichroic polarizers except that they transmit one component of polarization and reflect the other when the wavelength of the radiation is much longer than the grating or grid spacing. Wire grid and grating polarizers are covered in Par. 38.

None of these polarizers has as high a degree of polarization as the prism polarizers of Pars. 1 to 33. Thus it is frequently necessary to measure the polarizing properties of the particular polarizer used. A source of plane-polarized light is desirable for such a measurement. Lacking that, one of the procedures described in Par. 39 can be followed if there are two identical imperfect polarizers. Alternate methods are also described which are applicable to two nonidentical imperfect polarizers.

**35. Sheet Polarizers** Various types of sheet polarizers have been developed by Edwin H. Land and coworkers at the Polaroid Corporation, Cambridge, Mass. Sheet polarizers are also available from several European companies. The J sheet polarizer, the first type available in America (around 1930), consisted of submicroscopic needles of herapathite oriented parallel to one another in a sheet of cellulose acetate. Since this type of polarizer, being microcrystalline, had some tendency to scatter light, it was superseded by H and K sheet molecular polarizers, which exhibit virtually no scattering. The most widely used sheet polarizer is the H type, which consists of a sheet of polyvinyl alcohol that has been unidirectionally stretched and stained with iodine in a polymeric form. The K type is made by heating a sheet of polyvinyl alcohol in the presence of a catalyst to remove some of the water molecules and produce the dichromophore polyvinylene. It was developed primarily for applications where resistance to high temperature and high humidity are necessary. Another type of polarizing sheet, made from a combination of the H and K types, has an absorption maximum at about 1.5  $\mu\text{m}$  in the infrared and is designated as HR Polaroid.

The history of the development of the various kinds of sheet polarizers has been given by Land,<sup>81</sup> their chemical composition by Land and West,<sup>80</sup> and their optical performance by Shurcliff,<sup>82</sup> Baumeister and Evans,<sup>85</sup> Land and West,<sup>80</sup> and Land.<sup>81</sup> In addition, Blake *et al.*<sup>86</sup> mention the HR infrared polarizer, and Makas<sup>87</sup> describes the modified H-film polarizer for use in the near ultraviolet. Baxter *et al.*<sup>88</sup> describe a technique for measuring

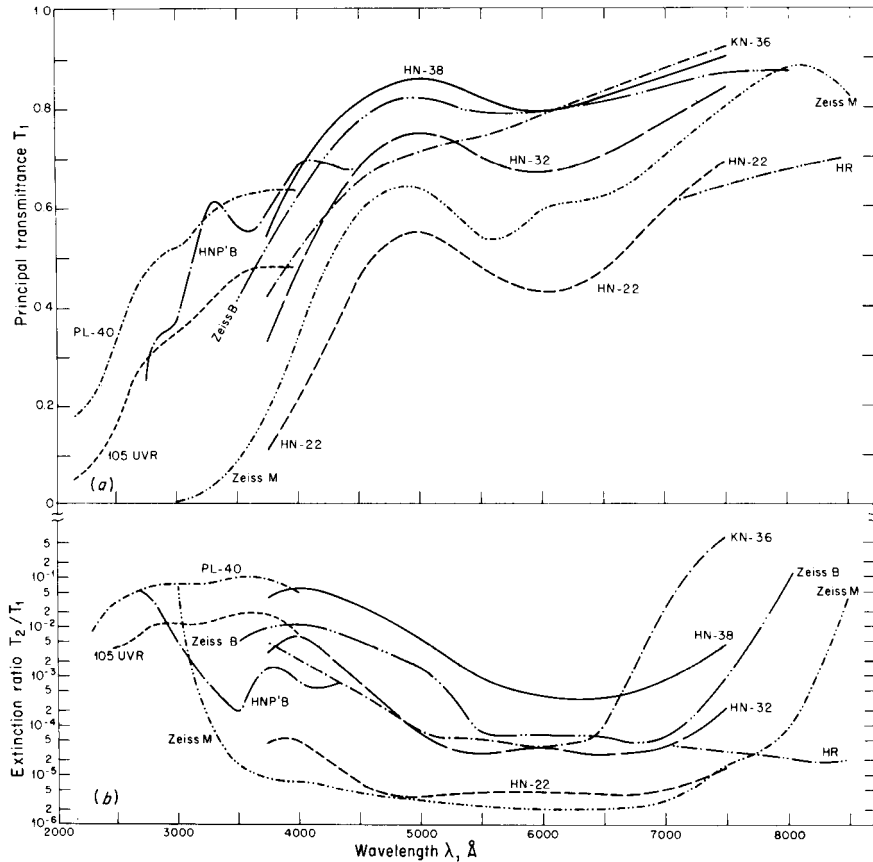


**FIGURE 13** (a) Principal transmittance and (b) extinction ratio for various types of dichroic polarizers: Polaroid sheet polarizers HN-22, HN-32, HN-38, and KN-36; Zeiss (Oberkochen) Bernotar and Micro Polarization filters; and Polacoat PL-40 and 105 UVR polarizing filters. The last is stated to have a transmittance (for unpolarized light) of 32 percent at 5460 Å. (Modified from curves of Shurcliff, Ref. 82, Baumeister and Evans, Ref. 85, Jones, Ref. 89, Haase, Ref. 90, and McDermott and Novick, Ref. 91.)

the optical density of high-extinction polarizers in the presence of instrumental polarization.

Figure 13 shows the principal transmittance  $T_1$  and extinction ratio  $T_2/T_1$  of various types of H and K sheet polarizers used in the visible and near ultraviolet.<sup>82,85,89</sup> In addition, curves for two sheet polarizers manufactured by Zeiss and two types of polarizing filters from Polacoat (Par. 36) are shown. The letter N in the designation of the Polaroid sheets stands for neutral (to distinguish them from sheet polarizers prepared from colored dyes), and the number 22, 32, etc., indicates the approximate transmittance of unpolarized visible light. Figure 14 gives the principal transmittance and extinction ratio of a typical plastic laminated HR infrared polarizer.<sup>82,89</sup> Sometimes the optical density  $D$  of a polarizer is plotted instead of its transmittance. The relation between these two quantities is

$$D = \log \frac{1}{T} \quad (8)$$

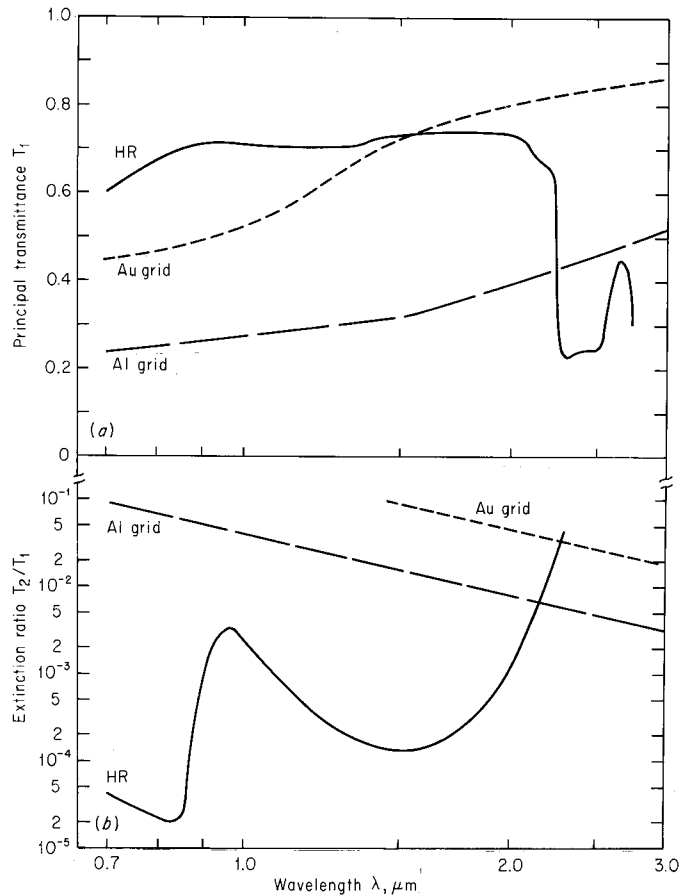


**FIGURE 14** (a) Principal transmittance and (b) extinction ratio for plastic laminated HR infrared polarizer (modified from curves of Shurcliff, Ref. 82, and Jones, Ref. 89) and two wire grid polarizers with 0.463- $\mu\text{m}$  grating spacings (Bird and Parrish, Ref. 92).

The extinction ratio of the HN-22 Polaroid compares favorably with that of Glan-Thompson prisms throughout the visible region, but the transmission of the Glan-Thompson is superior. In the ultraviolet, the new HNP'B material has a reasonably good extinction ratio (about  $10^{-3}$  or better) for wavelengths longer than 3200  $\text{\AA}$ . It is a specially purified form of HN-32, and its properties match those of the standard HNT-32 Polaroid at wavelengths longer than 4500  $\text{\AA}$ . Optical properties of various types of Polaroid dichroic polarizers have been described by Trapani.<sup>93</sup> According to West and Jones,<sup>48</sup> the extinction ratio for a dichroic polarizer of the Polaroid type has a practical limit of about  $10^{-5}$  because, as the concentration of dichromophore is increased beyond a certain value, the optical density no longer increases proportionately. Gunning and Foschaar<sup>94</sup> have described a method for the controlled bleaching of the iodine dichromophore in iodine-polyvinyl alcohol polarizers to achieve an increased internal transmission of up to 95 percent for the principal transmittance of linearly polarized light in the 5000- to 6000- $\text{\AA}$  wavelength region. This is achieved at the expense of degrading the extinction ratio and

drastically affecting the short wavelength performance of the polarizer. Baum<sup>95</sup> describes the application of sheet polarizers to liquid crystal displays and problems encountered in this application.

If Polaroids are used in applications where beam deviation is important, they should be checked for possible deviation. Most Polaroids, which are laminated in plastic sheets, do produce a slight beam deviation that can be observed through a telescope as a shift in the image position when the Polaroid is rotated. The amount of the deviation varies from point to point on the Polaroid and can be much worse if the material is mounted between glass plates. It is possible to order specially selected sheet Polaroid laminated between polished glass plates that deviates the beam by only about 5 seconds of arc.

Sheet polarizers made of stretched polyvinyl alcohol that has been stained with iodine or various dyes are also made in countries outside the United States, as described in the earlier Polarization chapter.<sup>1</sup>

King and Talim<sup>25</sup> have measured the axis wander and ellipticity of beams transmitted by various types of sheet polarizers in the same way as for Glan-Thompson prisms, (Par. 13). They found considerable variations from one type of sheet polarizer to another and also over a single sheet. Details are given in the earlier chapter on Polarization.<sup>1</sup>

**36. Dichroic Polarizing Coatings** Beilby-layer polarizers<sup>82</sup> are dichroic coatings that can be applied to the surface of glass or plastic. The process was developed by Dreyer,<sup>96</sup> who founded the company which manufactures Polacoat polarizing filters. There are three main steps in the production of these polarizers. First, the substrate (quartz, glass, plastic, etc.) is rubbed along parallel lines with filter paper, cotton, or rouge to produce a preferred surface orientation. (The affected region of minute scratches extends to a depth of less than 1  $\mu\text{m}$ .) Then the sheet is rinsed and treated with a solution of dichroic molecules, e.g., a 0.5 percent solution of methylene blue in ethanol or one or more azo dyes, and then dried in a controlled fashion. Presumably the molecules line up preferentially along the rubbing direction, resulting in a greater absorption for light, polarized in that direction. As a final step, the surface is treated with an acidic solution, often that of a metallic salt such as stannous chloride, which can increase the dichroism and produce a more neutral color. A protective coating over the polarized surface provides mechanical protection for the fragile layer with no loss in transmission. McDermott and Novick<sup>91</sup> give a somewhat more complete description of the Polacoat process, and Anderson<sup>97</sup> has investigated the absorption of methylene blue molecules on a unidirectionally polished surface. References to patents and related work are given by Shurcliff.<sup>82</sup>

The principal transmittance and extinction ratio of two standard Polacoat coatings, PL-40 and 105 UVR (32 percent transmission of unpolarized light at 5460  $\text{\AA}$ ), are shown in Fig. 13. These curves are taken from the data of McDermott and Novick.<sup>91</sup> Polacoat 105 UVR coating comes in various densities; the data shown are for the highest-density material with the best extinction ratio.\* A major advantage of Polacoat over sheet Polaroid is that it does not bleach upon exposure to intense ultraviolet radiation.

Kyser<sup>99</sup> tested a stock PL40 polarizing filter on fused quartz and found that it produced a large quantity of scattered light of the unwanted component. This light was dispersed spectrally and was scattered at angles up to about 20° as though the scratches on the rubbed surface were acting like rulings on a diffraction grating. There was relatively little of the unwanted component on axis; most of it was scattered at larger angles. Despite these difficulties, Polacoat PL40 polarizers appear to be the best large-aperture transmission-type polarizers available for work in the 2000- to 3000- $\text{\AA}$  wavelength range in the ultraviolet.

---

\* The company literature<sup>98</sup> is somewhat misleading in that the transmittance of this material is stated to be 35 percent, but the transmission curve (for unpolarized light) given in the bulletin does not rise above 30 percent until the wavelength becomes longer than 6500  $\text{\AA}$ .

**37. Pyrolytic-Graphite Polarizers** Pyrolytic graphite has a large anisotropy in both the electric conductivity and in the optical properties. If the  $E$  vector of an electromagnetic wave is pointing in the direction of the  $c$ -axis of the graphite, the absorption coefficient is a minimum, the reflectance is also a minimum, and hence the transmittance is a maximum. If the  $E$  vector lies in the plane perpendicular to the  $c$  direction, the absorption is a maximum, reflectance is a maximum, and transmittance is a minimum. Thus, pyrolytic graphite should be a good material from which to make a dichroic polarizer if a thin foil is cut and polished to contain the  $c$ -axis. Several such polarizers have been made by Rupprecht *et al.*<sup>100</sup>; two had thicknesses of  $9.2\ \mu\text{m}$ , and a third was  $4.2\ \mu\text{m}$  thick. The transmittances  $T_1$  of the thinner one and  $T_1$  and  $T_2$  of the two thicker ones were determined using one of the methods described in Par. 49 of the earlier Polarization chapter.<sup>1</sup> The principal transmittance and extinction ratio for one of the  $9.2\text{-}\mu\text{m}$ -thick ones are shown in Fig. 15 for infrared wavelengths from 2 to  $16\ \mu\text{m}$ , along with curves for various wire-grid polarizers (Par. 38). In the far infrared out to  $600\ \mu\text{m}$ ,  $T_1$  gradually increases to 0.50, and  $T_2/T_1$  drops down to the  $10^{-3}$  range.<sup>100</sup> The transmittance of the thinner pyrographite polarizer was larger than the curve shown, but its extinction ratio, although not given, was probably poorer. Pyrolytic-graphite polarizers have the advantages of being planar and thus easily rotatable, having large acceptance angles, and having reasonably high

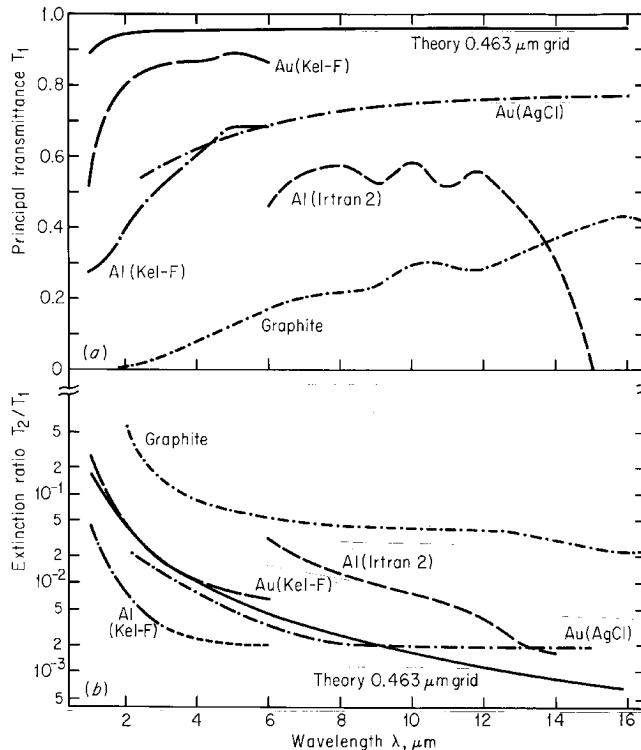


**FIGURE 15** (a) Principal transmittance and (b) extinction ratio for a pyrolytic-graphite polarizer (Rupprecht *et al.*, Ref. 100) and various wire-grid polarizers (Bird and Parrish, Ref. 92, Perkin-Elmer, Ref. 101 and Young *et al.*, Ref. 102). The substrate materials and metals used for the grids are indicated. Theoretical curves (solid lines) calculated from relations given in Ref. 1 with  $n = 1.5$  and  $d = 0.463$  are also shown for comparison.

transmittances and good extinction ratios in the far infrared. However, in the shorter-wavelength region shown in Fig. 15, they are inferior to all the wire-grid polarizers. In addition, they are fragile, and the largest clear aperture obtained by Rupprecht *et al.*<sup>100</sup> was about 12 mm diameter.

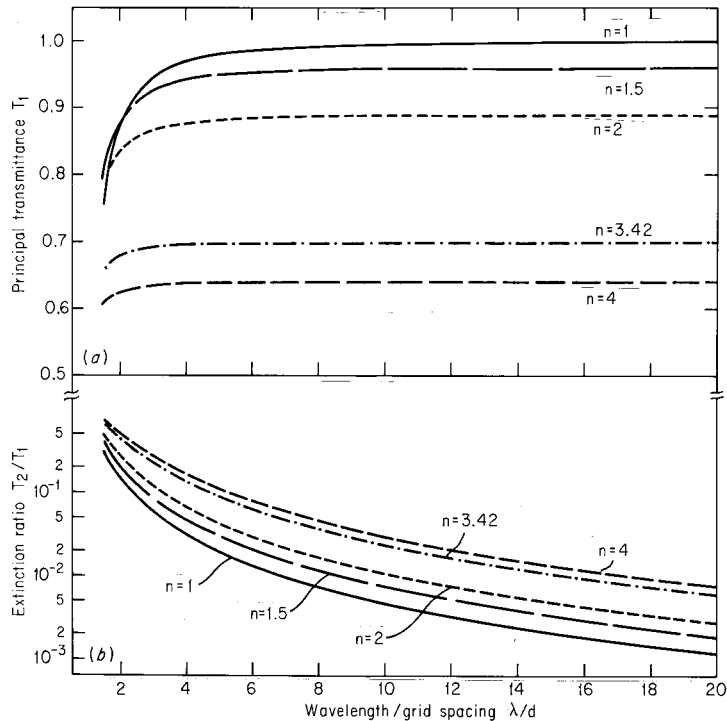
**38. Wire-Grid and Grating Polarizers** Wire grids\* have a long history of use as optical elements to disperse radiation and detect polarization in far-infrared radiation and radio waves.<sup>92</sup> They transmit radiation whose  $E$  vector is vibrating perpendicular to the grid wires and reflect radiation with the  $E$  vector vibrating parallel to the wires when the wavelength  $\lambda$  is much longer than the grid spacing  $d$ . When  $\lambda$  is comparable to  $d$ , both components are transmitted. For grids made of good conductors, absorption is negligible. Various aspects of the theory of reflection and transmission of radiation by wire grids are summarized in the earlier Polarization chapter.<sup>1</sup> In addition to that theoretical treatment, Casey and Lewis<sup>104,105</sup> considered the effect of the finite conductivity of the wires on the transmission and reflection of wire-grid polarizers when the light was polarized parallel to the wires. Mohebi, Liang, and Soileau<sup>106</sup> extended the treatment to the case for which light was polarized both parallel and perpendicular to the wires; they also calculated the absorption of the wire grids as a function of  $d/\lambda$ . In addition, they measured the absorption and surface damage of wire-grid polarizers consisting of aluminum strips (0.84  $\mu\text{m}$  period) deposited on ZnSe substrates at 10.6  $\mu\text{m}$ , 1.06  $\mu\text{m}$ , and 0.533  $\mu\text{m}$ . Stobie and Dignam<sup>107</sup> calculated the amplitude transmission coefficients for parallel and perpendicular components and relative phase retardation between them, both as a function of  $\lambda/d$ . Burton<sup>108</sup> proposed using wire-grid polarizers in the form of cylinders and paraboloids instead of planar structures in infrared interferometers, but did not show any experimental measurements.

Figure 16 shows values of the calculated principal transmittance and extinction ratio for various values of the refractive index  $n$  as a function of  $\lambda/d$ . These curves were calculated from relations given in the earlier Polarization chapter.<sup>1</sup> It is clear that the shortest wavelength for which a given grid will act as a useful polarizer is  $\lambda \approx 2d$ . Also, the best performance is obtained with the lowest refractive index substrate. Since absorption in the substrate material has been neglected, principal transmittances measured for real materials will be lower than the calculated values, but the extinction ratios should be unaffected. If one must use a high refractive index substrate such as silicon or germanium, the performance of the grid can be considerably improved by applying an antireflection coating to the substrate *before* depositing the conducting strips, since a perfectly antireflected substrate acts like an unsupported grid.<sup>109</sup> However, if the antireflecting layer is laid down *over* the grid strips, the performance of the wire grid polarizer is degraded.<sup>1</sup>

Many people have built and tested wire-grid polarizers including Bird and Parrish,<sup>92</sup> Young *et al.*,<sup>102</sup> Hass and O'Hara,<sup>110</sup> Hilton and Jones,<sup>111</sup> Auton,<sup>109</sup> Vickers *et al.*,<sup>112</sup> Cheo and Bass,<sup>113</sup> Auton and Hutley,<sup>114</sup> Costley *et al.*,<sup>115</sup> Beunen *et al.*,<sup>116</sup> Leonard,<sup>117</sup> Sonek *et al.*,<sup>118</sup> Eichhorn and Magner,<sup>119</sup> and Novak *et al.*<sup>120</sup> In addition, two types of wire grids are manufactured commercially by Buckbee Mears (see Ref. 110) and Perkin-Elmer,<sup>101</sup> and a third type composed of 152- $\mu\text{m}$ -diameter tungsten wires spaced 800 to the inch has been mentioned, but no performance characteristics have been given.<sup>121</sup> Hwang and Park<sup>122</sup> measured the polarization characteristics of two-dimensional wire mesh (64  $\mu\text{m}$  and 51  $\mu\text{m}$  spacings) at a laser wavelength of 118.8  $\mu\text{m}$ . The different wire-grid polarizers are listed in Table 2, and the principal transmittances and extinction ratios of several are shown in Figs 14 and 15.

The polarizers with grid spacings of 1.69  $\mu\text{m}$  and less were all made by evaporating the grid material at a very oblique angle onto a grating surface which had been prepared

\* *Wire grid* is being used here, as is customary, to denote a planar structure composed of a series of parallel wires or strips. Renk and Genzel<sup>103</sup> and a few others use the term to designate a two-dimensional array with two series of elements arranged at right angles to each other. They call a one-dimensional array a wire or strip grating.



**FIGURE 16** (a) Principal transmittance and (b) extinction ratio as a function of  $\lambda/d$  calculated from relations given in Ref. 1 for various values of  $n$  for the substrate. Substrate indexes correspond approximately to an antireflected substrate of air, organic plastic, silver chloride, silicon, and germanium.

either by replicating a diffraction grating with the appropriate substrate material (silver bromide, Kel-F, polymethyl methacrylate, etc.) or by ruling a series of lines directly onto the substrate (Irtran 2 and Irtran 4). The oblique evaporation (8 to 12° from the surface) produced metallic lines on the groove tips which acted like the conducting strips of the theory, while the rest of the surface was uncoated and became the transparent region between strips. Larger grid spaces (4 to 25.4  $\mu\text{m}$ ) were produced by a photoetching process, and one 25.4- $\mu\text{m}$  grid was made by an electroforming process. Still larger grid spacings were achieved by wrapping wires around suitable mandrels.

If a wire-grid polarizer is to be used in the near infrared, it is desirable to have the grid spacing as small as possible. Bird and Parrish<sup>92</sup> succeeded in obtaining a very good extinction ratio in the 2- to 6- $\mu\text{m}$  wavelength region with an aluminum-coated Kel-F substrate (Figs. 14 and 15). Unfortunately, Kel-F ( $\text{CF}_2\text{CFCl}$ )<sub>n</sub> has absorption bands at 7.7 to 9.2 and 10.0 to 11.0  $\mu\text{m}$ , making the polarizer useless in these regions, but it can be used at longer wavelengths out to 25  $\mu\text{m}$ .<sup>92</sup> Polyethylene would be an excellent substrate material since it has fewer absorption bands than Kel-F, but its insolubility in common solvents makes it much more difficult to use for replicating gratings.<sup>110</sup> It does, however, make an excellent substrate material for photoetched grids.<sup>109</sup>

For infrared wavelengths longer than about 24  $\mu\text{m}$ , a photoetched grid with 1- $\mu\text{m}$ -wide lines (close to the present limit for the photoetching process) and a 2- $\mu\text{m}$  spacing should have an extinction ratio of  $5 \times 10^{-3}$  or better if the refractive index of the substrate is about 1.5—for example, polyethylene. The extinction ratio would continue to decrease;

**TABLE 2** Types of Wire-Grid Polarizers

Grid spacing, $\mu\text{m}$	Grid material	Substrate	Wavelength range, $\mu\text{m}$	Reference
0.115	Evaporated Al	Quartz	0.2–0.8	Sonek <i>et al.</i> , Ref. 118
0.347	Evaporated Au	Silverchloride	2.5–30	Perkin-Elmer, Ref. 101
0.22–0.71	Evaporated Al	KRS-5	3–15, 3.39, 10.6	Auton and Hutley, Ref. 114
0.22–0.45	Evaporated Al	CaF <sub>2</sub>	3–10, 3.39	Auton and Hutley, Ref. 114
0.42	Evaporated Al	Glass	3–5	Auton and Hutley, Ref. 114
0.463	Evaporated Au	Kel-F	1.5–10*	Bird and Parrish, Ref. 92
0.463	Evaporated Al	Kel-F	0.7–15*	Bird and Parrish, Ref. 92
0.463	Evaporated Al	Polymethyl methacrylate	1–4000†	Hass and O'Hara, Ref. 110
1.67	Evaporated Al	Irtran 2	6–14	Young <i>et al.</i> , Ref. 102
1.67	Evaporated Al	Irtran 4	8–19	Young <i>et al.</i> , Ref. 102
1.69	Evaporated Al	Polyethylene	2.9–200‡	Hass and O'Hara, Ref. 110
2	Evaporated Cr	Silicon	10.6	Cheo and Bass, Ref. 113
?	?	BaF <sub>2</sub>	2–12	Leonard, Ref. 117
?	?	ZnSe	3–17	Leonard, Ref. 117
4	Photoetched Al	Polyethylene	>16	Auton, Ref. 109
5.1	Photoetched Al	Silicon	54.6	Hilton and Jones, Ref. 111
10	Photoetched Al	Polyethylene	>16	Auton, Ref. 109
25.4	Photoetched Al	Silicon	54.6	Hilton and Jones, Ref. 111
25.4	Evaporated Au	Mylar	>60	Hass and O'Hara, Ref. 110
25	Stainless steel wire 8 $\mu\text{m}$ diam	Air	80–135	Novak <i>et al.</i> , Ref. 120
32.4	Gold-coated W wire 21 $\mu\text{m}$ diam	Air	100–10,000	Eichhorn and Magner, Ref. 119
64, 51	Wire mesh (2D)	Air	118.8	Hwang and Park, Ref. 122
?	Stainless steel wire 50 $\mu\text{m}$ diam	Air	200–1000	Vickers <i>et al.</i> , Ref. 112
317	W wire 152 $\mu\text{m}$ diam	Air	40–300	Roberts and Coon, Ref. 121
25–1800	W wire 10 $\mu\text{m}$ diam	Air	>50	Costley <i>et al.</i> , Ref. 115
30–65	W wire 10 $\mu\text{m}$ diam	Air	22–500, 337	Beunen <i>et al.</i> , Ref. 116

\* Strong absorption bands near 8.3 and 10.5  $\mu\text{m}$ .

† Strong absorption bands between 5.7 and 12.5  $\mu\text{m}$ .

‡ Absorption bands between 6 and 15.5  $\mu\text{m}$ .

i.e., the polarization properties would improve as the wavelength increased. At very long wavelengths, grids with a larger spacing would have a high degree of polarization. The important factor is the ratio of wavelength to grid spacing, which should be kept as large as possible (Fig. 16b).

One definite advantage of the wire-grid polarizer is that it can be used in sharply converging beams, i.e. systems with high numerical apertures. Young *et al.*<sup>102</sup> found no decrease in percent of polarization for an Irtran 2 polarizer at 12  $\mu\text{m}$  used at angles of incidence from 0 to 45°. They did find, however, that the transmittance decreased from 0.55 at normal incidence to less than 0.40 at 45° incidence.

If a grid were to be used at a single wavelength, one might possibly make use of interference effects in the substrate to increase the transmission.<sup>109</sup> If the substrate has perfectly plane-parallel surfaces, it will act like a Fabry-Perot interferometer and transmit a maximum amount of light when twice the product of the thickness and refractive index is equal to an integral number of wavelengths. The 0.25-mm-thick pressed polyethylene

substrates used by Auton<sup>109</sup> were not uniform enough to show interference effects, but the Mylar film backing on the Buckbee Mears electroformed grid did show interference effects.<sup>110</sup>

Lamellar eutectics of two phases consist of thin needles of a conducting material embedded in a transparent matrix. The material is made by a controlled cooling process in which there is a unidirectional temperature gradient. This method of cooling orients conducting needles parallel to the temperature gradient, and hence the material can act like a wire-grid polarizer. Weiss and coworkers<sup>123-125</sup> have grown eutectic alloys of InSb and NiSb in which the conducting needles of NiSb are approximately 1  $\mu\text{m}$  in diameter and approximately 50  $\mu\text{m}$  long. A degree of polarization of more than 99 percent has been reported. Other eutectic alloys of InAs, GaSb, and InSb containing conducting needlelike crystals of Ni, Fe, Mn, Cr, and Co (or their compounds) have also been investigated. An advantage of this type of polarizer is that its performance can be optimized at a specific wavelength, e.g., that of a CO<sub>2</sub> laser line, by choosing the thickness of the crystalline film so that there will be an interference maximum at the desired wavelength.<sup>126</sup> Recently, Saito and Miyagi<sup>127</sup> have proposed using a thin film of anodized aluminum with implanted metallic columns to make a high-performance polarizer. Their theoretical calculations suggest that this type of polarizer should have a large extinction ratio and low loss in the infrared.

In summary, wire grids are very useful infrared polarizers, particularly for wavelengths much greater than the grid spacing. They are compact and easily rotatable and can be used with sharply converging beams. A major advantage is the extreme breadth of the wavelength band over which they have good polarizing properties. The long-wavelength limit is set by the transmission of the substrate material rather than by the loss of polarization of the grid. The short-wavelength limit is determined by the grid spacing; if gratings with smaller spacings could be successfully replicated and coated, the short-wavelength limit could be pushed closer to the visible region.

Another possible method of producing plane-polarized light is by using diffraction gratings or echelette gratings. Light reflected from diffraction gratings has long been known to be polarized, but the effect is generally small and extremely wavelength-dependent.<sup>128,129</sup> However, Roumiguieres<sup>130</sup> predicted that under certain conditions (rectangular groove grating with equal groove and land spacings and small groove depth), a high polarizing efficiency could be obtained. For wavelengths in the range  $1.1 < \lambda/d < 1.7$ , over 80 percent of the light polarized parallel to the grooves should be reflected in the zero order at a 50° angle of incidence and less than 5 percent of the other polarization. His predictions were verified by Knop<sup>131</sup> who fabricated gold-coated photoresist gratings as well as an electroplated nickel master grating. Knop's measured reflectances of the two polarized components were within  $\pm 3$  percent of the predicted values. In general, one tries to avoid polarization in the diffracted light to obtain high efficiencies in a blazed grating since polarization effects are frequently associated with grating anomalies.<sup>132,133</sup>

In contrast to diffraction gratings, echelette gratings have been found to produce an appreciable amount of plane-polarized light. Experimental studies have been made by Peters *et al.*,<sup>134</sup> Hadni *et al.*,<sup>135,136</sup> and Mitsuishi *et al.*,<sup>137</sup> as discussed in the earlier Polarization chapter.<sup>1</sup> The theory of the polarization of light reflected by echelette gratings in the far-infrared and microwave regions has been given by Janot and Hadni<sup>138</sup> and Rohrbaugh *et al.*<sup>139</sup> A general numerical technique published by Kalhor and Neureuther<sup>140</sup> should be useful for calculating the polarization effects of echelette gratings of arbitrary groove shape used in the visible region.

**39. Measuring Polarization of Imperfect Polarizers** In determining the principal transmittance, extinction ratio, and other properties of an imperfect polarizer, the effects of source polarization, instrumental polarization, and sensitivity of the detector to the plane of polarization must either be measured or eliminated from the calculations. This is easy if an auxiliary polarizer is available that has a much higher degree of polarization

than the one to be measured. In such a case, the “perfect” polarizer can be placed in the beam, and the transmittances  $T_1$  and  $T_2$  for the unknown polarizer can be measured directly.\* Source polarization, instrumental polarization, and variation of detector response with plane of polarization can all be lumped together as a product. If this product is different in the horizontal and vertical planes, the ratio of the signals obtained when the “perfect” polarizer is oriented horizontally and vertically will not equal unity. One should always take more than the minimum number of measurements, i.e., introduce redundancy, to make sure that no systematic errors are present.

If a high-quality polarizer is not available, two polarizers having unknown properties may be used instead. Several procedures have been described in detail in the earlier Polarization chapter.<sup>1</sup> The method of Hamm *et al.*<sup>141</sup> which yields the extinction ratio of each polarizer and the instrumental polarization was described in detail and a brief summary of the method of Kudo *et al.*<sup>142</sup> was given. The methods of Hamm *et al.*,<sup>141</sup> Horton *et al.*,<sup>143</sup> and Schledermann and Skibowski<sup>144</sup> were specifically developed for non-normal incidence reflection polarizers (see Par. 41).

### **NON-NORMAL-INCIDENCE REFLECTION AND TRANSMISSION POLARIZERS**

---

**40.** By far the largest class of polarizers used in the infrared and ultraviolet spectral regions (where dichroic sheet polarizers and calcite polarizing prisms cannot be used) is the so-called *pile-of-plates polarizers* from which light is reflected (or transmitted) at non-normal incidence. Since most of these polarizers operate at angles near the Brewster or polarizing angle [see Eq. (48) in Chap. 5, “Polarization,” in Vol. I of this handbook], they are frequently called Brewster angle polarizers. The plane-parallel plates which are used for Brewster angle transmission polarizers (Par. 42) are generally thick enough to ensure that although multiple reflections occur within each plate, the coherence of the light beam is lost and there are no interference effects. However, another class of non-normal-incidence transmission polarizers makes use of interference effects to enhance their polarizing properties, (Pars. 43 and 44). These include interference polarizers (Par. 43) and polarizing beam splitters (Par. 44). These thin-film devices are discussed in much more detail in the chapter on Optical and Physical Properties of Films and Coatings by J. A. Dóbrowolski (Chap. 42, Vol. I). A relation which is frequently used in connection with non-normal-incidence reflectance measurements is the Abelès condition, discussed in Par. 41.

**41. Brewster Angle Reflection Polarizers** Most reflection-type polarizers are made of plates which are either nonabsorbing or only slightly absorbing. The angle of incidence most often used is the Brewster angle at which the reflection of the  $p$  component, light polarized parallel to the plane of incidence, goes to 0. Thus the reflected light is completely plane polarized with the electric vector vibrating perpendicular to the plane of incidence ( $s$  component). Curves showing the reflectance and extinction ratio for various materials and angles near the Brewster angle are given in Fig. 5 of Chap. 5, “Polarization,” in Vol. I of this handbook. The polarizing efficiency of reflection-type polarizers can be experimentally determined using any of the methods given in Par. 49 of the earlier Polarization chapter;<sup>1</sup> the methods of Hamm *et al.*,<sup>141</sup> Horton *et al.*,<sup>143</sup> and Schledermann and Skibowski<sup>144</sup> were specifically developed for polarizers of this type.

Brewster angle reflection polarizers for the infrared are made from the semiconductors silicon, germanium, and selenium which are transparent beyond their absorption edges

---

\* When using an air-spaced polarizing prism, extreme care should be taken not to exceed the acceptance angle of the prism.

**TABLE 3** Infrared Brewster Angle Reflection Polarizers

Material	Description	Reference
Ge-Hg	Multiple internal reflections in Ge immersed in Hg	Harrick, Ref. 145
Ge	Single external reflection from 1-cm-thick polished Ge single crystal	Edwards and Bruemmer, Ref. 146
Ge	Proposed parallel and antiparallel arrangements of two Ge plates	Křízek, Ref. 147
Ge	Double-beam system: beam 1, single reflection; beam 2, one transmission, one reflection	Craig <i>et al.</i> , Ref. 148
Ge	Axial arrangement with reflections from two Ge wedges and two Al mirrors	Bor and Brooks, Ref. 149
Se	Reflections from two cast-Se films on roughened glass plates	Pfund, Ref. 150
Se	Axial arrangement with reflections from two Se films evaporated on NaCl and one Ag mirror	Barchewitz and Henry, Ref. 151
Se	Large-aperture, axial, venetian-blind arrangement with one or two reflections from evaporated Se films on roughened glass plates (additional reflections from Al mirrors)	Takahashi, Ref. 152
Si	Single reflection from polished single crystal Si	Walton and Moss, Ref. 153
Si	Axial arrangement with reflection from two Al mirrors and polished Si plate with roughened back	Baumel and Schnatterly, Ref. 154
PbS	Axial arrangement with reflections from two chemically deposited PbS films and one Al film	Grechushnikov and Petrov, Ref. 155
CdTe	Single plate	Leonard, Ref. 117
Al + Al <sub>2</sub> O <sub>3</sub>	Multiple reflections from Al <sub>2</sub> O <sub>3</sub> coated with metal at 10.6 μm (calculations only)	Cox and Hass, Ref. 156
Ti + SiO <sub>2</sub>	Multiple reflections from dielectric coated Ti at 2.8 μm (calculations only)	Thonn and Azzam, Ref. 157

and have high refractive indexes. Table 3 lists various infrared polarizers which have been described in the literature. All involve external reflections except the Ge-Hg polarizer described by Harrick,<sup>145</sup> in which light undergoes two or four reflections within a bar of germanium. While Harrick's polarizer has attractive features, it depends on maintaining polarization in the germanium, so that great care must be taken to obtain material with a minimum of strain birefringence.

In the ultraviolet, materials such as LiF, MgF<sub>2</sub>, CaF<sub>2</sub>, and Al<sub>2</sub>O<sub>3</sub>, can be used as polarizers. Biotite, a form of mica, has also been found to perform very well in the 1000- to 6000-Å region. In the extreme ultraviolet, metallic films, particularly Au, Ag, and Al, have been used as polarizers. Table 4 lists various non-normal-incidence ultraviolet reflection polarizers as well as authors who have made calculations and measurements on various materials for ultraviolet polarizers.

The most versatile non-normal-incidence reflection polarizer would be one which does not deviate or displace the beam from its axial position. One convenient arrangement would be a symmetric three-reflection system in which the light is incident on one side of a triangle, reflected to a plane mirror opposite the apex, and back to the other side of the triangle, as was done by Horton *et al.*,<sup>143</sup> and Barchewitz and Henry.<sup>151</sup> If the polarizer must have a good extinction ratio and the light beam is highly convergent, two of the reflections could be from the polarizing material and the third from a silvered or aluminized mirror. If the beam is highly collimated or more throughput is required, only one reflection may be from the polarizing material. The throughput can also be increased by using a plane-parallel plate for the polarizing reflection. The major drawback to a reflection polarizer is the extreme length of the device required to accommodate a beam of large cross-sectional area. For example, if a germanium polarizer were used at the

**TABLE 4** Ultraviolet Reflection Polarizers and Polarization Measurements

Material	Description	Wavelength range, Å	Reference
Al <sub>2</sub> O <sub>3</sub> , Al, Au, ZnS, glass, and others	Calculated values of $R_s$ and $(R_s/R_p)_{\max}$ vs. wavelength for a single reflection	500–2000	Hunter, Ref. 158
Al <sub>2</sub> O <sub>3</sub> , Al, glass, and others	Calculated values of $R_s$ and $(R_s - R_p)/(R_s + R_p)$ vs. angle of incidence for a single reflection; also principal angle and related angles	584	Damany, Ref. 159
Al <sub>2</sub> O <sub>3</sub> , CaF <sub>2</sub> , LiF, and Pyrex	Measured optical constants; calculated $R_s$ and $(R_s - R_p)/(R_s + R_p)$ vs. angle of incidence and wavelength for a single reflection	200–2000	Stephan <i>et al.</i> , Ref. 160
Al <sub>2</sub> O <sub>3</sub> and CaF <sub>2</sub>	Measured $(R_s - R_p)/(R_s + R_p)$ vs. angle of incidence at selected wavelengths for a single reflection; used both materials as single-reflection polarizers	1026–1600	de Chelle and Merdy, Ref. 161
LiF, Al <sub>2</sub> O <sub>3</sub> , MgF <sub>2</sub> , SiO <sub>2</sub> , ZnS	Used single-reflection LiF polarizer at Brewster angle to measure $R_s$ and $R_s/R_p$ for various materials; best polarizers were Al <sub>2</sub> O <sub>3</sub> and MgF <sub>2</sub>	1216	McIlrath, Ref. 162
Al, Ag, Au, MgF <sub>2</sub> , SiO <sub>2</sub> , ZnS	Measured polarization of uncoated aluminum grating and optical constants of all materials listed	304–1216	Cole and Oppenheimer, Ref. 163
Al, Au	Determined polarization of Au- and Al-coated gratings by measuring reflectance of Au and fused-silica mirrors at 45°	600–2000	Uzan <i>et al.</i> , Ref. 164
Al, Au, glass	Measured average reflectance and degree of polarization of Al, Au, and glass as a function of angle of incidence; measured polarization of a glass grating and an Al-coated grating	584	Rabinovitch <i>et al.</i> , Ref. 165
MgF <sub>2</sub>	Measured $R_p/R_s$ at 60° for a single reflection and compared it with calculated values	916, 1085, 1216	Sasaki and Fukutani, Ref. 166
MgF <sub>2</sub> + Al	Calculated performance, constructed axial triple-reflection polarizer and analyzer of MgF <sub>2</sub> -coated Al, and measured transmission	1216	Winter <i>et al.</i> , Ref. 167
MgF <sub>2</sub> , MgF <sub>2</sub> + Al	Calculated performance, constructed triple-reflection polarizer of a MgF <sub>2</sub> plate and two MgF <sub>2</sub> -coated Al mirrors, and measured transmission	300–2000	Hass and Hunter, Ref. 168

MgF <sub>2</sub> , MgF <sub>2</sub> + Al	Constructed four-reflection polarizers of a MgF <sub>2</sub> plate and three MgF <sub>2</sub> -coated Al mirrors, no performance properties measured; polarizer part of the UV spectrometer and polarimeter for the NASA Solar Maximum Mission	1150–visible	Spencer <i>et al.</i> , Ref. 169
MgF <sub>2</sub> , Au and other metals	Calculated values of $R_s$ and $(R_s/R_p)_{\max}$ vs. angle of incidence and wavelength for one and more reflections for a variety of materials	300–2000	Hunter, Ref. 170
Au, Ag	Measured $R_p/R_s$ at 45° for a single reflection and compared it with calculated values; measured $R_p/R_s$ for a platinumized grating	500–1300	Hamm <i>et al.</i> , Ref. 141
Au	Used single-reflection Au mirror at 60° as polarizer (Brewster angle about 55°)	600–1200	Ejiri, Ref. 171
Au	Used axial arrangement of eight Au mirrors at 60° as polarizer and analyzer to measure polarization of synchrotron radiation; determined polarizing properties of each polarizer	500–1000	Rosenbaum <i>et al.</i> , Ref. 172
Au	Constructed axial triple-reflection Au polarizer, measured extinction ratio and transmission for different angles of incidence on Au plates	500–5000	Horton <i>et al.</i> , Ref. 143
Au	Reflection from two cylindrical gold mirrors in a Seya-Namioka monochromator; measured polarization ratio	1200–3000	Rehfeld <i>et al.</i> , Ref. 173
Au	Calculated performance of a polarizer made of 2 concave Au-coated spherical mirrors used off axis, constructed polarizer, no measurements made of polarization or transmission	584	Van Hoof, Ref. 174
Au	Constructed a 4-reflection Au-coated polarizer of Van Hoof's design (2 plane, 2 spherical mirrors), measured transmission and degree of polarization	400–1300	Hibst and Bukow, Ref. 175
Au	Constructed a single-reflection Au-coated polarizer and measured the polarizing efficiency	584	Khakoo <i>et al.</i> , Ref. 176
Biotite	Constructed axial polarizer and analyzer each with 61° Brewster angle reflection from biotite and two reflections from MgF <sub>2</sub> -coated Al mirrors; measured transmission and extinction ratio	1100–6000	Robin <i>et al.</i> , Ref. 177
Biotite	Constructed two polarizers: (1) axial polarizer with two 60° reflections from biotite and 30° reflection from MgF <sub>2</sub> -coated Al mirror; (2) displaced-beam polarizer with 60° reflections from two biotite plates; measured degree of polarization of various gratings	1000–2000	Matsui and Walker, Ref. 178

Brewster angle ( $76^\circ$ ) and the beam width were about 25 mm, each Ge plate would have to be about 25 by 100 mm and the overall length of the polarizer would be greater than 200 mm if a three-reflection axial arrangement such as that described above were used.

The Abelès condition,<sup>179</sup> which applies to the amplitude reflectance at  $45^\circ$  angle of incidence (see Par. 4 in Chap. 5, "Polarization," in Vol. I) is useful for testing the quality of reflection polarizers. Schulz and Tangherlini<sup>180</sup> apparently rediscovered the Abelès condition and used the ratio  $R_s^2/R_p = 1$  as a test to evaluate their reflecting surfaces. They found that surface roughness made the ratio too small but annealing the metal films at temperatures higher than  $150^\circ\text{C}$  made the ratio larger than unity. Rabinovitch *et al.*<sup>165</sup> made use of the Abelès condition to determine the polarization of their Seya-Namioka vacuum-ultraviolet monochromator. They measured the reflectance at  $45^\circ$  of a sample whose plane of incidence was perpendicular or parallel to the exit slit. From these measurements they deduced the instrumental polarization by assuming the Abelès condition. Values of instrumental polarization obtained using carefully prepared gold and fused-silica samples were in excellent agreement, showing that neither of these materials had surface films which invalidated the Abelès condition. Surface films usually have relatively little effect on the Abelès condition in the visible region<sup>181</sup> but become important in the vacuum ultraviolet. Hamm *et al.*<sup>141</sup> eliminated the effect of instrumental polarization from their measurements of the reflectance of a sample in unpolarized light at  $45^\circ$  angle of incidence by making use of the Abelès condition. Although McIlrath<sup>162</sup> did not refer to the Abelès condition as such, he used it to determine the instrumental polarization of his vacuum-ultraviolet apparatus so he could measure the absolute reflectance of a sample at  $45^\circ$  angle of incidence. Thonn and Azzam<sup>157</sup> have calculated the polarizing properties of dielectric-coated metal mirrors at  $2.8\ \mu\text{m}$  in the infrared. Reflections from 2, 3, or 4 such mirrors at the Brewster angle should give excellent performance, although the polarizer would be quite long.

**42. Brewster Angle Transmission Polarizers** To help overcome the beam-deviation problem and the extreme length of reflection-type polarizers, Brewster angle polarizers are often used in transmission, particularly in the infrared, where transparent materials are available. At the Brewster angle, all of the  $p$  component and an appreciable fraction of the  $s$  component are transmitted. Thus, several plates must be used to achieve a reasonable degree of polarization. The higher the refractive index of the plates, the fewer are required.

Tables 1 and 2 in Chap. 5, "Polarization," in Vol. I of this handbook give equations for the transmittances and degree of polarization for a single plate and multiple plates at any angle of incidence in terms of  $R_s$  and  $R_p$  for a single surface, as well as these same quantities at the Brewster angle. Conn and Eaton<sup>182</sup> have shown that the formulas which assume incoherent multiple reflections within each plate and none between plates give the correct degree of polarization for a series of Zapon lacquer films ( $n = 1.54$ ) and also for a series of eight selenium films, whereas the formula of Provostaye and Desains<sup>183</sup> predicted values which were much too low. These authors also point out that the number of multiply reflected beams between plates that enter the optical system depends on the spacing between plates and the diaphragm used to limit the number of beams. One can use a fanned arrangement, as suggested by Bird and Shurcliff,<sup>184</sup> to eliminate these multiply reflected beams. Internal reflections within each plate can be removed by wedging the plates.<sup>184</sup>

Most of the infrared Brewster angle transmission polarizers described in the literature have been made of selenium, silver chloride, or polyethylene sheet; they are listed in Table 5. For wavelengths longer than  $3\ \mu\text{m}$ , where calcite polarizing prisms become highly absorbing, to about  $10\ \mu\text{m}$ , beyond which wire-grid polarizers have good extinction ratios, Brewster angle transmission polarizers are the most useful, since the better-extinction, on-axis reflection-type polarizers (Par. 41) are impossibly long. Some of the interference polarizers described in Pars. 43 and 44 are superior if the beam-convergence angle is

**TABLE 5** Infrared Brewster Angle Transmission Polarizers

Material	Description	Wavelength range, $\mu\text{m}$	Reference
Se	5 or 6 unbacked films (4 $\mu\text{m}$ thick) at 65° angle of incidence (Brewster angle 68.5°)	2–14	Elliott and Ambrose, Ref. 185; Elliott <i>et al.</i> , Ref. 186
Se	5 unbacked films at 65° incidence (different method of preparation from above)		Ames and Sampson, Ref. 187
Se	8 unbacked films at the Brewster angle		Conn and Eaton, Ref. 182
Se	Se films (3–8 $\mu\text{m}$ thick) evaporated on one side of collodion films; 68.5° angle of incidence	1–15	Barchewitz and Henry, Ref. 151
Se	1 to 6 unbacked films (1.44–8 $\mu\text{m}$ thick) at 68° angle of incidence	Visible–20	Duverney, Ref. 188
Se	3 unbacked films (0.95 $\mu\text{m}$ thick) at 71° angle of incidence	6–17	Hertz, Ref. 189
Se	5 Formvar films coated on both sides with Se (various thicknesses) at 65° angle of incidence	1.8–3.2	Buijs, Ref. 190
Se	Unbacked films (different method of preparation from Elliott <i>et al.</i> Ref. 186)		Bradbury and Elliott, Ref. 191
Se	4 to 6 plated unsupported films (4–8 $\mu\text{m}$ thick) at the Brewster angle	2.5–25	Greener <i>et al.</i> , Ref. 192
AgCl	3 plates (1 mm thick) at 63.5° angle of incidence	Visible–15	Wright, Ref. 193
AgCl	6 to 12 plates (0.05 mm thick) at 60–75° angle of incidence	2–20	Newman and Halford, Ref. 78
AgCl	6 plates (0.5 mm thick) at 63.5° stacked in alternate directions		Makas and Shureliff, Ref. 194
AgCl	Suggest 6 wedge-shaped plates at 68° stacked in alternate directions in a fanned arrangement		Bird and Shurcliff, Ref. 184
AgCl	2 V-shaped plates (3.2 mm thick) at 77° angle of incidence; large aperture		Bennett <i>et al.</i> , Ref. 195
KRS-5	1 to 3 thallium bromide-iodide plates (1 and 4 mm thick) at polarizing angle	1–15	Lagemann and Miller, Ref. 196
ZnS	4 glass plates (0.1 mm thick) coated on both sides with uniform ZnS films of same thickness (several sets of plates to cover extended wavelength range)	Visible–6	Huld and Staffin, Ref. 197
ZnSe	6 plates, extinction ratio of 800 at 4 $\mu\text{m}$	4	Leonard <i>et al.</i> , Ref. 198
Ge	1 single-crystal Ge plate (0.8 mm thick) at 76° angle of incidence		Meier and Günthard, Ref. 199
Ge	2 plates (1 mm thick) in an X-shaped arrangement at 76° angle of incidence		Harrick, Ref. 200
Ge	3 plates (2 wedged) at the Brewster angle	2–6	Murarka and Wilner, Ref. 201
Polyethylene	12 sheets (8 $\mu\text{m}$ thick) at the Brewster angle	6–20 (absorption bands 6–14)	Smith <i>et al.</i> , Ref. 202
Polyethylene	9 to 15 sheets (20–50 $\mu\text{m}$ thick) at the Brewster angle (55°)	30–200	Mitsuishi <i>et al.</i> , Ref. 137
Polyethylene	4 sheets at the Brewster angle	200–350	Hadri <i>et al.</i> , Ref. 136
Polyethylene	12 sheets (5 $\mu\text{m}$ thick) at the Brewster angle	1.5–13 (selected wavelengths)	Walton and Moss, Ref. 153
Polyethylene	1–15 stretched sheets (12.7 $\mu\text{m}$ thick) at the Brewster angle	10.6	Rampton and Grow, Ref. 203
Polyethylene	20 sheets (30 $\mu\text{m}$ thick) at the Brewster angle	45–200	Munier <i>et al.</i> , Ref. 204
Polyethylene	25 to 30 sheets at the Brewster angle	54.6	Hilton and Jones, Ref. 111
Melinex	11 to 13 polyethylene terephthalate (Melinex) sheets (4.25–9 $\mu\text{m}$ thick) at the Brewster angle	1–5	Walton <i>et al.</i> , Ref. 205

**TABLE 6** Ultraviolet Brewster Angle Transmission Polarizers

Material	Description	Wavelength range, Å	Reference
LiF	4 to 8 plates (0.3–0.8 mm thick) at 60° angle of incidence (Brewster angle 55.7–58.7°) stacked in alternate directions	1200–2000	Walker, Ref. 206
LiF	8 plates	1100–3000	Hinson, Ref. 207
LiF	8 plates (0.25–0.38 mm thick) at 60° angle of incidence stacked in groups of 4 in alternate directions	1200–2000	Heath, Ref. 208
CaF <sub>2</sub>	4 to 8 wedged plates stacked in alternate directions in fanned arrangement at 65° angle of incidence (Brewster angle 56.7)	1500–2500	Schellman <i>et al.</i> , Ref. 209
Al	Calculations of polarizing efficiency for 1000-Å-thick unbacked Al film, 1000- and 500-Å Al films each covered with 30-Å Al <sub>2</sub> O <sub>3</sub> and 100-Å Au films	300–800	Hunter, Ref. 158

small. Ultraviolet Brewster angle transmission polarizers are not nearly as common; LiF and CaF<sub>2</sub> have mainly been used from about 1500 to 2500 Å (see Table 6). In the wavelength region where calcite polarizing prisms are usable (>2140 Å), Brewster angle polarizers have the advantage of a larger linear aperture and less absorption.

Low-absorption glass pile-of-plates polarizers have been used in the visible spectral region by Weiser,<sup>210</sup> in preference to more absorbing Glan-Thompson prism polarizers, to increase the power output of giant-pulse ruby lasers. Weinberg<sup>211</sup> calculated the degree of polarization of glass and silver chloride plates, but he did not calculate the transmittance of his polarizers.

### Interference Polarizers

**43.** When the sheets or films constituting a non-normal-incidence transmission polarizer are thin and have very smooth surfaces, the internally reflected beams can interfere constructively or destructively. In this case, the transmittance of the *p* component remains unity at the Brewster angle (where  $R_p = 0$ ) and only oscillates slightly (with respect to wavelength) for angles close to the Brewster angle. However, the *s* transmittance varies from a maximum of unity to a minimum of  $(1 - R_s)^2 / (1 + R_s)^2$  whenever  $\lambda$  changes by an amount that will make the quantity  $(nd \cos \theta_i) / \lambda$  in Eq. (26) in Chap 5., “Polarization,” in Vol. I change by  $\frac{1}{2}$ .<sup>\*</sup> These transmittance oscillations are only  $\pm 0.225$  for a single film of refractive index 1.5 but can become as large as  $\pm 0.492$  when  $n = 4.0$ . Since the *p* transmittance remains essentially constant, the extinction ratio will vary cyclically with the *s* transmittance, as can be seen in the upper curve of Fig. 17 for a 2.016- $\mu\text{m}$ -thick selenium film.

If a transmission polarizer with a good extinction ratio is needed for use over a limited wavelength range, it can be made of several uniform films of a thickness that yields a minimum extinction ratio in the given wavelength region. The extinction ratio for a series of *m* films is  $(T_s/T_p)^m$  when there are no multiple reflections between them. In this way only *half* as many films would be needed to achieve a given extinction ratio as would be necessary if interference effects were not present. This rather surprising result can be seen from the expressions for  $(T_s)_{\text{sample}}$  for *m* plates with and without interference effects in Table 2 in Chap. 5, “Polarization,” in Vol. I of this handbook. Assuming no multiple reflections between plates, the expressions are  $[2n^2/(n^4 + 1)]^{2m}$  and  $[2n^2/(n^4 + 1)]^m$ ,

<sup>\*</sup> The approximate expression for this wavelength interval  $\Delta\lambda$  (assuming that the oscillations are sufficiently close together for  $\lambda_1\lambda_2 \approx \lambda_2$ ) is given in Eq. (27) in Chap. 5, “Polarization,” in Vol. I of this handbook.

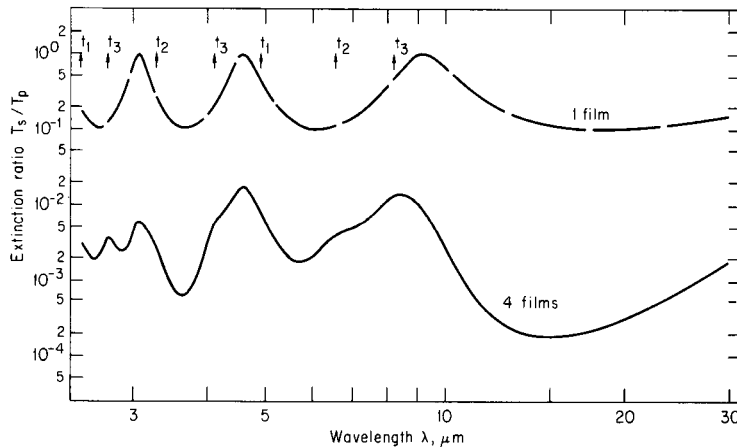


**FIGURE 17** Calculated extinction ratios for a series of selenium films ( $n = 2.46$ ) as a function of wavelength from 2.5 to 30  $\mu\text{m}$ . Light is incident at the Brewster angle,  $67.9^\circ$ , and multiply reflected beams interfere within the film. The upper curve is for a single film 2.016  $\mu\text{m}$  thick; arrows indicate positions of maxima for three thinner films:  $t_1 = 1.080 \mu\text{m}$ ,  $t_2 = 1.440 \mu\text{m}$ , and  $t_3 = 1.800 \mu\text{m}$ . The lower curve is the extinction ratio for the four films in series assuming no reflections between films. The calculated  $p$  transmittance for each film (and for four films in series) is unity at the Brewster angle.

respectively. Hertz<sup>189</sup> achieved a degree of polarization of 99.5 percent in the 6- to 17- $\mu\text{m}$  region using three unbacked selenium films 0.95  $\mu\text{m}$  thick. Conn and Eaton<sup>182</sup> obtained only a slightly better performance with eight thicker nonuniform selenium films.

As can be seen in Fig. 17, the calculated extinction ratio for the 2.016- $\mu\text{m}$ -thick film goes to unity at 3.0, 4.6, and 9.2  $\mu\text{m}$ , indicating that the  $s$  as well as the  $p$  transmittance at these wavelengths is unity. This ratio will remain unity at the above wavelengths if there are several nonabsorbing films of the same thickness. Even if the films have slightly different thicknesses, or if their surfaces are somewhat rough, interference effects may still persist, adversely affecting polarizer performance. Such effects have been observed by Elliott *et al.*,<sup>186</sup> Barchewitz and Henry,<sup>151</sup> Duverney,<sup>188</sup> Mitsuishi *et al.*,<sup>137</sup> and Walton *et al.*<sup>205</sup>

By choosing films of appropriate thicknesses, interference effects can be used to advantage. The lower curve in Fig. 17 shows the extinction ratio obtained if four selenium films of thicknesses 1.08, 1.44, 1.80, and 2.02  $\mu\text{m}$  are used at the Brewster angle as a transmission polarizer. (The wavelengths at which maxima occur for the three thinner films are indicated by arrows in the upper portion of the figure.) In this example the extinction ratio for the four films in series is better than  $2 \times 10^{-2}$  from 2.5 to 30  $\mu\text{m}$  and at most wavelengths is better than  $10^{-2}$  (corresponding to a degree of polarization in excess of 98 percent). In the 11- to 27- $\mu\text{m}$  wavelength region the extinction ratio is better than  $10^{-3}$ . Four thick or nonuniform selenium films without interference effects have a calculated extinction ratio of about  $10^{-2}$ , and six films are required to change this ratio to  $10^{-3}$ . Thus, in the 11- to 27- $\mu\text{m}$  wavelength region, *four* selenium films of appropriate thicknesses *with interference* have a superior extinction ratio to *six* selenium films *without interference*. If one wishes to optimize the extinction ratio over a more limited wavelength range, the film thicknesses can be adjusted accordingly and the extinction ratio improved. Unfortunately, the gain in extinction ratio is offset by a more sensitive angular function than that shown in Fig. 7 in Chap 5., "Polarization," in Vol. I, so that the incident beam must be very well collimated.

Interference effects can also be used to advantage in other types of non-normal-incidence polarizers. Bennett *et al.*<sup>212</sup> made a transmission polarizer from a series of four

germanium films (ranging in thickness from 0.164 to 0.593  $\mu\text{m}$ ), evaporated onto strain-free plates of sodium chloride. The plates were inclined at the Brewster angle for germanium and arranged in the form of an X so that the polarizer would have a large square aperture and would not deviate the beam. An extinction ratio better than  $3 \times 10^{-3}$  was measured at 2.5  $\mu\text{m}$ , and the plates transmitted from 2 to 13  $\mu\text{m}$ . (Calculated extinction ratios in this wavelength range vary from  $1 \times 10^{-3}$  to  $2 \times 10^{-4}$  for radiation incident at the Brewster angle.)

Polarizers consisting of a high refractive index transparent film on a lower refractive index transparent substrate have been suggested for use in the visible wavelength region by Schröder<sup>213</sup> and Abelès.<sup>214</sup> These still have a Brewster angle where  $R_p = 0$ , and furthermore  $R_s$  at this angle is greatly increased over its value for an uncoated low refractive index substrate. Thus, a large-aperture, high-efficiency polarizer with no absorption losses is possible, which should find numerous applications in laser systems. One polarizer of this type, suggested independently by Schröder and by Abelès, would consist of high refractive index titanium dioxide films ( $n \approx 2.5$ ) evaporated onto both sides of a glass substrate ( $n = 1.51$ ). At the Brewster angle,  $74.4^\circ$ ,  $R_s \approx 0.8$ , making this polarizer equivalent to one made from a material of refractive index 4 ( $\theta_B = 76.0^\circ$  as shown in Fig. 4 in Chap. 5, "Polarizers," in Vol. I of this handbook).<sup>\*</sup> Two glass plates coated on both sides with  $\text{TiO}_2$  films should have an extinction ratio of about  $1.6 \times 10^{-3}$  at 5500 Å and about twice that value at the extreme ends of the visible region, according to Abelès.<sup>214</sup> Schröder<sup>213</sup> measured the degree of polarization as a function of angle of incidence for one such  $\text{TiO}_2$ -coated glass plate and found values comparable to the calculated ones. Kubo<sup>215</sup> calculated the degree of polarization, reflectance, and transmittance (as a function of angle of incidence and wavelength) of a glass plate ( $n = 1.50$ ) covered with a thin transparent film of index, 2.20. His results are similar to those of Abelès and Schröder.

Schopper,<sup>216</sup> Ruiz-Urbieta and Sparrow,<sup>207-219</sup> and Abelès<sup>220</sup> have also investigated making non-normal-incidence reflection polarizers from a thin transparent or absorbing film deposited onto an absorbing substrate. Zaghoul and Azzam<sup>221</sup> proposed using silicon films on fused silica substrates as reflection polarizers for different mercury spectral lines in the visible and ultraviolet regions. Abelès designed some specialized reflection polarizers for use in the vacuum ultraviolet. Unfortunately the wavelength range covered by such a polarizer is very narrow; for one polarizer it was 25 Å at a wavelength of 1500 Å. However, the spectral range could possibly be increased by using several thin films instead of one.

Multilayer film stacks have also been used to produce non-normal-incidence reflection or transmission polarizers by Buchman *et al.*<sup>222</sup> Buchman<sup>223</sup> later improved the design performance of his polarizers by adding antireflection layers between the repeating groups of layers. Although this type of polarizer has a relatively narrow operating bandwidth, a small angular acceptance, tight wavelength centering, and layer thickness uniformity requirements, it can be used successfully in high power laser systems as shown by Refermat and Eastman.<sup>224</sup> Songer<sup>225</sup> described how to design and fabricate a Brewster angle multilayer interference polarizer out of a titanium dioxide, silicon dioxide multilayer on BK 7 glass for use in a 1.06- $\mu\text{m}$  laser beam. Blanc, Lissberger, and Roy<sup>226</sup> designed, built, and tested multilayer zinc sulfide-cryolite-coated glass and quartz polarizers for use with a pulsed 1.06- $\mu\text{m}$  laser. Recently, Maehara *et al.*<sup>227</sup> have reported excellent performance for a pair of polarizers coated with 21 ruthenium and silicon films on a silicon wafer over a wide wavelength range in the soft x-ray region. In several designs of multilayer film stacks, both the reflected and transmitted beams are used; they are discussed in Par. 44.

**44. Polarizing Beam Splitters** Polarizing beam splitters are a special form of non-normal-incidence interference polarizer in which the beam is incident on a multilayer

<sup>\*</sup> We are assuming no multiply reflected beams within the substrate in either case.

dielectric stack at  $45^\circ$ . The transmitted beam is almost entirely plane-polarized in the  $p$  direction, while the reflected beam is nearly all plane-polarized in the  $s$  direction. Generally the alternating high and low refractive index dielectric layers are deposited onto the hypotenuses of two right-angle prisms, which are then cemented together to form a cube. The beam enters a cube face normally and strikes the multilayers on the hypotenuse (the high refractive index layer is next to the glass), and the reflected and transmitted beams emerge normal to cube faces, being separated by  $90^\circ$ . Clapham *et al.*<sup>228</sup> have a good discussion of polarizing beam splitters, which were invented by S. M. MacNeille<sup>229</sup> and developed by Banning.<sup>230</sup> Banning's beam splitter was made with three zinc sulfide and two cryolite layers on each prism; the polarization for white light was greater than 98 percent over a  $5^\circ$ -angle on each side of the normal to the cube face for both the reflected and transmitted beams. Variations on this design have since been proposed by Dobrowolski and Waldorf,<sup>231</sup> Monga *et al.*,<sup>232</sup> and Mouchart *et al.*,<sup>233</sup> primarily to improve the laser damage resistance of the device and increase the angular field of view. Dobrowolski and Waldorf<sup>231</sup> designed and built a polarizing beam splitter consisting of a multilayer coating of  $\text{HfO}_2$  and  $\text{SiO}_2$  deposited onto fused silica and immersed in a water cell that acted like the MacNeille cube. Tests with a  $0.308\ \mu\text{m}$  excimer laser showed a high laser damage threshold. The multi-wavelength polarizing beam splitters designed by Monga *et al.*<sup>232</sup> could be made in large sizes and could withstand high laser power levels. The modified MacNeille cube polarizers designed by Mouchart *et al.*<sup>233</sup> had angular fields of view that could be increased to about  $\pm 10^\circ$  when the polarizers were used with monochromatic light sources.

Lees and Baumeister<sup>234</sup> designed a frustrated total internal reflection beam splitter that had a multilayer dielectric stack deposited onto the hypotenuse of a prism. Their designs, for use in the infrared spectral region, consisted of multilayer stacks of  $\text{PbF}_2$  and Ge deposited onto a germanium prism and covered by a second germanium prism. Azzam<sup>235</sup> designed polarization independent beam splitters for  $0.6328\ \mu\text{m}$  and  $10.6\ \mu\text{m}$  using single-layer coated zinc sulfide and germanium prisms. The devices were found to be reasonably achromatic and their beam-splitting ratio could be varied over a wide range with little degradation in polarization properties. Azzam<sup>236</sup> also proposed coating a low-refractive-index dielectric slab on both sides with high-refractive-index dielectric films to make an infrared polarizing beam splitter.

Various high- and low-refractive-index materials have been successfully used in the multilayer stacks. In addition to zinc sulfide and cryolite on glass by Banning<sup>230</sup> and Schröder and Schläfer,<sup>237</sup> layers of a controlled mixture of silicon dioxide and titanium dioxide have been alternated with pure titanium dioxide on fused-silica prisms by Pridatko and Krylova,<sup>238</sup> thorium dioxide and silicon dioxide have been used on fused-silica prisms by Sokolova and Krylova,<sup>239</sup> chiolite (a mixture of sodium and aluminum fluorides) and lead fluoride have been used on fused-silica prisms by Turner and Baumeister,<sup>240</sup> bismuth oxide and magnesium fluoride have been used on EDF glass prisms by Clapham *et al.*,<sup>228</sup> and zirconium oxide and magnesium fluoride have been used on dense flint-glass prisms by Clapham *et al.*<sup>228</sup> The calculations involved in optimizing these beam splitters for good polarizing characteristics, achromaticity, and relative insensitivity to angle of incidence are quite involved. Clapham *et al.*<sup>228</sup> and Turner and Baumeister<sup>240</sup> discuss various calculational techniques frequently used. Clapham<sup>241</sup> also gives the measured characteristics of a high-performance achromatic polarizing beam splitter made with zirconium oxide and magnesium fluoride multilayers.

Although polarizing beam splitters are generally designed so that the  $s$  and  $p$  polarized beams emerge at right angles to each other, Schröder and Schläfer<sup>237</sup> have an ingenious arrangement in which a half-wave plate and mirror are introduced into the path of the reflected beam to make it parallel to the transmitted beam and of the same polarization. Other optical schemes to accomplish the same purpose have been described in a later paper.<sup>242</sup>

For some purposes it is desirable to have a beam splitter that is insensitive to the

polarization of the incident beam. Baumeister<sup>243</sup> has discussed the design of such beam splitters made from multilayer dielectric stacks of alternating low- and high-refractive-index materials. One of his designs is composed of six dielectric layers for which the extinction ratio  $T_s/T_p$  varies from 0.93 to 0.99 in a bandwidth of about 800 Å, with a  $\pm 1^\circ$  variation in the angle of incidence. In principle, any multilayer filter which is nonreflecting at normal incidence will be nonpolarizing at all angles of incidence, according to Baumeister.<sup>244</sup> Costich<sup>245</sup> has described filter designs for use in the near infrared which are relatively independent of polarization at 45° angle of incidence.

## RETARDATION PLATES

**45. Introduction** The theory of retardation plates and especially quarter-wave retarders is given in Chap. 5, "Polarization," in Vol. I of this handbook. The basic relation for retardation plates, Eq. (73) in that section, is

$$N\lambda = d(n_e - n_o) \quad (9)$$

where  $n_o$  = refractive index of the ordinary ray,  $n_e$  = refractive index of the extraordinary ray,  $d$  = physical thickness of the plate, and  $\lambda$  = wavelength.

Retardation plates are generally made of mica, stretched polyvinyl alcohol, and quartz, although other stretched plastics such as cellophane, Mylar, cellulose acetate, cellulose nitrate, sapphire, magnesium fluoride, and other materials can also be used (see West and Makas<sup>246</sup>). Polyvinyl alcohol in sheet form transmits well into the ultraviolet beyond the cutoff for natural mica and is thus particularly useful for ultraviolet retardation plates, according to McDermott and Novick.<sup>91</sup> As suggested by Jacobs *et al.*,<sup>247</sup> permanent birefringence can be thermomechanically induced in the borosilicate optical glass ARG-2, making it an attractive alternate to natural crystalline quartz and mica for large aperture wave plates for laser systems. Refractive indexes and birefringences of some materials are listed in Tables 7 and 8. The birefringences reported for mica and apophyllite should be

**TABLE 7** Refractive Indices of Selected Materials at 5893 Å (Billings, Ref. 248)

Material	$n_o$	$n_e$
Positive uniaxial crystals		
Ice, H <sub>2</sub> O	1.309	1.313
Sellaite, MgF <sub>2</sub>	1.378	1.390
Apophyllite, 2[KCa <sub>4</sub> Si <sub>8</sub> O <sub>20</sub> (F, OH)·8H <sub>2</sub> O]	1.535±	1.537±
Crystalline quartz, SiO <sub>2</sub>	1.544	1.553
Diopase, CuSiO <sub>3</sub> ·H <sub>2</sub> O	1.654	1.707
Zircon, ZrSiO <sub>4</sub>	1.923±	1.968±
Rutile, TiO <sub>2</sub>	2.616	2.903
Negative uniaxial crystals		
Beryl (emerald), Be <sub>3</sub> Al <sub>2</sub> (SiO <sub>3</sub> ) <sub>6</sub>	1.581±	1.575±
Sodium nitrate, NaNO <sub>3</sub>	1.584	1.336
Muscovite mica (complex silicate)	1.5977±	1.5936±
Apatite, Ca <sub>10</sub> (F, Cl) <sub>2</sub> (PO <sub>4</sub> ) <sub>6</sub>	1.634	1.631
Calcite, CaCO <sub>3</sub>	1.658	1.486
Tourmaline (complex silicate)	1.669±	1.638±
Sapphire, Al <sub>2</sub> O <sub>3</sub>	1.768	1.760

**TABLE 8** Birefringence  $n_e - n_o$  of Various Optical Materials<sup>a</sup>

Wave-length, $\mu\text{m}$	Rutile <sup>b</sup> TiO <sub>2</sub>	CdSe <sup>b</sup>	Cryst- alline quartz <sup>c-e</sup>	MgF <sub>2</sub> <sup>d,h,i</sup>	CdS <sup>f-l</sup>	Apo- phyl- lite <sup>m</sup>	ZnS/ (Wurt- zite)	Cal- cite <sup>c</sup>	LiNbO <sub>3</sub> <sup>n</sup>	BaTiO <sub>3</sub> <sup>o</sup>	ADP <sup>p</sup>	KDP <sup>p</sup>	Sap- phire <sup>d,h,q,r</sup> (Al <sub>2</sub> O <sub>3</sub> )	Mica <sup>s</sup>
0.15	—	—	0.0214	0.0143	—	—	—	-0.326	—	—	-0.0613	-0.0587	-0.0111	—
0.20	—	—	0.0130	0.0134	—	—	—	-0.234	—	—	-0.0543	-0.0508	-0.0097	—
0.25	—	—	0.0111	0.0128	—	—	—	-0.206	—	—	-0.0511	-0.0474	-0.0091	—
0.30	—	—	0.0103	0.0125	—	—	—	-0.193	—	—	-0.0492	-0.0456	-0.0087	—
0.35	—	—	0.0098	0.0122	—	—	—	-0.184	—	—	-0.0482	-0.0442	-0.0085	—
0.40	—	—	0.0096	0.0121	—	—	0.004	-0.184	—	—	-0.0473	-0.0432	-0.0083	-0.00457
0.45	0.338	—	0.00937	0.0120	—	0.0019	0.004	-0.179	-0.1049	-0.097	-0.0473	-0.0432	-0.0082	-0.00468
0.50	0.313	—	0.00925	0.0119	—	0.0022	0.004	-0.176	-0.0998	-0.079	-0.0465	-0.0424	-0.0082	-0.00476
0.55	0.297	—	0.00917	0.0118	0.014	0.0024	0.004	-0.173	-0.0947	-0.070	-0.0458	-0.0417	-0.0081	—
0.60	0.287	—	0.00909	0.0118	0.018	0.0026	0.004	-0.172	-0.0919	-0.064	-0.0451	-0.0410	-0.0081	—
0.65	0.279	—	0.00903	0.0117	0.018	0.0028	0.004	-0.170	-0.0898	—	-0.0444	-0.0403	-0.0080	-0.00482
0.70	0.274	—	0.00898	0.0117	0.018	0.004	0.004	-0.169	-0.0882	—	-0.0438	-0.0396	-0.0080	-0.00483
0.80	0.265	—	0.0089	0.0116	0.018	0.004	0.004	-0.167	-0.0857	—	-0.0425	-0.0382	-0.0079	—
0.90	0.262	0.0195	0.0088	0.0115	0.018	0.004	0.004	-0.165	-0.0840	—	-0.0411	-0.0367	-0.0079	—
1.00	0.259	0.0195	0.0088	0.0114	0.018	0.004	0.004	-0.164	-0.0827	—	-0.0396	-0.0350	—	—
1.10	0.256	0.0195	0.0087	0.0114	0.018	0.004	0.004	-0.162	-0.0818	—	-0.0379	-0.0332	—	—
1.20	0.254	0.0195	0.0087	0.0114	0.017	0.004	0.004	-0.161	-0.0810	—	-0.0361	-0.0313	—	—
1.30	0.252	0.0195	0.0086	0.0113	0.017	0.004	0.004	-0.160	-0.0804	—	-0.342	-0.0292	—	—
1.40	0.251	0.0195	0.0085	0.0113	0.017	0.004	0.004	-0.158	-0.0798	—	-0.0321	-0.0269	—	—
1.50	0.250	0.0195	0.0085	0.0113	—	—	—	-0.157	-0.0793	—	-0.0298	-0.0245	—	—
1.60	0.249	0.0195	0.0084	0.0112	—	—	—	-0.156	-0.0788	—	-0.0274	-0.0219	—	—
1.70	0.248	0.0195	0.0084	0.0112	—	—	—	-0.154	-0.0782	—	-0.0248	-0.0191	—	—
1.80	0.247	0.0195	0.0083	0.0112	—	—	—	-0.153	-0.0777	—	-0.0221	-0.0162	—	—
1.90	0.246	0.0195	0.0082	0.0112	—	—	—	-0.151	-0.0774	—	-0.0192	-0.0130	—	—
2.00	0.246	0.0195	0.0081	0.0111	—	—	—	-0.150	-0.0771	—	-0.0161	-0.0097	—	—
2.10	0.245	0.0195	0.0081	0.0111	—	—	—	-0.148	-0.0766	—	—	—	—	—
2.20	0.244	0.0195	0.0080	0.0111	—	—	—	—	-0.0761	—	—	—	—	—
2.30	0.243	0.0195	0.0079	0.0110	—	—	—	—	-0.0752	—	—	—	—	—
2.40	0.241	0.0195	0.0078	0.0110	—	—	—	—	-0.0744	—	—	—	—	—
2.50	—	0.0195	0.0077	0.0110	—	—	—	—	-0.0739	—	—	—	—	—
2.60	—	0.0195	0.0076	0.0110	—	—	—	—	-0.0734	—	—	—	—	—

<sup>a</sup> Calculated values at 24.8°C obtained from analytical expressions are given for crystalline quartz, MgF<sub>2</sub>, calcite, ADP, and KDP by Beckers, Ref. 249.  
<sup>b</sup> Bond, Ref. 250.  
<sup>c</sup> Shields and Ellis, Ref. 251.  
<sup>d</sup> Chandrasekharan and Damany, Ref. 73.  
<sup>e</sup> Palik and Hennis, Ref. 252.  
<sup>f</sup> Boyd *et al.*, Ref. 253.  
<sup>g</sup> Jeppeson, Ref. 254.  
<sup>h</sup> Ballard *et al.*, Ref. 255.  
<sup>i</sup> Ennos and Opperman, Ref. 256.  
<sup>j</sup> Palik, Ref. 257.  
<sup>k</sup> Gobrecht and Bartschat, Ref. 258.  
<sup>l</sup> Shumate, Ref. 258a.  
<sup>m</sup> Loewenstein, Ref. 259.  
<sup>n</sup> Maillard, Ref. 261.  
<sup>o</sup> Bieniewski and Czyzak, Ref. 262.  
<sup>p</sup> Françon *et al.*, Ref. 263.  
<sup>q</sup> Zernike, Ref. 264.  
<sup>r</sup> Zernike, Ref. 264.  
<sup>s</sup> Einsporn, Ref. 265.

considered as approximate, since they are measurements made on single samples. There is good reason to believe that the birefringence of apophyllite may be different for other samples, (see Par. 53). Although calcite would seem at first to be a good material for retardation plates, its birefringence is so high that an extremely thin piece, less than  $1\ \mu\text{m}$ , would be required for a single  $\lambda/4$  retardation plate. If a “first-order” or multiple-order plate were constructed (Pars. 48 and 50), or if calcite were used as one component of an achromatic retardation plate (Par. 53), the tolerance on the thickness would be very stringent.

Retardation plates are generally made of a single piece of material, although when the thickness required for a plate is too small, two thicker pieces may be used with the fast axis of one aligned parallel to the slow axis of the other to cancel out all but the desired retardation. Plates which are a little too thin or a little too thick may be rotated about an axis parallel or perpendicular to the optic axis to change the retardation to the desired amount, as suggested by Gieselmann *et al.*,<sup>266</sup> and Daniels.<sup>267</sup> There are also some novel circular polarizers and polarization rotators for use in the far ultraviolet (see the papers by McIlrath,<sup>162</sup> Saito *et al.*,<sup>268</sup> and Westerveld *et al.*<sup>269</sup>), far infrared (Richards and Smith,<sup>270</sup> Johnston,<sup>271</sup> and Gonates *et al.*<sup>272</sup>), and visible region (Lostis,<sup>273</sup> and Greninger<sup>274</sup>).

Achromatic retardation plates which have the same retardation over a range of wavelengths can be made from two or more different materials or from two or more plates of the same material whose axes are oriented at appropriate angles with respect to each other. These latter devices are known as composite plates (Par. 55 and the earlier Polarization chapter<sup>1</sup>), and although they can change plane-polarized light into circularly polarized light, they do not have all the other properties of true retardation plates. By far the most achromatic  $\lambda/4$  retarders are devices, such as the Fresnel rhomb, which obtain their retardation from internal reflections at angles greater than the critical angle.

Mica retardation plates are mentioned in Par. 46 and are discussed in detail in the earlier Polarization chapter,<sup>1</sup> which includes the theory of multiple reflections; Pars. 47 to 52 are devoted to various types of crystalline-quartz retardation plates, and Par. 53 covers all achromatic retardation plates, except those of the rhomb-type; the latter are mentioned in Par. 54 and in detail by Bennett<sup>275</sup> and also in the earlier Polarization chapter.<sup>1</sup> Various types of composite plates and unusual retardation plates are also described in detail in Ref. 1.

Methods for making and testing quarter-wave plates including ways of splitting mica, how to distinguish between fast and slow axes, methods for measuring retardations close to  $\lambda/4$ , and the tolerance on plate thickness have all been described in detail in the earlier Polarization chapter.<sup>1</sup> An additional paper by Nakadate<sup>276</sup> shows how Young’s fringes can be used for a highly precise measurement of phase retardation.

Waveplates are all sensitive to some degree to temperature changes, variations in the angle of incidence, coherence effects in the light beam, and wavelength variations. Multiple-order plates are much more sensitive than “first-order” or single-order plates. Hale and Day<sup>277</sup> discuss these effects for various types of waveplates and suggest designs that are less sensitive to various parameters.

Most retardation plates are designed to be used in transmission, generally at normal incidence. However, there are also reflection devices that act as quarter-wave and half-wave retarders and polarization rotators. In the vacuum ultraviolet, Westerveld *et al.*<sup>269</sup> produced circularly polarized light by using Au-coated reflection optics. Saito *et al.*<sup>268</sup> used an evaporated Al mirror as a retardation plate at  $1216\ \text{\AA}$ , Lyman  $\alpha$  radiation, following earlier work by McIlrath.<sup>162</sup> Greninger<sup>274</sup> showed that a three-mirror device could be used in place of a half-wave plate to rotate the plane of polarization of a plane-polarized beam and preserve the collinearity of input and output beams. Johnston<sup>271</sup> used a different three-mirror arrangement for the same application in the far-infrared. Thonn and Azzam<sup>157</sup> designed three-reflection half-wave and quarter-wave retarders from single-layer dielectric coatings on metallic film substrates. They showed calculations for ZnS-Ag film-substrate retarders used at  $10.6\ \mu\text{m}$ . Previously Zaghloul, Azzam, and

Bashara<sup>278,279</sup> had proposed using a SiO<sub>2</sub> film on Si as an angle-of-incidence tunable reflection retarder for the 2537-Å mercury line in the ultraviolet spectral region. Kawabata and Suzuki<sup>280</sup> showed that a film of MgF<sub>2</sub> on Ag was superior to Zaghoul *et al.*'s design at 6328 Å. They also performed calculations using Al, Cu, and Au as the metals and concluded that Ag worked best.

**46. Mica Retardation Plates** Mica quarter-wave plates can be made by splitting thick sheets of mica down to the appropriate thickness, as described by Chu *et al.*,<sup>281</sup> and in the earlier Polarization chapter.<sup>1</sup> Since the difference between the velocities of the ordinary and extraordinary rays is very small, the mica sheets need not be split too thin; typical thicknesses lie in the range 0.032 to 0.036 mm for yellow light. The fast and slow axes of a mica quarter-wave plate can be distinguished using Tutton's test, as mentioned in Strong's book,<sup>282</sup> and the retardation can be measured using one of several rather simple tests.<sup>1</sup>

If the mica sheets are used without glass cover plates, multiply reflected beams in the mica can cause the retardation to oscillate around the value calculated from the simple theory, as described in the earlier Polarization chapter.<sup>1</sup> Fortunately this effect can be eliminated in one of several ways.<sup>1</sup> Mica does have one serious drawback. There are zones in the cleaved mica sheets which lie at angles to each other and which do not extinguish at the same angle, as noted by Smith.<sup>283</sup> Thus, extinction cannot be obtained over the whole sheet simultaneously. In very critical applications such as ellipsometry, much better extinction can be obtained using quarter-wave plates made of crystalline quartz (Pars. 47 to 50), which do not exhibit this effect. Properties of mica quarter-wave plates and methods for making and testing all  $\lambda/4$  plates are discussed in detail in the earlier Polarization chapter.<sup>1</sup>

### Crystalline-Quartz Retardation Plates

**47.** Crystalline quartz is also frequently used for retardation plates, particularly those of the highest quality. It escapes the problem of zones with different orientations like those found in mica. The thickness of quartz required for a single quarter-wave retardation at the 6328-Å helium-neon laser line is about 0.017 mm, much too thin for convenient polishing. If the plate is to be used in the infrared, single-order quarter-wave plates are feasible (Par. 49). Two types of quartz retardation plates are generally employed in the visible and ultraviolet regions: so-called "first-order" plates made of two pieces of material (Par. 48), which are the best for critical applications, and multiple-order plates made of one thick piece of crystalline quartz (Pars. 50 to 52). The multiple-order plates are generally not used for work of the highest accuracy since they are extremely sensitive to small temperature changes (Par. 51) and to angle of incidence. Also, they have  $\lambda/4$  retardation only at certain wavelengths; at other wavelengths the retardation may not even be close to  $\lambda/4$ .

When using any of the different types of retardation plates at a single wavelength, the methods for measuring the retardation and for distinguishing between fast and slow axes given in the earlier Polarization chapter<sup>1</sup> can be used.

**48. "First-Order" Plates** A so-called "first-order" plate is made by cementing together two nearly equal thicknesses of quartz such that the fast axis of one is aligned parallel to the slow axis of the other (both axes lie in planes parallel to the polished faces). The plate is then polished until the difference in thickness between the two pieces equals the thickness of a single  $\lambda/4$  plate. The retardation of this plate can be calculated from Eq. (9) by setting  $d$  equal to the *difference in thickness* between the two pieces. The "first-order" plate acts strictly like a single-order quarter-wave plate with respect to the variation of

retardation with wavelength, temperature coefficient of retardation, and angle of incidence.

The change in phase retardation with temperature at 6328 Å, as calculated from equations given in the earlier Polarization chapter,<sup>1</sup> is 0.0091°/°C, less than one-hundredth that of the 1.973-mm multiple-order plate discussed in Par 51. The change in retardation with angle of incidence\* at this wavelength is also small:  $(\Delta N)_{10^\circ} = 0.0016$ , as compared with 0.18 for the thick plate (see Par. 52).

A “first-order” quartz  $\lambda/4$  plate has several advantages over a mica  $\lambda/4$  plate. (1) Crystalline quartz has a uniform structure, so that extinction can be obtained over the entire area of the plate at a given angular setting. (2) Since the total plate thickness is generally large, of the order of 1 mm or so, the coherence of the multiple, internally reflected beams is lost and there are no oscillations in the transmitted light or in the phase retardation. (3) Crystalline quartz is not pleochroic, except in the infrared, so that the intensity transmitted along the two axes is the same. (4) Crystalline quartz transmits farther into the ultraviolet than mica, so that “first-order” plates can be used from about 0.185 to 2.0  $\mu\text{m}$  (see Table 8).

**49. Single-Order Plates in the Infrared** Although a crystalline-quartz retardation plate which is  $\lambda/4$  in the visible is too thin to make from a single piece of material, the thickness required for such a plate is larger in the infrared. Jacobs and coworkers<sup>266</sup> describe such a  $\lambda/4$  plate for use at the 3.39- $\mu\text{m}$  helium-neon laser line. They measured the birefringence of quartz at this wavelength and found it to be  $0.0065 \pm 0.0001$ , so that the thickness required for the plate was 0.1304 mm. The actual plate was slightly thinner (0.1278 mm), so that it was tipped at an angle of 10° (rotating it about an axis parallel to the optic axis) to give it exactly  $\lambda/4$  retardation (see Par. 52). Maillard<sup>261</sup> has also measured the birefringence of quartz at 3.39 and 3.51  $\mu\text{m}$  and obtained values of 0.00659 and 0.00642, respectively (both  $\pm 0.00002$ ), in agreement with Jacobs' value. These data lie on a smooth curve extrapolated from the values of Shields and Ellis.<sup>251</sup>

A problem encountered when using crystalline quartz in the infrared is that, in general, the ordinary and extraordinary rays have different absorption coefficients; thus it may be impossible to construct a perfect wave plate regardless of the relative retardation between the rays. For an absorbing wave plate to have a retardation of exactly  $\lambda/4$ , the requirement

$$\left(\frac{n_o + 1}{n_e + 1}\right)^2 \exp\left[-\frac{(\alpha_e - \alpha_o)\lambda}{8(n_e - n_o)}\right] = 1 \quad (10)$$

must be met;<sup>266</sup>  $\alpha_e$  and  $\alpha_o$  are the absorption coefficients for the extraordinary and ordinary rays, respectively. At wavelengths shorter than 3.39  $\mu\text{m}$ , the birefringence is small enough for it to be possible to approximate the condition in Eq. (10) closely whenever  $\alpha_e \approx \alpha_o$ . Values of these quantities are given by Drummond.<sup>285</sup> Gonatas *et al.*<sup>272</sup> concluded that, in the far infrared and submillimeter wavelength region, the effect of different absorption coefficients in the crystalline quartz was small and could be corrected for.

Another problem which occurs for crystalline quartz and also for sapphire<sup>272</sup> in the infrared is that the Fresnel reflection coefficients are slightly different for the ordinary and extraordinary rays since the refractive indexes and absorption coefficients are in general different. One possible solution is to deposit isotropic thin films on the crystal surfaces.<sup>272</sup> The refractive index of these films is chosen to balance the anisotropic absorption effect by making the Fresnel reflection coefficients appropriately anisotropic. On the other hand, if anisotropic Fresnel reflection proves to be undesirable, it can be greatly diminished by using an antireflection coating, as suggested by Gieselmann *et al.*<sup>266</sup>

\* Grechushnikov<sup>284</sup> has an incorrect relation for the change in phase retardation with angle of incidence [his eq. (2)]. He assumed that the retardations in the two halves of the plate add rather than subtract, yielding a retardation comparable to that of a thick quartz plate.

If a single-order, crystalline-quartz plate is to be used for a continuous range of wavelengths, both the phase retardation and the transmittance of the ordinary and extraordinary rays will oscillate as a function of wavelength because of multiple coherent reflections in the quartz. The separation between adjacent maxima in the phase retardation can be calculated from Eq. (144) in the earlier Polarization chapter.<sup>1</sup> Using  $\lambda = 3.3913 \mu\text{m}$ ,  $n \approx 1.4881$ , and  $d = 127.8 \mu\text{m}$ ,  $\Delta\lambda = 0.03024 \mu\text{m}$ , an amount which should be well-resolved with most infrared instruments. Thus, if a wave plate is to be used over a range of wavelengths, it would be well to antireflect the surfaces to eliminate the phase oscillations.

**50. Multiple-Order Plates** Thick plates made from crystalline quartz are sometimes used to produce circularly polarized light at a single wavelength or a discrete series of wavelengths. The plate thickness is generally of the order of one or more millimeters so that the retardation is an integral number of wavelengths plus  $\lambda/4$ , hence the name multiple-order wave plate. This plate acts like a single  $\lambda/4$  plate providing it is used only at certain specific wavelengths; at other wavelengths it may not even approximate the desired retardation. For example, a 1.973-mm-thick quartz plate was purchased which had an order of interference  $N = 28.25$  at  $6328 \text{ \AA}$ . From Eq. (9) and Table 8, this plate would have  $N = 30.52$  at  $5890 \text{ \AA}$ , and would thus be an almost perfect half-wave plate at this latter wavelength.

If a multiple-order plate is used to produce circularly polarized light at unspecified discrete wavelengths, e.g., to measure circular or linear dichroism, it can be placed following a polarizer and oriented at  $45^\circ$  to the plane of vibration of the polarized beam. When the wavelengths are such that  $N$  calculated from Eq. (9) equals  $1/4$ ,  $3/4$ , or in general  $(2M - 1)/4$  (where  $M$  is a positive integer), the emerging beam will be alternately right and left circularly polarized. The frequency interval  $\Delta\nu$  between wavelengths at which circular polarization occurs is

$$\Delta\nu = \frac{1}{2d(n_e - n_o)} \quad (11)$$

where  $\nu = 1/\lambda$ . If the birefringence is independent of wavelength, the retardation plate will thus produce circularly polarized light at equal intervals on a frequency scale and can conveniently be used to measure circular dichroism, as described by Holzwarth.<sup>286</sup>

In order to approximately calibrate a multiple-order retardation plate at a series of wavelengths, it can be inserted between crossed polarizers and oriented at  $45^\circ$  to the polarizer axis. Transmission maxima will occur when the plate retardation is  $\lambda/2$  or an odd multiple thereof; minima will occur when the retardation is a full wave or multiple thereof. If the axes of the two polarizers are parallel, maxima in the transmitted beam will occur when the plate retardation is a multiple of a full wavelength. The birefringence of the retardation plate can be determined by measuring the wavelengths at which maxima or minima occur if the plate thickness is known. Otherwise  $d$  can be measured with a micrometer, and an approximate value of  $n_e - n_o$  can be obtained.

Palik<sup>287</sup> made and tested a 2.070-mm-thick CdS plate for the 2- to 15- $\mu\text{m}$  infrared region and also made thick retardation plates of SnSe, sapphire, and crystalline quartz to be used in various parts of the infrared. Holzwarth<sup>286</sup> used a cultured-quartz retardation plate 0.8 mm thick to measure circular dichroism in the 1850- to 2500- $\text{\AA}$  region of the ultraviolet; Jaffe *et al.*<sup>288</sup> measured linear dichroism in the ultraviolet using a thick quartz plate and linear polarizer.

**51. Sensitivity to Temperature Changes** Small temperature changes can have a large effect on the retardation of a multiple-order plate. The method for calculating this effect was given in the earlier Polarization chapter.<sup>1</sup> For the 1.973-mm-thick quartz plate

mentioned in Par. 50 ( $N = 28.25$  at  $6328 \text{ \AA}$ ), the phase retardation will decrease  $1.03^\circ$  for each Celsius degree increase in temperature. If the temperature of the wave plate is not controlled extremely accurately, the large temperature coefficient of retardation can introduce sizable errors in precise ellipsometric measurements in which polarizer and analyzer settings can be made to  $\pm 0.01^\circ$ .

**52. Sensitivity to Angle of Incidence** The effect of angle of incidence (and hence field angle) on the retardation was calculated in the earlier Polarization chapter.<sup>1</sup> It was shown there that the change in phase retardation with angle of incidence,  $2\pi(\Delta N)_\theta$ , is proportional to the total thickness of the plate (which is incorporated into  $N$ ) and the square of the angle of incidence when the rotation is about an axis parallel to the optic axis. If the 1.973-mm-thick plate mentioned previously is rotated parallel to the optic axis through an angle of  $10^\circ$  at a wavelength of  $6328 \text{ \AA}$ , the total retardation changes from 28.25 to 28.43, so that the  $\lambda/4$  plate is now nearly a  $\lambda/2$  plate.

If the plate had been rotated about an axis *perpendicular* to the direction of the optic axis, in the limit when the angle of incidence is  $90^\circ$ , the beam would have been traveling along the optic axis; in this case the ordinary and extraordinary rays would be traveling with the same velocities, and there would have been *no retardation* of one relative to the other. For any intermediate angle of incidence the retardation would have been *less than* the value at normal incidence. The relation for the retardation as a function of angle of incidence is not simple, but the retardation will be approximately as angle-sensitive as it was in the other case. An advantage of rotation about either axis is that, with care, one can adjust the retardation of an inexact wave plate to a desired value. Rotation about an axis *parallel* to the optic axis will *increase* the retardation, while rotation about an axis *perpendicular* to the optic axis will *decrease* the retardation.

### Achromatic Retardation Plates

**53.** Achromatic retardation plates are those for which the phase retardation is independent of wavelength. The name arose because when a plate of this type is placed between polarizers, it does not appear colored and hence is achromatic, as shown by Gaudefroy.<sup>289</sup> In many applications, a truly achromatic retardation plate is not required. Since the wavelength of light changes by less than a factor of 2 across the visible region, a quarter- or half-wave mica plate often introduces only tolerable errors even in white light. The errors that do occur cancel out in many kinds of experiments.

Achromatic retardation plates can be made in various ways. The most achromatic are based on the principle of the Fresnel rhomb, in which the phase retardation occurs when light undergoes two or more total internal reflections (Par. 54 and Ref. 1). A material with the appropriate variation of birefringence with wavelength can also be used. Such materials are uncommon, but plates of two or more different birefringent materials can be combined to produce a reasonably achromatic combination. Composite plates, consisting of two or more plates of the same material whose axes are oriented at the appropriate angles, can be used as achromatic circular polarizers or achromatic polarization rotators,<sup>1</sup> although they do not have all the properties of true  $\lambda/4$  or  $\lambda/2$  plates. One unusual achromatic half-wave plate is described in the earlier Polarization chapter.<sup>1</sup>

The simplest type of achromatic retardation plate could be made from a single material if its birefringence satisfied the requirement that  $(n_e - n_o)/\lambda$  be independent of wavelength, i.e., that  $n_e - n_o$  be directly proportional to  $\lambda$ . This result follows from Eq. (9) since  $d(n_e - n_o)/\lambda$  must be independent of  $\lambda$  to make  $N$  independent of wavelength. (The plate thickness  $d$  is constant.) The birefringences of various materials are listed in Table 8 and

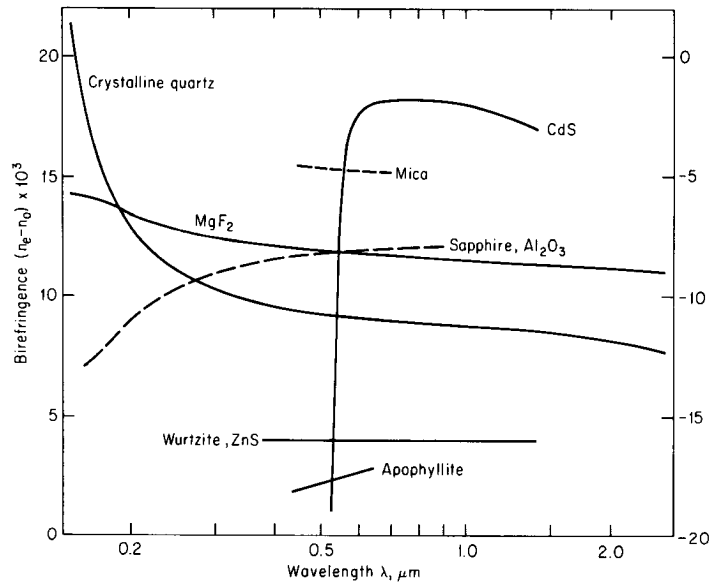


**FIGURE 18** Birefringence of various optical materials as a function of wavelength. The scale at the left is for materials having a positive birefringence (*solid curves*), and the scale at the right is for materials with a negative birefringence (*dashed curves*).

plotted in Figs. 18 and 19. Only one material, the mineral apophyllite, has a birefringence which increases in the correct manner with increasing wavelength.<sup>263</sup> \* A curve of the phase retardation vs. wavelength for a quarter-wave apophyllite plate is shown as curve *D* in Fig. 20. Also included are curves for other so-called achromatic  $\lambda/4$  plates as well as for simple  $\lambda/4$  plates of quartz and mica. The phase retardation of apophyllite is not as constant with  $\lambda$  as that of the rhomb-type retarders, but it is considerably more constant than that of the other "achromatic"  $\lambda/4$  plates. Since the birefringence of apophyllite is small, a  $\lambda/4$  plate needs a thickness of about  $56.8 \mu\text{m}$ , which is enough for it to be made as a single piece rather than as a "first-order" plate. Unfortunately optical-grade apophyllite is rare, the sample for which data are reported here having come from Sweden. There is some indication that the optical properties of other apophyllite samples may be different. Isotropic, positive, and negative-birefringent specimens have been reported by Deer *et al.*<sup>290</sup> According to them, the optical properties of apophyllite are often anomalous, some specimens being isotropic, uniaxial negative, or even biaxial with crossed dispersion of optic axial planes. Whether many samples have the favorable birefringence of the Swedish sample is uncertain.

Certain types of plastic film stretched during the manufacturing process have birefringences which are nearly proportional to wavelength and can serve as achromatic retardation plates if they have the proper thickness, as pointed out by West and Makas.<sup>246</sup> Curve *C* in Fig. 20 is the retardation of a stretched cellulose nitrate film as measured by West and Makas.<sup>246</sup> A combination of stretched cellulose acetate and cellulose nitrate sheets with their axes parallel will also make a reasonably achromatic  $\lambda/4$  plate over the visible region. The advantages of using stretched plastic films for retardation plates are that they are cheap, readily available, have a retardation which is uniform over large areas,

\* For materials having a negative birefringence the requirement is that  $-(n_e - n_o)$  be proportional to  $\lambda$ .

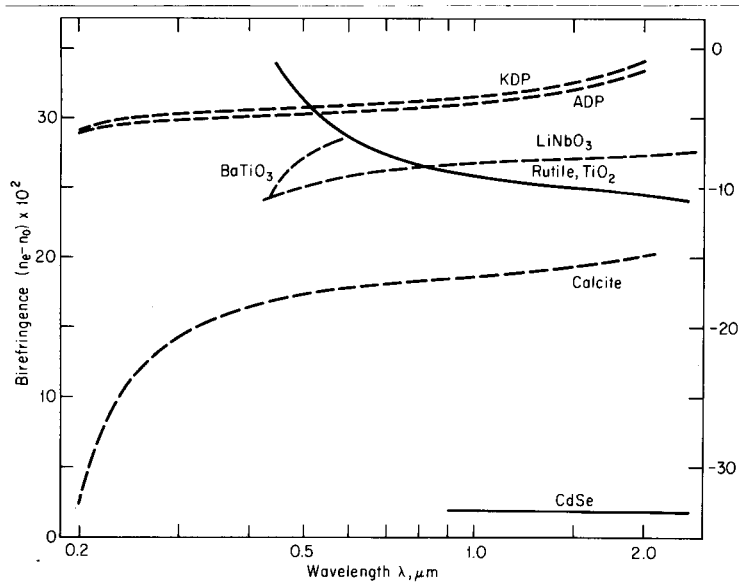


**FIGURE 19** Birefringence of various optical materials which have larger birefringences than those shown in Fig. 18. The scale at the left is for materials having a positive birefringence (*solid curves*), and the scale at the right is for materials with a negative birefringence (*dashed curves*).

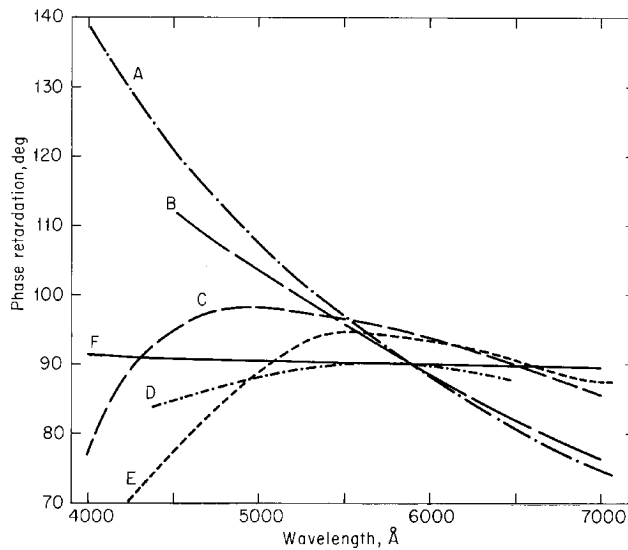


**FIGURE 20** Curves of the phase retardation vs. wavelength for  $\lambda/4$  plates; *A*, quartz; *B*, mica; *C*, stretched plastic film; *D*, apophyllite; and *E*, quartz-calcite achromatic combination. Curve *F* is for a Fresnel rhomb but is representative of all the rhomb-type devices. (*Bennett, Ref. 275.*)

and can be used in strongly convergent light. However, each sheet must be individually selected since the birefringence is a strong function of the treatment during the manufacturing process and the sheets come in various thicknesses, with the result that their retardations are not necessarily  $\lambda/4$  or  $\lambda/2$ . Also, Ennos<sup>291</sup> found that while the magnitude of the retardation was uniform over large areas of the sheets, the direction of the effective crystal axis varied from point to point by as much as  $1.5^\circ$  on the samples he was testing. Thus, film retarders appear to be excellent for many applications but are probably not suitable for measurements of the highest precision.

A reasonably achromatic retardation plate can be constructed from pairs of readily available birefringent materials such as crystalline quartz, sapphire, magnesium fluoride, calcite, or others whose birefringences are listed in Table 8. Assume that the plate is to be made of materials  $a$  and  $b$  having thicknesses  $d_a$  and  $d_b$ , respectively (to be calculated), and that it is to be achromatized at wavelengths  $\lambda_1$  and  $\lambda_2$ . From Eq. (9) we can obtain the relations

$$N\lambda_1 = d_a \Delta n_{1a} + d_b \Delta n_{1b} \quad (12)$$

$$N\lambda_2 = d_a \Delta n_{2a} + d_b \Delta n_{2b}$$

where  $N = \frac{1}{4}$  for a  $\lambda/4$  plate,  $\frac{1}{2}$  for a  $\lambda/2$  plate, etc., and the  $\Delta n$ 's are values of  $n_e - n_o$  for the particular materials at the wavelengths specified;  $\Delta n$  will be positive for a positive uniaxial crystal and negative for a negative uniaxial crystal. (A positive uniaxial material can be used with its fast axis crossed with that of another positive uniaxial material; in this case the first material will have a negative  $\Delta n$ .) Equations (12) can be solved for  $d_a$  and  $d_b$ :

$$d_a = \frac{N(\lambda_1 \Delta n_{2b} - \lambda_2 \Delta n_{1b})}{\Delta n_{1a} \Delta n_{2b} - \Delta n_{1b} \Delta n_{2a}} \quad d_b = \frac{N(\lambda_2 \Delta n_{1a} - \lambda_1 \Delta n_{2a})}{\Delta n_{1a} \Delta n_{2b} - \Delta n_{1b} \Delta n_{2a}} \quad (13)$$

As an example of a compound plate, let us design a  $\lambda/4$  plate of crystalline quartz and calcite and achromatize it at wavelengths  $\lambda_1 = 0.508 \mu\text{m}$  and  $\lambda_2 = 0.656 \mu\text{m}$ . Quartz has a positive birefringence and calcite a negative birefringence (Table 8) so that  $\Delta n_{1a}$  and  $\Delta n_{2a}$  (for quartz) are positive and  $\Delta n_{1b}$  and  $\Delta n_{2b}$  (for calcite) are negative. Equations (13) are satisfied for  $d_{\text{qtz}} = 426.2 \mu\text{m}$  and  $d_{\text{calc}} = 21.69 \mu\text{m}$ ; thus the phase retardation is exactly  $90^\circ$  at these two wavelengths. An equation of the form of those in Eqs. (12) is now used to calculate  $N$  for all wavelengths in the visible region using birefringence values listed in Table 8, and the results are plotted as curve  $E$  in Fig. 20. Although the achromatization for this quartz-calcite combination is not as good as can be obtained with a rhomb-type device or apophyllite, the phase retardation is within  $\pm 5^\circ$  of  $90^\circ$  in the wavelength region 4900 to 7000 Å and is thus much more constant than the retardation of a single mica or quartz  $\lambda/4$  plate. Better two-plate combinations have been calculated by Beckers,<sup>249</sup> the best being  $\text{MgF}_2$ -ADP and  $\text{MgF}_2$ -KDP, which have maximum deviations of  $\pm 0.5$  and  $\pm 0.4$  percent, respectively, compared with  $\pm 7.2$  percent for a quartz-calcite combination over the same 4000- to 7000-Å wavelength region. The thicknesses of the materials which are required to produce  $\lambda/4$  retardation\* are  $d_{\text{MgF}_2} = 113.79 \mu\text{m}$ ,  $d_{\text{ADP}} = 26.38 \mu\text{m}$ , and  $d_{\text{MgF}_2} = 94.47 \mu\text{m}$ ,  $d_{\text{KDP}} = 23.49 \mu\text{m}$ . Since the ADP and KDP must be so thin, these components could be made in two pieces as "first-order" plates.

Other two-component compound plates have been proposed by Chandrasekharan and Damany,<sup>260</sup> Gaudefroy,<sup>289</sup> Ioffe and Smirnova,<sup>292</sup> and Mitchell.<sup>293</sup> The paper by Ioffe and Smirnova describes a quartz-calcite combination similar to the one illustrated above, but it contains various numerical errors which partially invalidate the results.

\* Beckers' tables II to V give the thickness of materials required to produce one full-wave retardation. To obtain values of thicknesses for  $\lambda/4$  retardation, for example, multiply all  $d$  values in the table by 0.25. The percent deviations should remain unchanged.

If better achromatization is desired and one does not wish to use a rhomb-type  $\lambda/4$  device, three materials can be used which satisfy the relations

$$\begin{aligned} N\lambda_1 &= d_a \Delta n_{1a} + d_b \Delta n_{1b} + d_c \Delta n_{1c} \\ N\lambda_2 &= d_a \Delta n_{2a} + d_b \Delta n_{2b} + d_c \Delta n_{2c} \\ N\lambda_3 &= d_a \Delta n_{3a} + d_b \Delta n_{3b} + d_c \Delta n_{3c} \end{aligned} \quad (14)$$

where the  $\Delta n$ 's are birefringences of the various materials at wavelengths  $\lambda_1$ ,  $\lambda_2$ , and  $\lambda_3$ .

Instead of using only three wavelengths, Beckers<sup>249</sup> suggested that the thicknesses can be optimized such that the maximum deviations from achromatization are minimized over the entire wavelength interval desired. In this way, he obtained a three-component combination of quartz, calcite, and  $\text{MgF}_2$  which has a retardation of a full wavelength and a maximum deviation of only  $\pm 0.2$  percent over the 4000- to 7000-Å wavelength region. The maximum deviation of slightly different thicknesses of these same three materials rises to  $\pm 2.6$  percent if the wavelength interval is extended to 3000 to 11,000 Å. Chandrasekharan and Damany<sup>260</sup> have designed a three-component  $\lambda/4$  plate from quartz,  $\text{MgF}_2$ , and sapphire for use in the vacuum ultraviolet. Title<sup>294</sup> has designed achromatic combinations of three-element, four-element, nine-element, and ten-element waveplates using Jones matrix techniques. The nine-element combination is achromatic to within  $1^\circ$  from 3500 to 10,000 Å. He constructed and tested several waveplate combinations, and they performed as designed.

### Rhombs as Achromatic $\lambda/4$ Retarders

54. The simplest stable, highly achromatic  $\lambda/4$  retarder with a reasonable acceptance angle and convenient size appears to be a rhomb-type retarder. Several types are available; the choice of which one to use for a specific application depends on (1) the geometry of the optical system (can a deviated or displaced beam be tolerated?), (2) wavelength range, (3) degree of collimation of the beam, (4) beam diameter (determining the aperture of the retarder), (5) space available, and (6) accuracy required. Table 9 summarizes the properties of the various achromatic rhombs. This subject has been covered in detail by

**TABLE 9** Properties of Achromatic Rhombs (Bennett, Ref. 275)

Name	Light path	Internal angle of incidence, deg	Material	Variation of phase retardation					
				Refractive index		With wavelength		With angle of incidence	
				$n$	Wave-length, Å	Var., deg	Wave-length, Å	Var., deg.	Angle, deg
Fresnel rhomb	Translated	54.7	Crown glass	1.511	5893	2.5	3650–7682	9.1	–7 to +7
Coated Fr. rhomb	Translated	51.5	Crown glass	1.5217	5461	0.4	3341–5461	2.5	–4 to +6
	Translated	54.0	Fused quartz	1.4880	3000	0.7	2148–3341	<0.5	–1.5 to +1.5
Mooney rhomb	Deviated	60.0	Flint glass	1.650	5893	1.9	4047–6708	0.7	–7 to +7
AD-1	Undeviated	74.3	Fused quartz	1.4702	4000	2.0	3000–8000	0.7	–7 to +7
AD-2	Undeviated	73.2, 56.4	Fused quartz	1.4702	4000	2.9	3000–8000	13.2	–3 to +3
Coated AD-2	Undeviated	72.2	Fused quartz	1.4601	5461	0.3	2140–5461	6.0	–1.5 to +1.5
AD	Undeviated	53.5	Crown glass	1.511	5893	1.6	3650–7682	9.4	–7 to +7

Bennett,<sup>275</sup> and is condensed from that reference in the earlier Polarization chapter.<sup>1</sup> Anderson<sup>295</sup> has compared the retardation of a CdS  $\lambda/4$  plate and a Fresnel rhomb in the 10- $\mu\text{m}$  CO<sub>2</sub> laser emission region. Wizinowich<sup>296</sup> used a Fresnel rhomb along with some additional optics to change an unpolarized light beam from a faint star object into linearly polarized light to improve the throughput of a grating spectrograph and make it independent of the input polarization.

### Composite Retardation Plates

**55.** A composite retardation plate is made up of two or more elements of the same material combined so that their optic axes are at appropriate angles to each other. Some of the composite plates have nearly all the properties of a true retardation plate, whereas others do not. In the earlier Polarization chapter,<sup>1</sup> composite plates were described which produced circularly polarized light at a given wavelength, those which acted as achromatic circular polarizers, and those which acted as achromatic polarization rotators or pseudo  $\lambda/2$  plates. The effect of combining several birefringent plates with their axes at arbitrary angles to each other can be easily understood using the Poincaré sphere. A general treatment of this subject has been given by Ramachandran and Ramaseshan.<sup>297</sup>

## VARIABLE RETARDATION PLATES AND COMPENSATORS

---

**56.** Variable retardation plates can be used to modulate or vary the phase of a beam of plane-polarized light, to measure birefringence in mineral specimens, flow birefringence, or stress in transparent materials, or to analyze a beam of elliptically polarized light such as might be produced by transmission through a birefringent material or by reflection from a metal or film-covered surface. The term compensator is frequently applied to a variable retardation plate since it can be used to compensate for the phase retardation produced by a specimen. Common types of variable compensators include the Babinet and Soleil compensators, in which the total thickness of birefringent material in the light path is changed, the Sénarmont compensator,<sup>1</sup> which consists of a fixed quarter-wave plate and rotatable analyzer to compensate for varying amounts of ellipticity in a light beam, and tilting-plate compensators,<sup>1</sup> with which the total thickness of birefringent material in the light beam is changed by changing the angle of incidence. Electro-optic and piezo-optic modulators can also be used as variable retardation plates since their birefringence can be changed by varying the electric field or pressure. However, they are generally used for modulating the amplitude, phase, frequency, or direction of a light beam, in particular a laser beam, at frequencies too high for mechanical shutters or moving mirrors to follow. Information on electro-optic materials and devices is contained in the chapter on Electro-Optic Modulators by T. A. Maldonado (Chap. 13, Vol II) and in the earlier Polarization chapter.<sup>1</sup>

**57. Babinet Compensator** There are many devices which compensate for differences in phase retardation by having a variable thickness of a birefringent material (such as crystalline quartz) in the light beam, as discussed by Johansen,<sup>298</sup> and Jerrard.<sup>299</sup> One such device, described by Hunt,<sup>300</sup> can compensate for a residual wedge angle between the entrance and exit faces of birefringent optical components such as optical modulators and waveplates.

The most common variable retardation plates are the Babinet compensator and the Soleil compensator. The Babinet compensator was proposed by Babinet in 1837 and later

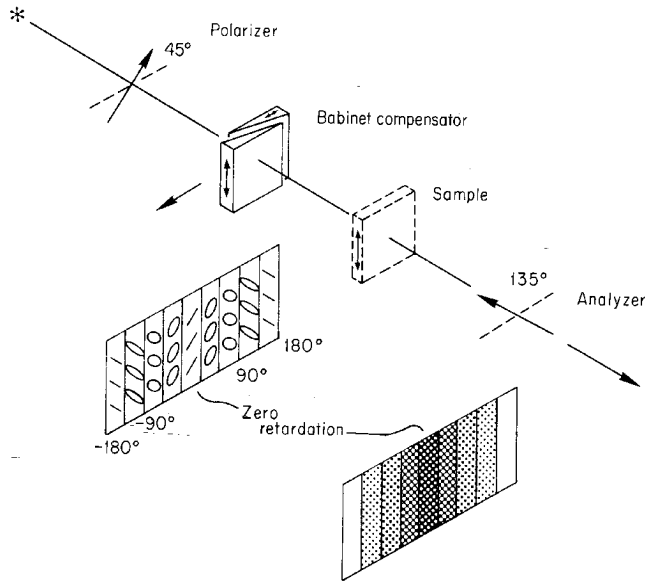


**FIGURE 21** Arrangement of a Babinet compensator, polarizer, and analyzer for measuring the retardation of a sample. The appearance of the field after the light has passed through the compensator is shown to the left of the sample position. Retardations are indicated for alternate regions. After the beam passes through the analyzer, the field is crossed by a series of dark bands, one of which is shown to the left of the analyzer.

modified by Jamin; references to the voluminous early literature are given by Partington.<sup>301</sup> Ellerbroek and Groosmuller<sup>302</sup> have a good description of the theory of operation (in German), and Jerrard<sup>303-305</sup> and Archard<sup>306</sup> describe various optical and mechanical defects of Babinet compensators.

The Babinet compensator, shown schematically in Fig. 21, consists of two crystalline-quartz wedges, each with its optic axis in the plane of the face but with the two optic axes exactly 90° apart. One wedge is stationary, and the other is movable by means of a micrometer screw in the direction indicated by the arrow, so that the total amount of quartz through which the light passes can be varied uniformly. In the first wedge, the extraordinary ray vibrates in a horizontal plane and is retarded relative to the ordinary ray (crystalline quartz has a positive birefringence; see Table 8). When the rays enter the second wedge, the ray vibrating in the horizontal plane becomes the ordinary ray and is advanced relative to the ray vibrating in the vertical plane. Thus, the total retardation is proportional to the difference in thickness between the two wedges:

$$N\lambda = (d_1 - d_2)(n_e - n_o) \tag{15}$$

where  $N$  = retardation in integral and fractional parts of a wavelength

$d_1, d_2$  = thickness of the first and second wedges where light passes through

$n_o, n_e$  = ordinary and extraordinary refractive indexes for crystalline quartz

If light polarized at an angle of 45° to one of the axes of the compensator passes through

it, the field will appear as shown in Fig. 21; the wedges have been set so there is zero retardation at the center of the field. (If the angle  $\alpha$  of the incident plane-polarized beam were different from  $45^\circ$ , the beam retarded or advanced by  $180^\circ$  in phase angle would make an angle of  $2\alpha$  instead of  $90^\circ$  with the original beam.) When an analyzer whose axis is crossed with that of the polarizer is used to observe the beam passing through the compensator, a series of light and dark bands is observed in monochromatic light. In white light only one band, that for which the retardation is zero, remains black. All the other bands are colored. These are the bands for which the retardation is multiples of  $2\pi$  (or, expressed in terms of path differences, integral numbers of wavelengths). On one side of the central black band one ray is advanced in phase relative to the other ray; on the other side it is retarded. If one wedge is moved, the whole fringe system translates across the field of view. The reference line is scribed on the stationary wedge so that it remains in the center of the field. Information on calibrating and using a Babinet compensator is given in the earlier Polarization chapter.<sup>1</sup>

**58. Soleil Compensator** The Soleil compensator (see Wood<sup>307</sup> and Ditchburn<sup>308</sup>), sometimes called a Babinet-Soleil compensator, is shown in Fig. 22. It is similar to the Babinet compensator in the way it is used, but instead of having a field crossed with alternating light and dark bands in monochromatic light, the field has a uniform tint if the compensator is constructed correctly. This is because the ratio of the thicknesses of the two quartz blocks (one composed of a fixed and a movable wedge) is the same over the entire field. The Soleil compensator will produce light of varying ellipticity depending on the position of the movable wedge. Calibration of the Soleil compensator is similar to that of

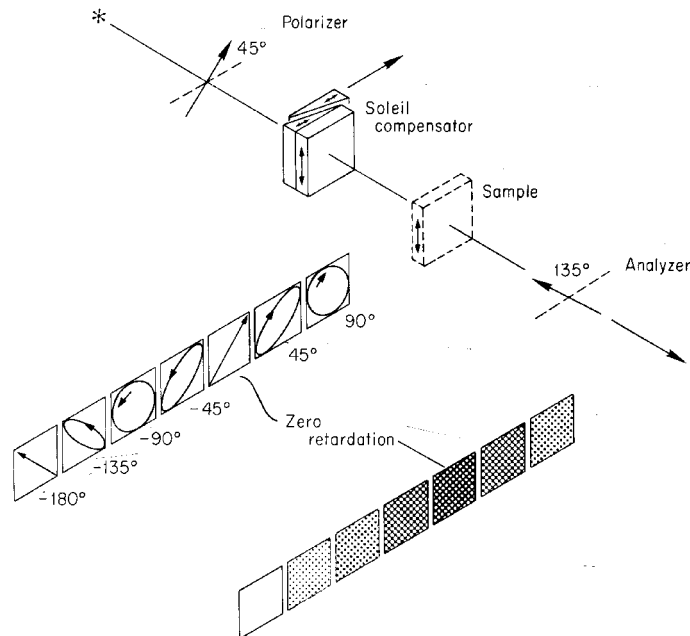


**FIGURE 22** Arrangement of a Soleil compensator, polarizer, and analyzer for measuring the retardation of a sample. The appearance of the field after the light has passed through the compensator is shown to the left of the sample position. After the beam passes through the analyzer, the field appears as one of the shades of gray shown to the left of the analyzer.

the Babinet compensator.<sup>1</sup> The zero-retardation position is found in the same manner except that now the entire field is dark. The compensator is used in the same way as a Babinet compensator with the uniformly dark field (in white light) of the Soleil corresponding to the black zero-retardation band in the Babinet.

The major advantage of the Soleil compensator is that a photoelectric detector can be used to make the settings. The compensator is offset a small amount on each side of the null position so that equal-intensity readings are obtained. The average of the two drum positions gives the null position. Photoelectric setting can be much more precise than visual setting, but this will not necessarily imply increased accuracy unless the compensator is properly constructed. Since Soleil compensators are composed of three pieces of crystalline quartz, all of which must be very accurately made, they are subject to more optical and mechanical defects than Babinet compensators. Jerrard<sup>309-311</sup> has described many of these defects in detail. Ives and Briggs<sup>312</sup> found random departures of about  $\pm 1.5^\circ$  from their straight-line calibration curve of micrometer reading for extinction vs. wedge position. This variation was considerably larger than the setting error with a half-shade plate and was attributed to variations in thickness of the order of  $\pm \lambda/4$  along the quartz wedges.

Soleil compensators have been used for measurements of retardation in the infrared. They have been made of crystalline quartz, cadmium sulfide, and magnesium fluoride (see the work of Palik<sup>257,313</sup> and Palik and Hervis<sup>252</sup>). A by-product of this work was the measurement of the birefringence of these materials in the infrared.

Two other uniform-field compensators have been proposed. Jerrard,<sup>310</sup> following a suggestion by Soleil, has taken the Babinet wedges and reversed one of them so the light passes through the thicker portions of each wedge. This reversed Babinet compensator is less subject to mechanical imperfections than the Soleil compensator but does produce a small deviation of the main beam. Hariharan and Sen<sup>314</sup> suggest double-passing a Babinet compensator (with a reflection between the two passes) to obtain a uniform field.

## HALF-SHADE DEVICES

---

**59.** It is sometimes necessary to measure accurately the azimuth of a beam of plane-polarized light, i.e., the angle the plane of vibration makes with a reference coordinate system. This can be done most easily by using a polarizer as an analyzer and rotating it to the position where the field appears the darkest. The analyzer azimuth is then exactly  $90^\circ$  from the azimuth of the plane-polarized beam. A more sensitive method is to use a photoelectric detector and offset on either side of the extinction position at angles where the intensities are equal. The average of these two angles is generally more accurate than the value measured directly, but care must be taken to keep the angles small so that asymmetries will not become important.

Before the advent of sensitive photoelectric detectors, the most accurate method of setting on a minimum was to use a half-shade device as the analyzer or in conjunction with the analyzer. The device generally consisted of two polarizers having their axes inclined at an angle  $\alpha$  to each other (angle fixed in some types and variable in others). As the device was rotated, one part of the field became darker while the other part became lighter. At the match position, both parts of the field appeared equally bright. The Jellett-Cornu prism, Lippich and Laurent half shades, Nakamura biplate, and Savart plate are examples of half-shade devices.<sup>1</sup>

Ellipticity half-shade devices are useful for detecting very small amounts of ellipticity in a nominally plane-polarized beam and hence can indicate when a compensator has completely converted elliptically polarized light into plane-polarized light. Two of these devices are the Bravais biplate and the Brace half-shade plate. Half-shade devices for both

plane and elliptically polarized light are described in detail in the earlier Polarization chapter.<sup>1</sup>

## MINIATURE POLARIZATION DEVICES

---

**60. Polarization Devices for Optical Fibers** Single-mode optical fiber-type polarizers are important devices for optical fiber communication and fiber sensor systems. These polarizers have been made by a variety of techniques. Polarizers have been made by bending<sup>315</sup> or by tapering<sup>316</sup> a birefringent fiber to induce differential attenuation in the orthogonal modes. In most cases a fiber was polished laterally and some device was placed in contact with the exposed guiding region of the fiber to couple out the unwanted polarization. Bergh *et al.*<sup>317</sup> used a birefringent crystal as the outcoupling device and obtained a high extinction ratio polarizer. Optical fiber polarizers made with a metal film coated onto the polished area to eliminate the unwanted polarization state seem to be preferred because they are stable and rugged. The original version by Eickhoff<sup>318</sup> used the thin cladding remaining after polishing as the buffer layer, but it had an insufficient extinction ratio. Other designs using metal coatings were suggested by Gruchmann *et al.*,<sup>319</sup> and Hosaka *et al.*<sup>320</sup> Feth and Chang<sup>321</sup> used a fiber polished into its core to which a superstrate coated with a very thin metal layer was attached by an index-matching oil. Yu and Wu<sup>322</sup> gave a theoretical analysis of metal-clad single-mode fiber-type polarizers. Dyott *et al.*<sup>323</sup> made a metal-fiber polarizer from an etched D-shaped fiber coated with indium.

In the above approaches, either expensive components are used or the structure of the polarizer is complicated and fragile. Lee and Chen<sup>324</sup> suggested a new way of fabricating high-quality metal-clad polarizers by polishing a fiber  $\sim 0.4\ \mu\text{m}$  into its core and then overcoating it with a 265-nm  $\text{MgF}_2$  film as the buffer layer followed by a 100-nm Al film. Polarizers fabricated in this way had an average extinction ratio of 28 dB with a 2-dB insertion loss at a 0.63- $\mu\text{m}$  wavelength or a 34-dB extinction ratio with a 3-dB insertion loss at 0.82  $\mu\text{m}$ .<sup>324</sup>

Other devices for optical fibers have also been designed. Ulrich and Johnson<sup>325</sup> made a single-mode fiber-optical polarization rotator by mechanically twisting successive half-wave fiber sections in alternating directions; Hosaka *et al.*'s fiber circular polarizer<sup>326</sup> was composed of a metal-coated fiber polarizer and a  $\lambda/4$  platelet fabricated on a birefringent fiber; polished-type couplers acting as polarizing beam splitters were made by Snyder and Stevenson.<sup>327</sup> The patent literature contains references to other polarization devices for optical fibers.

**61. Polarization Devices for Integrated Circuits** Small and highly efficient polarization devices are also needed for integrated circuits. Some such devices have been proposed and fabricated. Uehara *et al.*<sup>328</sup> made an optical waveguiding polarizer for optical fiber transmission out of a plate of calcite attached to borosilicate glass into which a three-dimensional high-index region had been formed by ion migration to act as the waveguide. Mahlein<sup>329</sup> deposited a multilayer dielectric film onto a glass superstrate which was then contacted to a planar waveguide to couple out the TM polarization. This paper contains a good description of the polarizer design as well as extensive references. Suchoski *et al.*<sup>330</sup> fabricated low-loss, high-extinction polarizers in  $\text{LiNbO}_3$  by proton exchange. Noé *et al.*<sup>331</sup> achieved automatic endless polarization control with integrated optical  $\text{Ti}:\text{LiNbO}_3$  polarization transformers. This was a better method of matching polarization states between two superposed waves than techniques that had been used previously. Finally, Baba *et al.*<sup>332</sup> proposed making a polarizer for integrated circuits out of periodic metal-dielectric laminated layers (Lamipol structures). Their experiments with  $\text{Al-SiO}_2$  structures were encouraging. Patents have been filed for other polarization devices for integrated circuits.

## REFERENCES\*

1. H. E. Bennett and J. M. Bennett, "Polarization," in W. G. Driscoll and W. Vaughan, (eds.), *Handbook of Optics*, 1st ed., McGraw-Hill, New York, 1978, pp. 10-1-10-164.
2. H. J. Nickl and H. K. Henisch, *J. Electrochem. Soc.* **116**, pp. 1258-1260, 1969.
3. R. N. Smartt, *J. Sci. Instrum.* **38**, p. 165, 1961.
4. E. E. Wahlstrom, *Optical Crystallography*, 4th ed. Wiley, New York, 1969, pp. 236-267.
5. E. Uzan, H. Damany, and V. Chandrasekharan, *Opt. Commun.* **1**, pp. 221-222, 1969.
6. S. S. Ballard, J. S. Browder, and J. F. Ebersole, in D. E. Gray (ed.), *American Institute of Physics Handbook*, 3d ed., McGraw-Hill, New York, 1972, p. 6-20.
7. J. Schnellman, V. Chandrasekharan, H. Damany, and J. Romand, *C. R. Acad. Sci.* **260**, pp. 117-120, 1965.
8. Y. Bouriau and J. Lenoble, *Rev. Opt.* **36**, pp. 531-543, 1957.
9. S. S. Ballard, J. S. Browder, and J. F. Ebersole, in D. E. Gray, (ed.), *American Institute of Physics Handbook*, 3d ed., McGraw-Hill, New York, 1972, p. 6-65.
10. H. Damany, Laboratoire des Hautes Pressions, Bellevue, France, private communication, 1970.
11. E. Uzan, H. Damany, and V. Chandrasekharan, *Opt. Commun.* **2**, pp. 273-275, 1970.
12. M. Born and E. Wolf, *Principles of Optics*, 6th ed. Pergamon Press, New York, 1980, p. 680.
13. L. C. Martin, *Technical Optics*, vol. 1, Pitman, London, 1948, pp. 196-198.
14. R. W. Ditchburn, *Light*, 2d ed. Interscience, New York, 1963, pp. 595-616.
15. A. Schuster, *Theory of Optics*, 2d ed, Arnold, London, 1920, pp. 168-187.
16. R. Müller, *Optik* **20**, pp. 510-511, 1963.
17. C. Dévé, *Optical Workshop Principles*, T. L. Tippell (trans.), Hilger & Watts, London, 1954, p. 295.
18. P. Jacquinot, *J. Opt. Soc. Am.* **44**, pp. 761-765, 1954.
19. L. Mertz, *Transformations in Optics*, Wiley, New York, 1965, pp. 15-16.
20. P. Glan, *Carl's Repert.* **16**, p. 570, 1880.
21. S. P. Thompson, *Phil. Mag.*, ser. 5, **12**, p. 349, 1881.
22. S. P. Thompson, *Proc. Opt. Conv.*, 1905, pp. 216-235.
23. R. T. Glazebrook, *Phil. Mag.*, ser. 5, **15**, p. 352, 1883.
24. C. E. Moeller and D. R. Grieser, *Appl. Opt.* **8**, pp. 206-207, 1969.
25. R. J. King and S. P. Talim, *J. Phys. (GB)*, ser. E, **4**, pp. 93-96, 1971.
26. J. W. Ellis and J. Bath, *J. Chem. Phys.* **6**, pp. 221-222, 1938.
27. F. Lippich, *Wien Akad. Sitzungsber.*, ser. III, **91**, p. 1059, 1885.
28. A. C. Hardy and F. H. Perrin, *The Principles of Optics*, McGraw-Hill, New York, 1932, p. 611.
29. J. F. Archard and A. M. Taylor, *J. Sci. Instrum.* **25**, pp. 407-409, 1948.
30. Karl Lambrecht Corp., Bull. P-73, Chicago, 1973.
31. J. Swartz, D. K. Wilson, and R. J. Kapash, *High Efficiency Laser Polarizers*, Electro-Opt. 1971 West Conf., Anaheim, Calif., May, 1971.
32. A. Lambrecht, Karl Lambrecht Corp., Chicago, Ill., private communication, 1969.
33. A. V. Shustov, *Sov. J. Opt. Technol.* **34**, pp. 177-181, 1967.
34. F. Twyman, *Prism and Lens Making*, 2d ed., Hilger & Watts, London, 1952, pp. 244, 599.
35. J. F. Archard, *J. Sci. Instrum.* **26**, pp. 188-192, 1949.

---

\* In all references to the Russian literature, volume and pages cited are for the English translation.

36. H. E. Bennett and J. M. Bennett, "Precision Measurements in Thin Film Optics," in G. Hass and R. E. Thun (eds.), *Physics of Thin Films*, vol. 4, Academic Press, New York, 1967, pp. 69–78.
37. D. L. Decker, J. L. Stanford, and H. E. Bennett, *J. Opt. Soc. Am.* **60**, p. 1557A, 1970.
38. R. L. Rowell, A. B. Levit, and G. M. Aval, *Appl. Opt.* **8**, p. 1734, 1969.
39. D. E. Aspnes, *Appl. Opt.* **9**, pp. 1708–1709, 1970.
40. R. L. Rowell, *Appl. Opt.* **9**, p. 1709, 1970.
41. W. Nicol, *Edinb. New Phil. J.* **6**, p. 83, 1828–1829, as quoted in A. Johannsen, *Manual of Petrographic Methods*, 2d ed. Hafner, New York, 1968, p. 158; (originally published in 1918).
42. S. P. Thompson, *Phil. Mag.*, ser. 5, **21**, p. 476, 1886.
43. B. Halle, *Dtsch. Mech. Z.*, no. 1, pp. 6–7, Jan. 1, 1908.
44. B. Halle, *Dtsch. Mech. Z.*, no. 2, pp. 16–19, Jan. 15, 1908.
45. A. B. Dale, in R. Glazebrook (ed.), *A Dictionary of Applied Physics*, vol. 4, Macmillan, London, 1923, pp. 496–497.
46. Hartnack and Prazmowski, *Ann. Chim. Phys.*, ser. 4, **7**, p. 181, 1866.
47. L. Foucault, *C. R. Acad. Sci.* **45**, p. 238, 1857.
48. C. D. West, and R. C. Jones, *J. Opt. Soc. Am.* **41**, pp. 976–982, 1951.
49. D. L. Steinmetz, W. G. Phillips, M. Wirick, and F. F. Forbes, *Appl. Opt.* **6**, pp. 1001–1004, 1967.
50. G. C. Morris and A. S. Abramson, *Appl. Opt.* **8**, pp. 1249–1250, 1969.
51. E. O. Ammann and G. A. Massey, *J. Opt. Soc. Am.* **58**, pp. 1427–1433, 1968.
52. A. C. Hardy, *J. Opt. Soc. Am.* **25**, pp. 305–311, 1935.
53. C. Bouhet and R. LaFont, *Rev. Opt.* **28**, pp. 490–493, 1949.
54. A. Cotton, *C. R. Acad. Sci.* **193**, pp. 268–271, 1931.
55. W. C. Johnson, Jr., *Rev. Sci. Instrum.* **35**, pp. 1375–1376, 1964.
56. L. V. Foster, *J. Opt. Soc. Am.* **28**, pp. 124–126, 127–129, 1938.
57. K. Feussner, *Z. Instrumentenk.* **4**, p. 41, 1884.
58. A. Johannsen, *Manual of Petrographic Methods*, 2d ed., Hafner, New York, 1968, pp. 169, 283–285; (originally published in 1918).
59. W. L. Hyde, New York Univ., Bronx N.Y., 1970, private communication.
60. E. Bertrand, *C. R. Acad. Sci.* **49**, p. 538, 1884.
61. L. Wulff, *Sitz. Preuss. Akad. Wiss.* **135**, p. 879, 1896.
62. P. Stöber, *Z. Krist.* **61**, p. 299, 1924.
63. P. Stöber, *Neues Jahrb. Mineral.* **A57**, p. 139, 1928.
64. P. Stöber, *Chem. Erde* **6**, p. 357, 453, 1930.
65. E. Tzekhnovitzer, *J. Phys. Chem. (USSR)* **5**, p. 1452, 1934.
66. C. D. West, *J. Opt. Soc. Am.* **35**, pp. 26–31, 1945.
67. M. Huot de Longchamp, *Rev. Opt.* **26**, pp. 94–98, 1947.
68. T. Yamaguti, *J. Phys. Soc. Jap.* **10**, pp. 219–221, 1955.
69. T. Yamaguti, I. Makino, S. Shinoda, and I. Kuroha, *J. Phys. Soc. Jap.* **14**, p. 199–201, 1959.
70. F. J. Dumont and R. N. Smartt, *J. Opt. Soc. Am.* **59**, p. 1541A, 1969
71. F. J. Dumont, *J. Opt. Soc. Am.* **60**, p. 719A, 1970
72. L. G. DeShazer, Dept. of Electrical Engineering, Univ. Southern California, Los Angeles, private communication, 1971.
73. V. Chandrasekharan and H. Damany, *Appl. Opt.* **8**, pp. 675–675, 1969.
74. V. Chandrasekharan and H. Damany, *Appl. Opt.* **10**, pp. 681–682, 1971.
75. E. Landais, *Bull. Soc. Fr. Mineral. Cristallogr.* **91**, pp. 350–354, 1968.
76. T. J. Bridges and J. W. Kluver, *Appl. Opt.* **4**, pp. 1121–1125, 1965.

77. J. J. Loferski, *Phys. Rev.* **87**, pp. 905–906, 1952.
78. R. Newman and R. S. Halford, *Rev. Sci. Instrum.* **19**, pp. 270–271, 1948.
79. W. L. Hyde, *J. Opt. Soc. Am.* **38**, p. 663A, 1948.
80. E. H. Land and C. D. West, in J. Alexander (ed.), *Colloid Chemistry*, vol. 6, Reinhold, New York, 1946, pp. 160–190.
81. E. H. Land, *J. Opt. Soc. Am.* **41**, pp. 957–963, 1951.
82. W. A. Shurcliff, *Polarized Light*, Harvard University Press, Cambridge, Mass., 1962, pp. 43–64.
83. S. D. Stookey and R. J. Araujo, *Appl. Opt.* **7**, pp. 777–779, 1968.
84. T. Yamaguti, *J. Opt. Soc. Am.* **45**, pp. 891–892, 1955.
85. P. Baumeister and J. Evans, in D. E. Gray (ed.), *American Institute of Physics Handbook*, 3rd ed., McGraw-Hill, New York, 1972, pp. 6-171–6-172.
86. R. P. Blake, A. S. Makas, and C. D. West, *J. Opt. Soc. Am.* **39**, p. 1054A, 1949.
87. A. S. Makas, *J. Opt. Soc. Am.* **52**, pp. 43–44, 1962.
88. L. Baxter, A. S. Makas, and W. A. Shurcliff, *J. Opt. Soc. Am.* **46**, p. 229, 1956.
89. R. C. Jones, Polaroid Corporation, Cambridge, Mass., private communication, 1970.
90. M. Haase, *Zeiss-Mitt.* **2**, p. 173, 1961.
91. M. N. McDermott and R. Novick, *J. Opt. Soc. Am.* **51**, pp. 1008–1010, 1961.
92. G. R. Bird and M. Parrish, Jr., *J. Opt. Soc. Am.* **50**, pp. 886–891, 1960.
93. G. B. Trapani, *Proc. Soc. Photo-Opt. Instrum. Eng.* **88**, pp. 105–113, 1976.
94. W. J. Gunning and J. Foschaar, *Appl. Opt.* **22**, pp. 3229–3231, 1983.
95. S. J. Baum, *Proc. Soc. Photo-Opt. Instrum. Eng.* **88**, pp. 50–56, 1976.
96. J. F. Dreyer, *J. Opt. Soc. Am.* **37**, p. 983A, 1947.
97. S. Anderson, *J. Opt. Soc. Am.* **39**, pp. 49–56, 1949.
98. Polacoat Bull. P-108 and P-112, Polacoat, Inc., Cincinnati, Ohio, 1967.
99. D. S. Kyser, Michelson Laboratory, Naval Weapons Center, China Lake, Calif., private communication, 1970.
100. G. Rupprecht, D. M. Ginsberg, and J. D. Leslie, *J. Opt. Soc. Am.* **52**, pp. 665–669, 1962.
101. Perkin-Elmer Corp., Instrument Division, Norwalk, Conn., “Wire Grid Polarizer Accessory,” Sheet no. D-454, 1966.
102. J. B. Young, H. A. Graham, and E. W. Peterson, *Appl. Opt.* **4**, pp. 1023–1026, 1965.
103. K. F. Renk and L. Genzel, *Appl. Opt.* **1**, pp. 643–648, 1962.
104. J. P. Casey and E. A. Lewis, *J. Opt. Soc. Am.* **42**, pp. 971–977, 1952.
105. E. A. Lewis and J. P. Casey, *J. Appl. Phys.* **23**, pp. 605–608, 1952.
106. M. Mohebi, J. Q. Liang, and M. J. Soileau, *Appl. Opt.* **28**, pp. 3681–3683, 1989.
107. R. W. Stobie and J. J. Dignam, *Appl. Opt.* **12**, pp. 1390–1391, 1973.
108. C. H. Burton, *Appl. Opt.* **18**, pp. 420–422, 1979.
109. J. P. Auton, *Appl. Opt.* **6**, pp. 1023–1027, 1967.
110. M. Hass and M. O’Hara, *Appl. Opt.* **4**, pp. 1027–1031, 1965.
111. A. R. Hilton and C. E. Jones, *J. Electrochem. Soc.* **113**, pp. 472–478, 1966.
112. D. G. Vickers, E. I. Robson, and J. E. Beckman, *Appl. Opt.* **10**, pp. 682–684, 1971.
113. P. K. Cheo and C. D. Bass, *Appl. Phys. Lett.* **18**, pp. 565–567, 1971.
114. J. P. Auton and M. C. Hutley, *Infrared Phys.* **12**, pp. 95–100, 1972.
115. A. E. Costley, K. H. Hursey, G. F. Neill, and J. M. Ward, *J. Opt. Soc. Am.* **67**, pp. 979–981, 1977.
116. J. A. Beunen, A. E. Costley, G. F. Neill, C. L. Mok, T. J. Parker, and G. Tait, *J. Opt. Soc. Am.* **71**, pp. 184–188, 1981.

117. T. A. Leonard, *Soc. Photo-Opt. Instrum. Eng.* **288**, pp. 129–135, 1981.
118. G. J. Sonek, D. K. Wanger, and J. M. Ballantyne, *Appl. Opt.* **22**, pp. 1270–1272, 1983.
119. W. L. Eichhorn and T. J. Magner, *Opt. Eng.* **25**, pp. 541–544, 1986.
120. G. Novak, R. J. Pernic, and J. L. Sundwall, *Appl. Opt.* **28**, pp. 3425–3427, 1989.
121. S. Roberts and D. D. Coon, *J. Opt. Soc. Am.* **52**, pp. 1023–1029, 1962.
122. Y. S. Hwang and H. K. Park, *Appl. Opt.* **28**, pp. 4999–5001, 1989.
123. H. Weiss and M. Wilhelm, *Z. Phys.* **176**, pp. 399–408, 1963.
124. B. Paul, H. Weiss, and M. Wilhelm, *Solid State Electron. (GB)* **7**, pp. 835–842, 1964.
125. A. Mueller and M. Wilhelm, *J. Phys. Chem. Solids* **26**, p. 2029, 1965.
126. N. M. Davis, A. R. Clawson, and H. H. Wieder, *Appl. Phys. Lett.* **15**, pp. 213–215, 1969.
127. M. Saito and M. Miyagi, *Appl. Opt.* **28**, pp. 3529–3533, 1989.
128. A. Hidalgo, J. Pastor, and J. M. Serratos, *J. Opt. Soc. Am.* **52**, pp. 1081–1082, 1962.
129. T. G. R. Rawlins, *J. Opt. Soc. Am.* **54**, pp. 423–424, 1964.
130. J.-L. Roumiguieres, *Opt. Commun.* **19**, pp. 76–78, 1976.
131. K. Knop, *Opt. Commun.* **26**, pp. 281–283, 1978.
132. G. W. Stroke, *Phys. Lett. (Neth.)* **5**, pp. 45–48, 1963.
133. G. W. Stroke, *J. Opt. Soc. Am.* **54**, p. 846, 1964.
134. C. W. Peters, T. F. Zipf, and P. V. Deibel, *J. Opt. Soc. Am.* **43**, p. 816A, 1953.
135. A. Hadni, E. Décamps, and P. Delorme, *J. Phys. Radium*, ser. 8, **19**, 793–794, 1958.
136. A. Hadni, E. Décamps, D. Grandjean, and C. Janot, *C. R. Acad. Sci.* **250**, pp. 2007–2009, 1960.
137. A. Mitsuishi, Y. Yamada, S. Fujita, and H. Yoshinaga, *J. Opt. Soc. Am.* **50**, pp. 433–436, 1960.
138. C. Janot and A. Hadni, *J. Phys. Radium*, ser. 8, **24**, pp. 1073–1077, 1963.
139. J. H. Rohrbaugh, C. Pine, W. G. Zoellner, and R. D. Hatcher, *J. Opt. Soc. Am.* **48**, pp. 710–711, 1958; [see also R. D. Hatcher and J. H. Rohrbaugh, *J. Opt. Soc. Am.* **46**, pp. 104–110, 1956 and J. H. Rohrbaugh and R. D. Hatcher, *J. Opt. Soc. Am.* **48**, pp. 704–709, 1958].
140. H. A. Kalthor and A. R. Neureuther, *J. Opt. Soc. Am.* **61**, pp. 43–48, 1971.
141. R. N. Hamm, R. A. MacRae, and E. T. Arakawa, *J. Opt. Soc. Am.* **55**, pp. 1460–1463, 1965.
142. K. Kudo, T. Arai, and T. Ogawa, *J. Opt. Soc. Am.* **60**, pp. 1046–1050, 1970.
143. V. G. Horton, E. T. Arakawa, R. N. Hamm, and M. W. Williams, *Appl. Opt.* **8**, pp. 667–670, 1969.
144. M. Schledermann and M. Skibowski, *Appl. Opt.* **10**, pp. 321–326, 1971.
145. N. J. Harrick, *J. Opt. Soc. Am.* **49**, pp. 376–379, 379–380, 1959.
146. D. F. Edwards and M. J. Bruemmer, *J. Opt. Soc. Am.* **49**, pp. 860–861, 1959.
147. M. Krížek, *Czech. J. Phys.* **13B**, pp. 599–610, 683–691, 1963.
148. J. P. Craig, R. F. Gribble, and A. A. Dougal, *Rev. Sci. Instrum.* **35**, pp. 1501–1503, 1964.
149. J. Bor, and L. A. Brooks, *J. Sci. Instrum.* **43**, p. 944, 1966.
150. A. H. Pfund, *J. Opt. Soc. Am.* **37**, pp. 558–559, 1947.
151. P. Barchewitz and L. Henry, *J. Phys. Radium*, ser. 8, **15**, pp. 639–640, 1954.
152. S. Takahashi, *J. Opt. Soc. Am.* **51**, pp. 441–444, 1961.
153. A. K. Walton and T. S. Moss, *Proc. Phys. Soc. (GB)* **78**, pp. 1393–1407, 1961.
154. R. T. Baumel and S. E. Schnatterly, *J. Opt. Soc. Am.* **61**, pp. 832–833, 1971.
155. B. N. Grechushnikov and I. P. Petrov, *Opt. Spectrosc. (USSR)* **14**, pp. 160–161, 1963.
156. J. T. Cox and G. Hass, *Appl. Opt.* **17**, pp. 1657–1658, 1978.
157. T. F. Thonn and R. M. A. Azzam, *Opt. Eng.* **24**, pp. 202–206, 1985.
158. W. R. Hunter, *Jap. J. Appl. Phys.* **4**, suppl. 1, p. 520, 1965; (*Proc. Conf. Photogr. Spectrosc. Opt.*, 1964).

159. H. Damany, *Opt. Acta* **12**, pp. 95–107, 1965.
160. G. Stephan, J.-C. Lemonnier, Y. LeCalvez, and S. Robin, *C. R. Acad. Sci.* **262B**, pp. 1272–1275, 1966.
161. F. de Celle and H. Merdy, *C. R. Acad. Sci.* **265B**, pp. 968–971, 1967.
162. T. J. McIlrath, *J. Opt. Soc. Am.* **58**, pp. 506–510, 1968.
163. T. T. Cole and F. Oppenheimer, *Appl. Opt.* **1**, pp. 709–710, 1962.
164. E. Uzan, H. Damany, and J. Romand, *C. R. Acad. Sci.* **260**, pp. 5735–5737, 1965.
165. K. Rabinovitch, L. R. Canfield, and R. P. Madden, *Appl. Opt.* **4**, pp. 1005–1010, 1965.
166. T. Sasaki and H. Fukutani, *Jap. J. Appl. Phys.* **3**, pp. 125–126, 1964.
167. H. Winter, H. H. Bukow, and P. H. Heckmann, *Opt. Commun.* **11**, pp. 299–300, 1974.
168. G. Hass and W. R. Hunter, *Appl. Opt.* **17**, pp. 76–82, 1978.
169. R. S. Spencer, G. J. Bergen, C. M. Fleetwood, H. Herzig, L. Miner, S. H. Rice, E. Smigocki, B. E. Woodgate, and J. J. Zaniewski, *Opt. Eng.* **24**, pp. 548–554, 1985.
170. W. R. Hunter, *Appl. Opt.* **17**, pp. 1259–1270, 1978.
171. A. Ejiri, *J. Phys. Soc. Jap.* **23**, p. 901, 1967.
172. G. Rosenbaum, B. Feuerbacher, R. P. Godwin, and M. Skibowski, *Appl. Opt.* **7**, pp. 1917–1920, 1968.
173. N. Rehfeld, U. Gerhardt, and E. Dietz, *Appl. Phys.* **1**, pp. 229–232, 1973.
174. H. A. Van Hoof, *Appl. Opt.* **19**, pp. 189–190, 1980.
175. R. Hibst and H. H. Bukow, *Appl. Opt.* **28**, pp. 1806–1812, 1989.
176. M. A. Khakoo, P. Hammond, and J. W. McConkey, *Appl. Opt.* **26**, pp. 3492–3494, 1987.
177. M. B. Robin, N. A. Kuebler, and Y.-H. Pao, *Rev. Sci. Instrum.* **37**, pp. 922–924, 1966.
178. A. Matsui and W. C. Walker, *J. Opt. Soc. Am.* **60**, pp. 64–65, 1970.
179. F. Abelès, *C. R. Acad. Sci.* **230**, pp. 1942–1943, 1950.
180. L. G. Schulz and F. R. Tangherlini, *J. Opt. Soc. Am.* **44**, pp. 362–368, 1954.
181. D. K. Burge and H. E. Bennett, *J. Opt. Soc. Am.* **54**, pp. 1428–1433, 1964.
182. G. K. T. Conn and G. K. Eaton, *J. Opt. Soc. Am.* **44**, pp. 553–557, 1954.
183. M. F. de la Provostaye and P. Desains, *Ann. Chim. Phys.*, ser. 3, **30**, p. 158, 1850.
184. G. R. Bird and W. A. Shurcliff, *J. Opt. Soc. Am.* **49**, pp. 235–237, 1959.
185. A. Elliott and E. J. Ambrose, *Nature* **159**, pp. 641–642, 1947.
186. A. Elliott, E. J. Ambrose, and R. Temple, *J. Opt. Soc. Am.* **38**, pp. 212–216, 1948.
187. J. Ames and A. M. D. Sampson, *J. Sci. Instrum.* **26**, p. 132, 1949.
188. R. Duverney, *J. Phys. Radium*, ser. 8, **20**, suppl. 7, p. 66A, 1959.
189. J. H. Hertz, *Exper. Tech. der Phys.* **7**, pp. 277–280, 1959.
190. K. Buijs, *Appl. Spectrosc.* **14**, pp. 81–82, 1960.
191. E. M. Bradbury and A. Elliott, *J. Sci. Instrum.* **39**, p. 390, 1962.
192. R. G. Greenler, K. W. Adolph, and G. M. Emmons, *Appl. Opt.* **5**, pp. 1468–1469, 1966.
193. N. Wright, *J. Opt. Soc. Am.* **38**, pp. 69–70, 1948.
194. A. S. Makas and W. A. Shurcliff, *J. Opt. Soc. Am.* **45**, pp. 998–999, 1955.
195. H. E. Bennett, J. M. Bennett, and M. R. Nagel, *J. Opt. Soc. Am.* **51**, p. 237, 1961.
196. R. T. Lagemann and T. G. Miller, *J. Opt. Soc. Am.* **41**, pp. 1063–1064, 1951.
197. L. Huld and T. Staffin, *Opt. Acta* **6**, pp. 27–36, 1959.
198. T. A. Leonard, J. Loomis, K. G. Harding, and M. Scott, *Opt. Eng.* **21**, pp. 971–975, 1982.
199. R. Meier and H. H. Günthard, *J. Opt. Soc. Am.* **49**, pp. 1122–1123, 1959.
200. N. J. Harrick, *J. Opt. Soc. Am.* **54**, pp. 1281–1282, 1964.

201. N. P. Murarka and K. Wilner, *Appl. Opt.* **20**, pp. 3275–3276, 1981.
202. S. D. Smith, T. S. Moss, and K. W. Taylor, *J. Phys. Chem. Solids* **11**, pp. 131–139, 1959.
203. D. T. Rampton and R. W. Grow, *Appl. Opt.* **15**, pp. 1034–1036, 1976.
204. J.-M. Munier, J. Claudel, E. Décamps, and A. Hadni, *Rev. Opt.* **41**, pp. 245–253, 1962.
205. A. K. Walton, T. S. Moss, and B. Ellis, *J. Sci. Instrum.* **41**, pp. 687–688, 1964.
206. W. C. Walker, *Appl. Opt.* **3**, pp. 1457–1459, 1964.
207. D. C. Hinson, *J. Opt. Soc. Am.* **56**, p. 408, 1966.
208. D. F. Heath, *Appl. Opt.* **7**, pp. 455–459, 1968.
209. J. Schellman, V. Chandrasekharan, and H. Damany, *C. R. Acad. Sci.* **259**, pp. 4560–4563, 1964.
210. G. Weiser, *Proc. IEEE* **52**, p. 966, 1964.
211. J. L. Weinberg, *Appl. Opt.* **3**, pp. 1057–1061, 1964.
212. J. M. Bennett, D. L. Decker, and E. J. Ashley, *J. Opt. Soc. Am.* **60**, p. 1577A, 1970.
213. H. Schröder, *Optik* **3**, pp. 499–503, 1948.
214. F. Abelès, *J. Phys. Radium* ser. 8, **11**, pp. 403–406, 1950.
215. K. Kubo, *J. Sci. Res. Instrum.* (Tokyo Inst. Phys. Chem. Res.) **47**, pp. 1–6, 1953.
216. H. Schopper, *Optik* **10**, pp. 426–438, 1953.
217. M. Ruiz-Urbietta and E. M. Sparrow, *J. Opt. Soc. Am.* **62**, pp. 1188–1194, 1972.
218. M. Ruiz-Urbietta and E. M. Sparrow, *J. Opt. Soc. Am.* **63**, pp. 194–200, 1973.
219. M. Ruiz-Urbietta, E. M. Sparrow, and G. W. Goldman, *Appl. Opt.* **12**, pp. 590–596, 1973.
220. F. Abelès, *Jap. J. Appl. Phys.* **4**, suppl. 1, p. 517, 1965; (Proc. Conf. Photogr. Spectrosc. Opt., 1964).
221. A.-R. M. Zaghoul and R. M. A. Azzam, *Appl. Opt.* **16**, pp. 1488–1489, 1977.
222. W. W. Buchman, S. J. Holmes, and F. J. Woodberry, *J. Opt. Soc. Am.* **61**, pp. 1604–1606, 1971.
223. W. W. Buchman, *Appl. Opt.* **14**, pp. 1220–1224, 1975.
224. S. Refermat and J. Eastman, *Proc. Soc. Photo-Opt. Instrum. Eng.* **88**, pp. 28–33, 1976.
225. L. Songer, *Optical Spectra* **12** (10), pp. 49–50, October 1978.
226. D. Blanc, P. H. Lissberger, and A. Roy, *Thin Solid Films* **57**, pp. 191–198, 1979.
227. T. Maehara, H. Kimura, H. Nomura, M. Yanagihara, and T. Namioka, *Appl. Opt.* **30**, pp. 5018–5020, 1991.
228. P. B. Clapham, M. J. Downs, and R. J. King, *Appl. Opt.* **8**, pp. 1965–1974, 1969. [See also P. B. Clapham, *Thin Solid Films* **4**, pp. 291–305, 1969].
229. S. M. MacNeille, U.S. Patent 2,403,731, July 9, 1946.
230. M. Banning, *J. Opt. Soc. Am.* **37**, pp. 792–797, 1947.
231. J. A. Dobrowolski and A. Waldorf, *Appl. Opt.* **20**, pp. 111–116, 1981.
232. J. C. Monga, P. D. Gupta, and D. D. Bhawalkar, *Appl. Opt.* **23**, pp. 3538–3540, 1984.
233. J. Mouchart, J. Begel, and E. Duda, *Appl. Opt.* **28**, pp. 2847–2853, 1989.
234. D. Lees and P. Baumeister, *Opt. Lett.* **4**, pp. 66–67, 1979.
235. R. M. A. Azzam, *Opt. Lett.* **10**, pp. 110–112, 1985.
236. R. M. A. Azzam, *Appl. Opt.* **25**, pp. 4225–4227, 1986.
237. H. Schröder and R. Schläfer, *Z. Naturforsch.* **4a**, pp. 576–577, 1949.
238. G. Pridatko and T. Krylova, *Opt.-Mekh. Prom.* **3**, p. 23, 1958.
239. R. S. Sokolova and T. N. Krylova, *Opt. Spectrosc.* (USSR) **14**, pp. 213–215, 1963.
240. A. F. Turner and P. W. Baumeister, *Appl. Opt.* **5**, pp. 69–76, 1966.
241. P. B. Clapham, *Opt. Acta* **18**, pp. 563–575, 1971.
242. H. Schröder, *Optik* **13**, pp. 158–168, 169–174, 1956.
243. P. Baumeister, *Opt. Acta* **8**, pp. 105–119, 1961.

244. P. Baumeister, Institute of Optics, Univ. Rochester, Rochester, N.Y., private communication, 1971.
245. V. R. Costich, *Appl. Opt.* **9**, pp. 866–870, 1970.
246. C. D. West and A. S. Makas, *J. Opt. Soc. Am.* **39**, pp. 791–794, 1949.
247. S. D. Jacobs, Y. Asahara, and T. Izumitani, *Appl. Opt.* **21**, pp. 4526–4532, 1982.
248. B. H. Billings, in D. E. Gray, (ed.), *American Institute of Physics Handbook*, 3d ed., McGraw-Hill, New York, 1972, pp. 6-37,6-40, 6-46, 6-112, and 6-113.
249. J. M. Beckers, *Appl. Opt.* **10**, pp. 973–975, 1971.
250. W. L. Bond, *J. Appl. Phys.* **36**, pp. 1674–1677, 1965.
251. J. H. Shields and J. W. Ellis, *J. Opt. Soc. Am.* **46**, pp. 263–265, 1956.
252. E. D. Palik and B. W. Henvis, *Appl. Opt.* **6**, pp. 2198–2199, 1967.
253. G. D. Boyd, W. L. Bond, and H. L. Carter, *J. Appl. Phys.* **38**, pp. 1941–1943, 1967.
254. M. A. Jeppesen, *J. Opt. Soc. Am.* **48**, pp. 629–632, 1958.
255. S. S. Ballard, J. S. Browder, and J. F. Ebersole, in D. E. Gray (ed.), *American Institute of Physics Handbook*, 3d ed., McGraw-Hill, New York, 1972, pp. 6-20, 6-27, and 6-35.
256. A. E. Ennos and K. W. Opperman, *Appl. Opt.* **5**, p. 170, 1966.
257. E. D. Palik, *Appl. Opt.* **7**, pp. 978–979, 1968.
258. H. Gobrecht and A. Bartschat, *Z. Phys.* **156**, pp. 131–143, 1959.
- 258a. M. S. Shumate, *Appl. Opt.* **5**, pp. 327–332, 1966.
259. E. V. Loewenstein, *J. Opt. Soc. Am.* **51**, pp. 108–112, 1961.
260. V. Chandrasekharan and H. Damany, *Appl. Opt.* **7**, pp. 939–941, 1968.
261. J.-P. Maillard, *Opt. Commun.* **4**, pp. 175–177, 1971.
262. T. M. Bieniewski and S. J. Czyzak, *J. Opt. Soc. Am.* **53**, pp. 496–497, 1963.
263. M. Françon, S. Mallick, and J. Vulmière, *J. Opt. Soc. Am.* **55**, p. 1553, 1965.
264. F. Zernicke, Jr., *J. Opt. Soc. Am.* **54**, pp. 1215–1220, 1964, [erratum in *J. Opt. Soc. Am.* **55**, pp. 210–211, 1965].
265. E. Einsporn, *Phys. Z.* **37**, pp. 83–88, 1936.
266. E. L. Gieselmann, S. F. Jacobs, and H. E. Morrow, *J. Opt. Soc. Am.* **59**, pp. 1381–1383, 1969 [erratum in *J. Opt. Soc. Am.* **60**, p. 705, 1970].
267. J. M. Daniels, *Rev. Sci. Instrum.* **38**, pp. 284–285, 1967.
268. T. Saito, A. Ejiri, and H. Onuki, *Appl. Opt.* **29**, pp. 4538–4540, 1990.
269. W. B. Westerveld, K. Becker, P. W. Zetner, J. J. Corr, and J. W. McConkey, *Appl. Opt.* **14**, pp. 2256–2262, 1985.
270. P. L. Richards and G. E. Smith, *Rev. Sci. Instrum.* **35**, pp. 1535–1537, 1964.
271. L. H. Johnston, *Appl. Opt.* **16**, pp. 1082–1084, 1977.
272. D. P. Gonatas, X. D. Wu, G. Novak, and R. H. Hildebrand, *Appl. Opt.* **28**, pp. 1000–1006, 1989.
273. P. Lostis, *J. Phys. Radium*, ser. 8, **18**, p. 51S, 1957.
274. C. E. Greninger, *Appl. Opt.* **27**, pp. 774–776, 1988.
275. J. M. Bennett, *Appl. Opt.* **9**, pp. 2123–2129, 1970.
276. S. Nakadate, *Appl. Opt.* **29**, pp. 242–246, 1990.
277. P. D. Hale and G. W. Day, *Appl. Opt.* **27**, pp. 5146–5153, 1988.
278. A.-R. M. Zaghloul, R. M. A. Azzam, and N. M. Bashara, *Opt. Commun.* **14**, pp. 260–262, 1975.
279. A.-R. M. Zaghloul, R. M. A. Azzam, and N. M. Bashara, *J. Opt. Soc. Am.* **65**, pp. 1043–1049, 1975.
280. S. Kawabata and M. Suzuki, *Appl. Opt.* **19**, pp. 484–485, 1980.
281. S. Chu, R. Conti, P. Bucksbaum, and E. Commins, *Appl. Opt.* **18**, pp. 1138–1139, 1979.
282. J. Strong, *Procedures in Experimental Physics*, Prentice-Hall, Englewood Cliffs, N.J., 1938, pp. 388–389.

283. P. H. Smith, *Proc. Symp. Recent Dev. Ellipsometry, Surf. Sci.* **16**, pp. 34–66, 1969.
284. B. N. Grechushnikov, *Opt. Spectrosc.* (USSR) **12**, p. 69, 1962.
285. D. G. Drummond, *Proc. Roy. Soc. (Lond.)* **153A**, pp. 318–339, 1936.
286. G. Holzwarth, *Rev. Sci. Instrum.* **36**, pp. 59–63, 1965.
287. E. D. Palik, *Appl. Opt.* **2**, pp. 527–539, 1963.
288. J. H. Jaffe, H. Jaffe, and K. Rosenbeck, *Rev. Sci. Instrum.* **38**, pp. 935–938, 1967.
289. C. Gaudefroy, *C. R. Acad. Sci.* **189**, pp. 1289–1291, 1929.
290. W. A. Deer, R. A. Howie, and J. Zussman, *Rock-forming Minerals*, vol. 3; *Sheet Silicates*, Wiley, New York, 1962, pp. 258–262.
291. A. E. Ennos, *J. Sci. Instrum.* **40**, pp. 316–317, 1963.
292. S. B. Ioffe and T. A. Smirnova, *Opt. Spectrosc.* (USSR) **16**, pp. 484–485, 1964.
293. S. Mitchell, *Nature* **212**, pp. 65–66, 1966.
294. A. M. Title, *Appl. Opt.* **14**, pp. 229–237, 1975.
295. R. Anderson, *Appl. Opt.* **27**, pp. 2746–2747, 1988.
296. P. L. Wizinowich, *Opt. Eng.* **28**, p. 157–159, 1989.
297. G. N. Ramachandran and S. Ramaseshan, “Crystal Optics,” in S. Flügge (ed.), *Handbuch der Physik*, vol. 25/1, Springer, Berlin, 1961, pp. 156–158.
298. A. Johannsen, *Manual of Petrographic Methods*, 2d ed. Hafner, New York, 1968, pp. 369–385 (originally published in 1918).
299. H. G. Jerrard, *J. Opt. Soc. Am.* **38**, pp. 35–59, 1948.
300. R. P. Hunt, *Appl. Opt.* **9**, pp. 1220–1221, 1970.
301. J. R. Partington, *An Advanced Treatise on Physical Chemistry*, vol. 4, Wiley, New York, 1953, pp. 173–177.
302. J. Ellerbroek and J. T. Groosmuller, *Phys. Z.* **27**, pp. 468–471, 1926.
303. H. G. Jerrard, *J. Opt. Soc. Am.* **39**, pp. 1031–1035, 1949.
304. H. G. Jerrard, *J. Sci. Instrum.* **26**, pp. 353–357, 1949.
305. H. G. Jerrard, *J. Sci. Instrum.* **27**, pp. 62–66, 1950.
306. J. F. Archard, *J. Sci. Instrum.* **27**, pp. 238–241, 1950.
307. R. W. Wood, *Physical Optics*, 3d ed., Macmillan, New York, 1934, pp. 356–361.
308. R. W. Ditchburn, *Light*, 2d ed., Interscience, New York, 1963b, pp. 483–485.
309. H. G. Jerrard, *J. Sci. Instrum.* **27**, pp. 164–167, 1950.
310. H. G. Jerrard, *J. Sci. Instrum.* **28**, pp. 10–14, 1951.
311. H. G. Jerrard, *J. Sci. Instrum.* **30**, pp. 65–70, 1953.
312. H. E. Ives and H. B. Briggs, *J. Opt. Soc. Am.* **26**, pp. 238–246, 1936.
313. E. D. Palik, *Appl. Opt.* **4**, pp. 1017–1021, 1965.
314. P. Hariharan and D. Sen, *J. Sci. Instrum.* **37**, pp. 278–281, 1960.
315. M. P. Varnham, D. N. Payne, A. J. Barlow, and E. J. Tarbox, *Opt. Lett.* **9**, pp. 306–308, 1984.
316. C. A. Villarruel, M. Abebe, W. K. Burns, and R. P. Moeller, in *Digest of the Seventh Topical Conference on Optical Fiber Communication*, vol. 84.1, Optical Society of America, Washington, D.C., 1984.
317. R. A. Bergh, H. C. Lefevre, and H. J. Shaw, *Opt. Lett.* **5**, pp. 479–481, 1980.
318. W. Eickhoff, *Electron. Lett.* **16**, pp. 762–763, 1980.
319. D. Gruchmann, K. Petermann, L. Satandigel, and E. Weidel, in *Proceedings of the European Conference on Optical Communication*, North Holland, Amsterdam, 1983, pp. 305–308.
320. T. Hosaka, K. Okamoto, and T. Edahiro, *Opt. Lett.* **8**, pp. 124–126, 1983.
321. J. R. Feth and C. L. Chang, *Opt. Lett.* **11**, pp. 386–388, 1986.
322. T. Yu and Y. Wu, *Opt. Lett.* **13**, pp. 832–834, 1988.

323. R. B. Dyott, J. Bello, and V. A. Handerek, *Opt. Lett.* **12**, pp. 287–289, 1987.
324. S. C. Lee and J.-I. Chen, *Appl. Opt.* **29**, pp. 2667–2668, 1990.
325. R. Ulrich and M. Johnson, *Appl. Opt.* **18**, pp. 1857–1861, 1979.
326. T. Hosaka, K. Okamoto, and T. Edauro, *Appl. Opt.* **22**, pp. 3850–3858, 1983.
327. A. W. Snyder and A. J. Stevenson, *Opt. Lett.* **11**, pp. 254–256, 1986.
328. S. Uehara, T. Izawa, and H. Nakagome, *Appl. Opt.* **13**, pp. 1753–1754, 1974.
329. H. F. Mahlein, *Opt. Commun.* **16**, pp. 420–424, 1976.
330. P. G. Suchoski, T. K. Findakly, and F. J. Leonberger, *Opt. Lett.* **13**, pp. 172–174, 1988.
331. R. Noé, H. Heidrich, and D. Hoffmann, *Opt. Lett.* **13**, pp. 527–529, 1988.
332. K. Baba, K. Shiraiishi, K. Obi, T. Kataoka, and S. Kawakami, *Appl. Opt.* **27**, pp. 2554–2560, 1988.